Modal Characteristics of Satellite Appendages using On-Orbit Output-Only Modal Testing

Md Mashiul Alam

A Thesis
in
The Department
of
Mechanical and Industrial Engineering

Presented in the partial fulfillment of the requirements
For the degree of Master of Applied Science (Mechanical Engineering) at
Concordia University,
Montreal, Quebec, Canada

May 2007

Your file Votre référence
ISBN: 978-0-494-34679-2
Our file Notre référence
ISBN: 978-0-494-34679-2

ABSTRACT

Modal Characteristics of Satellite Appendages

using On-Orbit Output-Only Modal Testing

Md Mashiul Alam

Output-only modal testing is an attractive new technique with potential applications in civil, mechanical, and aerospace engineering. It may effectively be used for model validation, model updating, quality control, and health monitoring through the determination of modal characteristics of the structures. This approach to modal testing has great potential for ground and on-orbit modal testing of space hardware, especially for flexible structures such as membrane payloads where the operating excitations, such as firing of AC thrusters and ambient thermal shock, are difficult or impossible to measure. The latest versions of output only modal testing technique that considers a noise model to have better estimation of modal parameters from output response time series data is very new and can be very successfully employed to test satellite structures.

The main objective of this research is to validate the output-only modal technique approach to extract modal parameters of the appendages with the help of finite element transient analysis and to further verify it through experiments. This research includes a study of the dynamics of satellite appendages and associated excitation method to investigate analytically and experimentally the output-only modal testing approach. Application of the proposed method is investigated and the efficiency over traditional FRF modal testing approach is shown.

For identification of modal parameters, satellite solar panel, antennas or other satellite appendages are modeled as linear plate or beam models. It has been proven analytically that the multiple-point excitation is a better loading condition compared with driven base or single point excitation using output-only modal testing technique. It has also been established experimentally that the driven base excitation is better loading condition compared to single point excitation. The effect of using less number of nodal responses instead of using all the nodal response has been investigated.

Finally, it has been confirmed both analytically and experimentally that the new versions of output only modal testing approach can be employed to identify the modal parameters of satellite appendages on orbit efficiently.

ACKNOWLEDGEMENT

I would like to take the opportunity to express my gratefulness to some people without whose help completion of this dissertation would not have been possible. First of all, I would like to convey my sincere gratitude to my professor Dr. Ramin Sedaghati, for his stimulating supervision, discussions and invaluable constructive suggestions to complete this thesis. I am deeply thankful for his endless co-operation, support and comments on this thesis.

I would like to thank Canadian Space Agency (CSA) in St. Hubert, Quebec for their support and for initiating this research. Especially, I am grateful to Dr. Yvan Soucy, the thesis co-supervisor from Canadian Space Agency, for his continuous support, sharing his insights and for the kindness. He helped me to overcome the difficult and critical situations and made me believe in myself. Also, I would like to extend my thankfulness to all the manufacturing departmental staff in CSA, as well as Mr. Mondor Sylvain, space technologies technician. Special thanks goes to Mr. F. R. Vigneron, formerly with CSA, for giving us some critical information and help time to time on spacecraft engineering.

I wish to extend my gratitude to Dr. Rama Bhat, my co-supervisor, for his enormous advice and help from the beginning to the end of my research work. He made me to be strong analytically and more thoughtful about giving something more towards my dissertation.

Finally, I would like to thank my wife, Imrana Rahman, for her inspiration and encouragement all through my thesis work.

TABLE OF CONTENTS

LIST OF FIGURES

LIST OF TABLES

NOMENCLATURE

The symbols used in this thesis are listed below:

a	Length
A	$2n \times 2n$ the system matrix
A_k	kth residue matrix of the output PSD
b	Width
B	$2n \times n$ input matrix
C	$n \times n$ time-invariant damping matrix
d_k	scalar constant
$e(t)$	$n \times 1$ vector of external excitation of n degrees of freedom
E	Modulus of elasticity
f	Natural frequency
$F(t)$	$2n \times 2n$ state transition matrix of the linear dynamic structure
F, G	Constant matrix
$< g_i >$	the operational reference factors
G_{xx}	Power Spectral Density (PSD) matrix of the input
G_{yy}	PSD matrix of the response
$\hat{G}_{yy}$	the output PSD at discrete frequencies $\omega = \omega_i$
h	Thickness
H	p$\times 2n$ observation matrix
$[H(\omega)]$	FRF matrix

$[K]$	Stiffness matrix
K	$n \times n$ time-invariant mass stiffness matrix
L	$p \times n$ matrix specifies at which points of the structure the output are measured
m	Mass per unit length
$[M]$	Mass matrix
M	$n \times n$ time-invariant mass matrix
n	Number of modes
P	Number of segments
Q	Maximum number of time lags at which the correlations are estimated
r	Number of inputs
R_i	Correlation
R_k	Residue
S_i	Diagonal matrix holding the scalar singular values s_{ij}
$Sub(\omega)$	Set of modes
$[S_{uu}]$	Input spectra
$[S_{yy}]$	Output spectra
t	Time in seconds
U_i	a unitary matrix holding singular vectors u_{ij}
$U(t)$	$n \times 1$ vector of displacement
$\dot{U}(t)$	$n \times 1$ vector of velocity
$\ddot{U}(t)$	$n \times 1$ vector of acceleration

$\{\gamma_i^l\}$ Modal participation factors

w_k Time window

$x^T(t)$ State vector

$y(k)$ Measured discrete observation data

$y(t)$ $p \times 1$ vector of measurements

$\bullet^*$ Complex conjugate of a matrix

$\bullet^H$ Complex conjugate transpose (Hermitian) of a matrix

α_i Scaling factor

λ Eigenvalue of the system

λ_i Eigenvalues of i-degrees-of-freedom

λ_k Pole

ρ Density

γ Mass per unit area

ν Poisson's ratio

Δt Time steps in seconds

ω_i Eigen frequencies

ω_q Natural frequency (rad/s) of the i-th mode

ξ Damping ratio

ξ_i Damping ratio of i-th mode

η_q Damping ratio of q-th mode

$\hat{\phi}$	Mode shape
$[\Phi]$	Matrix of the system eigenvectors
Φ_i	Eigenvectors of i-degrees-of-freedom
$\{\Phi\}$	Unscaled mode identified by output-only modal analysis
$\{\Psi\}$	Eigenvector of the system
$[\Sigma]$	Diagonal matrix of singular values

ASCII	American Standard Code for Information Interchange
B&K	Brüel & Kjaer
BFD	Basic Frequency Domain
CSA	Canadian Space Agency
CU	Concordia University
CVA	Canonical Variate Analysis
DFT	Discrete Fourier Transform
DoF	Degree of Freedom
DoFs	Degrees of Freedom
EFDD	Enhanced Frequency Domain Decomposition
ERA	Eigen Realization Algorithm
FDD	Frequency Domain Decomposition
FEA	Finite Element Analysis
FRF	Frequency Response Function
ITD	Ibrahim Time Domain
LSCF	Least-Squares Complex Frequency domain

MAC	Media Assurance Criterion
N4SID	Numerical Algorithm for Subspace state space IDentification
OLE	Object Linking and Embedding
O&M	Operation and Maintenance
OOMT	Out-put Only Modal Testing
PC	Principal Component
PSD	Power Spectral Density
R&D	Research and Development
SDoF	Single Degree of Freedom
SSI	Stochastic Subspace Identification
SVD	Singular Value Decomposition
SVS	Structural Vibration Solution
UFF	Universal File Format
UPC	Unweighted Principle Components

CHAPTER 1

INTRODUCTION

1.1 BACKGROUND

The number of spacecraft is increasing in space as well as their age. The older a spacecraft structure becomes, the more difficult it is to perform normal operation under space environmental conditions that include intermittent or impulsive non-gravitational acceleration, ionizing radiation, and extremes of thermal temperatures. It is under these conditions that the spacecraft structures need increased monitoring and subsequent life management. One of the ways in which the engineers accomplish this is through identification of modal parameters.

Modal identification is the process of estimating modal parameters from vibration measurements obtained from different locations on a structure. The modal parameters of a structure include the mode shapes, natural (or resonance) frequencies and the damping properties of each mode that influence the response of the structure in a frequency range of interest. Modal parameters are important because they describe the inherent dynamic properties of the structure. Since these dynamic properties are directly related to the mass and the stiffness, experimentally obtained modal parameters provide information about these two physical properties of a structure. These modal parameters are also used for model validation, model updating, and health monitoring.

The engineers use different kinds of modal parameter identification techniques. One well-known technique is input-output based Frequency Response Function (FRF) method. In this technique, a response function is generated based on the input and the resulting output of the structure. In this process the instrumentation is demanding due to the need for simultaneous measurement of input and output data and the tests are done mostly in the laboratory. The limitations of this method are difficulties in the generation of the real operation conditions, measurement of input excitation and the need for scaling in modeling of the real structure.

To overcome these problems a new technique was introduced which is called Output-Only Modal Testing (OOMT) technique. This technique has applications in civil and mechanical engineering field and has been used in ground structural systems for quite sometime. With this new technique some of the problems associated with traditional FRF method are eliminated. The testing is done in-situ under real operation conditions without bringing the structure into the laboratory. The advantages of this technique in satellite applications while in operation are quite obvious. This thesis attempts to introduce analytically and experimentally the potential application of this novel technique for on-orbit satellite applications.

1.2 LITERATURE REVIEW

The concept of output-only modal testing is not new but the development of this technique has a brief history. For quite some time people working in modal analysis have been performing output only modal identification using the commonly accepted fact that

if only one mode contributes to a certain band of the spectral matrix, then any row or column in that matrix can be used as a mode shape estimate. By picking a peak in one of the spectral density functions one can get the mode shape from one of the columns or rows in the spectral matrix. This classical approach, also known as Basic Frequency Domain (BFD) technique, is based on the simple signal processing technique using a discrete Fourier transform, and hinges on the fact that well separated modes can be estimated directly from the matrix of the frequency response functions [1].

This classical technique gives reasonable estimates of the natural frequencies and mode shapes if the modes are well separated. However, in the case of closely spaced modes, it can be difficult to detect the modes, and, even in the case where close modes are detected, estimated frequencies and mode shapes become heavily biased. Furthermore, the estimated frequencies are limited by the frequency resolution of the estimated spectral density and, in all cases, damping estimation is uncertain or impossible.

The first time-domain technique that really became known for serious output-only identification was introduced by Ibrahim and Milkulcik [2-4] and is known as the Ibrahim Time Domain (ITD) method. Shortly after that the Polyreference method were introduced by Vold et al. [5] and Vold and Rocklin [6]. After that the Eigen Realization Algorithm (ERA) developed by Juan and Pappa [7] was introduced and used for space application in the past [8, 9]. The two last techniques, i.e. Polyreference and ERA, use multiple inputs but ITD also can be formulated as a multiple input method as described by Fukuzono [10]. Recently, Zhang et al. [11] has given a common formulation for all these techniques.

What they have in common is that they assume that a free response function can be obtained. These time domain techniques are all based on a function represented by exponential decay and there are no provisions for separate noise modeling. Noise is basically accounted for by adding extra modes, which are called the noise modes. A more modern approach called Stochastic Subspace Identification (SSI) has been introduced in which the noise mode has been considered. This method is time domain method that directly works with time data, without any conversion to correlations or spectra functions. The algorithm for this new stochastic subspace time domain technique was described by Van Overschee and De Moor [12-15]. Also, more detailed information on stochastic subspace method can be found in [16-19]. Two simulation examples including a spring-mass-system and a horizontal cantilever beam in transverse vibration were demonstrated by Lardies [20] to investigate the efficiency of this stochastic subspace method.

The main advantage of the classical i.e. BFD technique is that it is more user-friendly, faster and provides the user a 'feeling' of the data. Working directly with the spectral density functions basically helps the user to find out the structural properties just by examining the spectral density functions.

The disadvantages associated with classical approach are further removed by another method called Frequency Domain Decomposition technique (FDD) that was extensively investigated by Ren and Zong [21] and Brincker et al. [22-24]. This method contains all the advantages of the classical technique and also provides clear indication of harmonic components in the response signal. It has been described that the spectral matrix can be

decomposed with the Singular Value Decomposition (SVD) method into a set of auto spectral density functions, each corresponding to a Single Degree of Freedom (SDoF) system. The results achieved are exact in the case where the excitation is white noise, the structure is lightly damped and the mode shapes of closely spaced modes are geometrically orthogonal.

Scaling of the mode has been a critical issue in some applications since the exciting forces are not measured. All these techniques involve either detailed knowledge of the material characteristics, finite element method [25], or make very restrictive assumptions about the excitation [26]. Randall et al. [27] performed an additional forced vibration test, at a limited number of points, in order to re-scale the in-operational mode shape estimates. Parloo et al. [28] proposed a method for the re-scaling to get the correct scaled mode. It is shown that by adding, for instance, one or more known masses to the test structure, the operational mode shapes can be mass-normalized by means of the measured shift in natural frequencies between the original and mass-loaded condition. Sestieri and D'Ambrogio [29] proposed a scaling technique based on the same phenomenon but for the undamped (or lightly damped) system.

The added masses should be small enough to permit a first order approximation while it should be appropriately located to permit a significant measurable shift of the natural frequencies. This emphasis on a critical point location is possibly the real weakness of the method, because small difference in the shift estimation can lead to significant errors in

the determination of the scaled factor. Therefore the method must be appropriately optimized, by performing a careful analysis on the mass distribution and location(s) [30].

Abdelghani et al. [31] presented the results of the performance of output only identification algorithm for modal analysis of aircraft structure under white noise excitations. It was found that the subspace-based algorithm performs well. Richardson and Schwarz also discussed the different aspects of operational modal analysis in [32].

The PolyMAX is a further evolution of the so-called Least-Square Complex Frequency (LSCF) domain method. Originally, LSCF was introduced to find initial values of the iterative maximum likelihood method [33]. The method estimates a so-called common-denominator transfer function model [34]. The most important advantage of LSCF estimator over the available and widely applied parameter estimator techniques [35] is that very clear stabilization diagrams are obtained. A thorough analysis of different variants of the common-denominator LSCF method can be found in [36]. A complete background on frequency-domain system identification can be found in [37].

It was found that the identified common-denominator model closely fitted the measured frequency response function (FRF) data. However, when converting this model to a modal model by reducing the residues to a rank-one matrix using the singular value decomposition (SVD), the quality of the fit decreased [38]. Another feature of the common-denominator implementation is that the stabilization diagram can only be constructed using pole information (eigenfrequencies and damping ratios). Neither

participation factors nor mode shapes are available. The theoretically associated drawback is that closely spaced poles will erroneously show up as a single pole.

These two reasons provided the motivation for a polyreference version of the LSCF method known as PolyMAX using the so-called right matrix-fraction model. In this approach, also the participation factors are available when constructing the stabilization diagram. The main benefits of PolyMAX method are that the SVD step to decompose the residues can be avoided so that closely spaced poles can be separated. The detailed discussion regarding this method can be found in references [39, 40].

Combined with the new automatic modal parameter selection tool, an intelligent rule-based technique, Operational Modal Analysis (OMA) is performed in an appropriate, timeless and user-independent way. Through PolyMAX, the LMS modal parameter identification algorithm with its clear stabilization diagrams, the modal analysis process of highly damped structures and noisy data has become straightforward. This enables engineers to fine-tune the numerical model [41]. The output time series data are converted to correlations and the spectra are computed as the Fourier transforms of the positive time lags of the correlation functions [42].

1.3 DYNAMICS OF SPACECRAFT APPENDAGES

The appendages of a spacecraft consist of lightweight, flexible, deployable members in the form of solar panels, antennas, and booms. Because satellites must survive the launch and must operate in the harsh environment of space, they require unique and durable

technologies. Satellites have to carry their own power source because they cannot receive power from Earth. They must remain pointed in a specific direction, or orientation, to accomplish their mission. Satellites need to maintain proper temperature in the face of direct rays from the Sun and in the cold blackness of space.

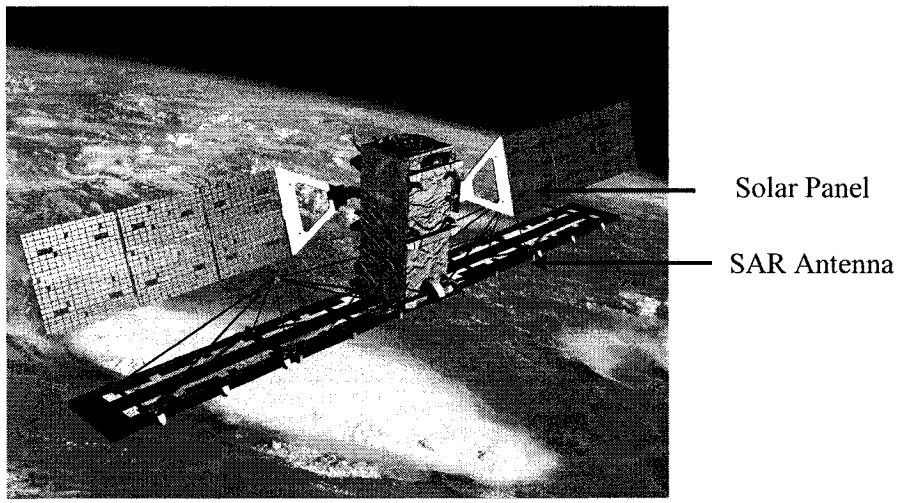

Figure 1-1: Canadian RADARSAT-2 Satellite [43]

The satellite keeps the solar panels pointed toward the Sun. Maintaining proper orientation is typically accomplished by small rocket engines, known as attitude thrusters. These thrusters/attitude controllers perform some functions such as pointing the antennas in a desired direction, pointing solar panels toward the sun, keeping sensors and sensitive equipment away from the sun's light and heat, and pointing the control jets in the desired direction to accomplish efficient maneuvers [44].

Attitude thrusters can make large changes to orientation quickly and can create significant vibration in the satellite body. They are the largest source of torque on the spacecraft. If they are used to achieve accurate pointing, the small amount of torque should be applied as consistent impulses for minimum switch-on time of several milliseconds [44, 45].

The Figure 1-2 represents the simple model of satellite during attitude control. Thrusters of front and back face provide F1 and F2 forces, respectively. The satellite body rotates due to the torque created by the forces which eventually will create vibrations.

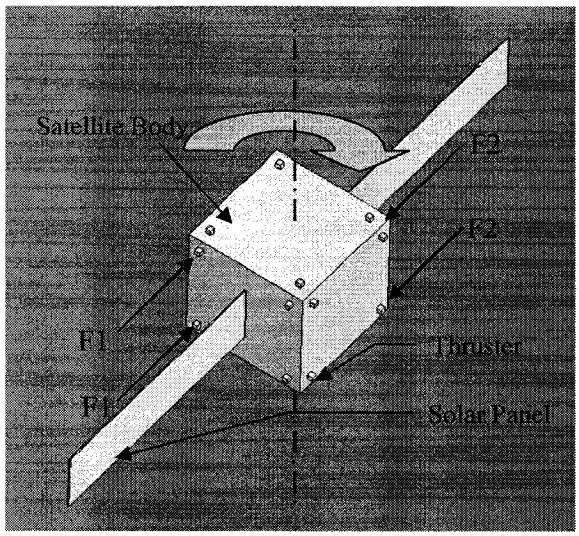

Figure 1-2: Simple model of a satellite

Spacecraft thrusters are of two basic types. There are cold-gas thrusters and hot-gas thrusters. Cold gas thrusters produce small amount of thrust, typically 5 N or less and are useful for small spacecraft and for fine attitude control, whereas the hot gas thrusters can produce thrusts as low as 0.5 N up to 9000N, but are usually used for higher thrust applications [46]. The excitation may exist for approximately 10-15 seconds including steady state thrust for 4~5 seconds.

The thruster thrust profile is shown in Figure 1-3 [46].

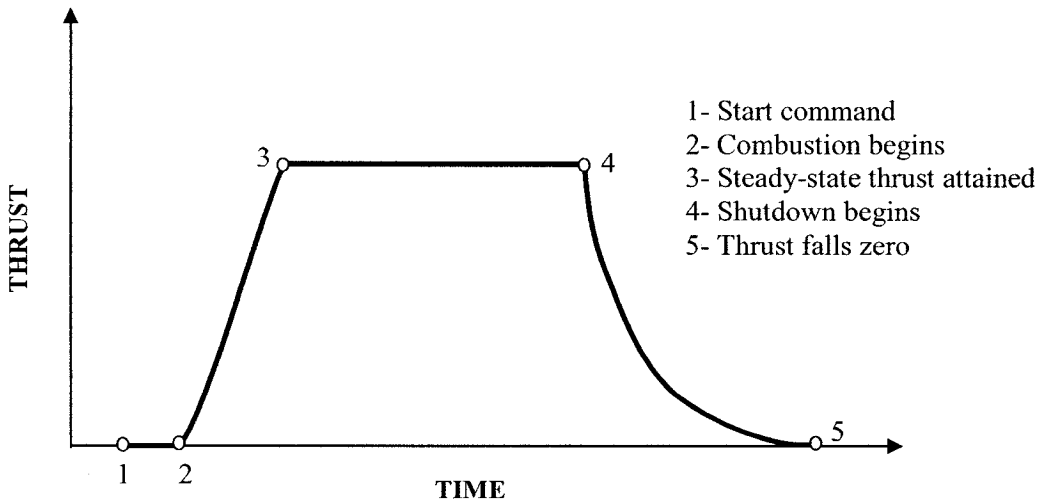

Figure 1-3: Thrust profile of a hot-gas thruster

On the other hand, exposure to the harsh space environment can cause a range of problems and challenges to spacecraft structure especially when there is a variation in both the temperature level and distribution due to solar radiation and shadowing. This may cause severe damage of the sophisticated equipments. For example, one side of satellite, exposed to sunlight in space, may be at about +150°C whereas the opposite side, in the shadow and facing the blackness of space, may be at –120°C [47]. The effects of both temperature level and temperature distribution on satellites structures are discussed in Ref. [48]. A unified finite element model had been used in thermal analysis to obtain the temperature distributions and structural analysis to give distortion results of the reflector.

The analytical investigation of the structural dynamics of a flexible solar array had been done by Vigneron et al. [49]. The analysis focused on two representative array units of Communication Technology Satellite (CTS) employed in ground-test program.

Frequencies and mode shapes were identified by (a) Rayleigh-Ritz method on a simplified continuum model and by (b) NASTRAN finite – element program. Extrapolation of modal information to on-orbit conditions have also been discussed. The formulation of complex system dynamics due to interactions between librational motion, transverse vibration, and thermal deformations has been elaborated in Ref. [50]. Also, more research has already been done on satellite structure dynamics in Ref. [51].

In this study only vibrations induced by the attitude control thrusters are considered for identification of modal parameters of the panel. Some assumptions and considerations made during design and manufacturing of the test article for experimental testing based on the above discussion are:

- The test article can be considered as linear beam or plate type of structure representative of solar panel
- It can be considered as cantilevered planar type of structure for simplicity
- The material of the test article are representative of spacecraft hardware material e.g. Aluminum
- The fundamental frequency of the test article should be 3~4 Hz and the fixtures should be rigid in this frequency range
- The analysis is considered as transient response analysis with step input loading

Based on the above considerations a test article has been designed and manufactured. The drawings of the test article along slip table configuration of the vibration testing equipment are enclosed in APPENDIX-II.

1.4 OBJECTIVES AND CONTRIBUTION OF THIS RESEARCH

The objectives of this study are twofold: (1) Investigate, for ground modal testing, the proper test procedures and the various advanced modal identification methods for processing the response data; (2) Perform a feasibility study of the applicability of the Output-Only Modal Testing for on-orbit characterization considering the type and/or location of ambient and operational excitations.

It is found that the output-only modal testing works well with randomly distributed loading condition [23], this work attempts to demonstrate the applicability of the modern output-only modal testing (e.g. EFDD, SSI and Operational PolyMAX) on satellite appendages under base rotational excitation (induced by thrusters) which is completely different environment than desired loading conditions.

The workability of these new output only approaches with response data for few seconds will also be investigated since one of the criteria for good estimation of modal parameters using output only approach is to acquire data for minimum of 500 cycles of lowest natural frequency. For instance, if the satellite appendage has the natural frequency of 3.5 Hz then it needs at least 140 seconds of response data. But from the dynamics of satellite appendages it is found that the excitation could remain for only

approximately about 4~5 seconds. The responses dies down within short period time say about 10~12 seconds. So, investigation of output-only modal testing methods and their capability to capture modal parameters with this limited number of response data is very important.

The results of the study will help to apply the output-only modal testing approach on flight hardware for the ground modal testing (with simulated on-orbit excitation on the ground) and to compare the derived modal parameters with their counterpart obtained from subsequent measurements on orbit.

1.5 THESIS ORGANIZAION

Chapter 1 explains the concepts of output-only modal testing for on-orbit applications. Literature review related to output only modal has been done. The dynamics of space appendages are studied. At the end objectives and contribution to this research have been outlined

Chapter 2 explains a brief overview of output only modal testing has been presented. This includes description of the different methods of output-only modal testing and their algorithms. This chapter also indicates the criteria to obtain better estimation of modal parameters from output only data.

Chapter 3 presents the analytical methodology to extract modal parameters from transient analysis of solar panel modeled as beam and plate type structures. Three types of

excitation methods have been used to identify the kind of excitation that the output only modal testing works best with from the comparison of results obtained.

Chapter 4 presents the experimental testing and identification of modal parameters using output-only modal testing software from the experimental data. The results are then compared with the LMS FRF based PolyMAX and LMS Operational PolyMAX results.

Chapter 5 presents the final simulation of solar panel considering the analytical and experimental study. Modal parameters of satellite appendage e.g. solar panel have been identified from transient response analysis using step-input acceleration applied at the base of the panel. Also, few nodal responses have been processed considering real satellite case scenario. The results are discussed and compared with modal parameters from modal analysis.

Chapter 6 presents the conclusions and discussion along with recommendations for the future work.

CHAPTER 2

DESCRIPTION OF OUTPUT-ONLY MODAL TESTING TECHNIQUE

2.1 INTRODUCTION

The output-only modal testing technique allows the identification of modal parameters from response data recorded under the natural (ambient or operational) conditions. This means, for instance, that if a bridge is going to be tested, the bridge traffic and normal operation need not be interrupted during the test. On the contrary, the traffic will be used as the excitation source, and the natural response of the bridge to that loading – and to other natural loads acting on the structure at the same time – will be measured and used to perform an output-only modal identification.

Similarly, it is more desirable to test spacecraft structures that are operating under normal conditions. For instance the responses from satellite appendages, due to excitation from the thrusters for attitude control, may be measured to find modal parameters using output-only identification approach.

Whenever these techniques of output-only modal identification are used instead of traditional modal identification, the basic idea is the same. Instead of exciting the structure artificially with known input force, the natural environmental excitation is used as input source. The input forces are not measured in ambient vibration testing. Instead of that the reference sensor signal is used as an "input" and the coherence functions are computed for each measurement point with respect to this reference sensor. This will not

only help in the identification of the resonances, but also the operational shapes that are not the mode shapes, but almost always correspond to them. The coherence function computed for two simultaneously recorded output signals has values close to unity near the resonance frequencies because of the high signal-to-noise ratio at these frequencies.

The main advantages of this kind of testing are [52]

- ***Structures that are impossible or difficult to be excited by externally applied forces can be tested***: In many cases, artificial inputs cannot be applied to a structure or they cannot be measured correctly due to the structure's boundary conditions or physical size, thereby making traditional modal analysis impractical.
- ***Modal model represents real operating conditions***: As the measurements are done under real operating conditions, true boundary conditions and actual force and vibration levels are guaranteed ensuring an optimal modal model. This is particularly important for non-linear structures.
- ***Testing can be done in-situ without interruption of operation and in parallel with other applications***: The structure does not have to be moved into a laboratory to do testing under controlled conditions. Costly downtime is consequently avoided. Furthermore, the test does not affect or interrupt the daily use of the structure and can even be applied in parallel with other applications.
- ***Simple and fast setup***: No shakers or hammers are used, making the physical setup very straightforward and fast. Notorious difficult aspects of traditional modal analysis such as dynamic loading from shakers and mechanical coupling between shakers and structures are no longer of concern.

- ***Accurate estimation of modal parameters:*** For estimating some modal parameters very accurately we need a very long testing time. This is not feasible performing traditional modal testing because the lab, test-rig and equipment and the structure itself will be tied-up in testing.
- ***Easier operation and maintenance:*** The output-only modal testing process can be monitored or even maintained through internet or wireless network which is not possible in traditional approach. Thus practically output-only modal testing requires less manpower.

There are different methods of output only modal testing technique, which have already been established in the civil, mechanical and aerospace industries. These include peak picking based methods including Frequency Domain Decomposition (FDD) and Enhanced Frequency Domain Decomposition (EFDD) methods and Stochastic subspace Identification (SSI) methods based on Unweighted Principal Component (UPC), Principal Component (PC) and Canonical Variate Analysis (CVA) methods. In this research these methods will be used for both analytical and experimental testing whereas the LMS Operational PolyMAX method will be used for experimental testing only.

The different methods of output-only modal testing technique are summarized in the Figure 2-1.

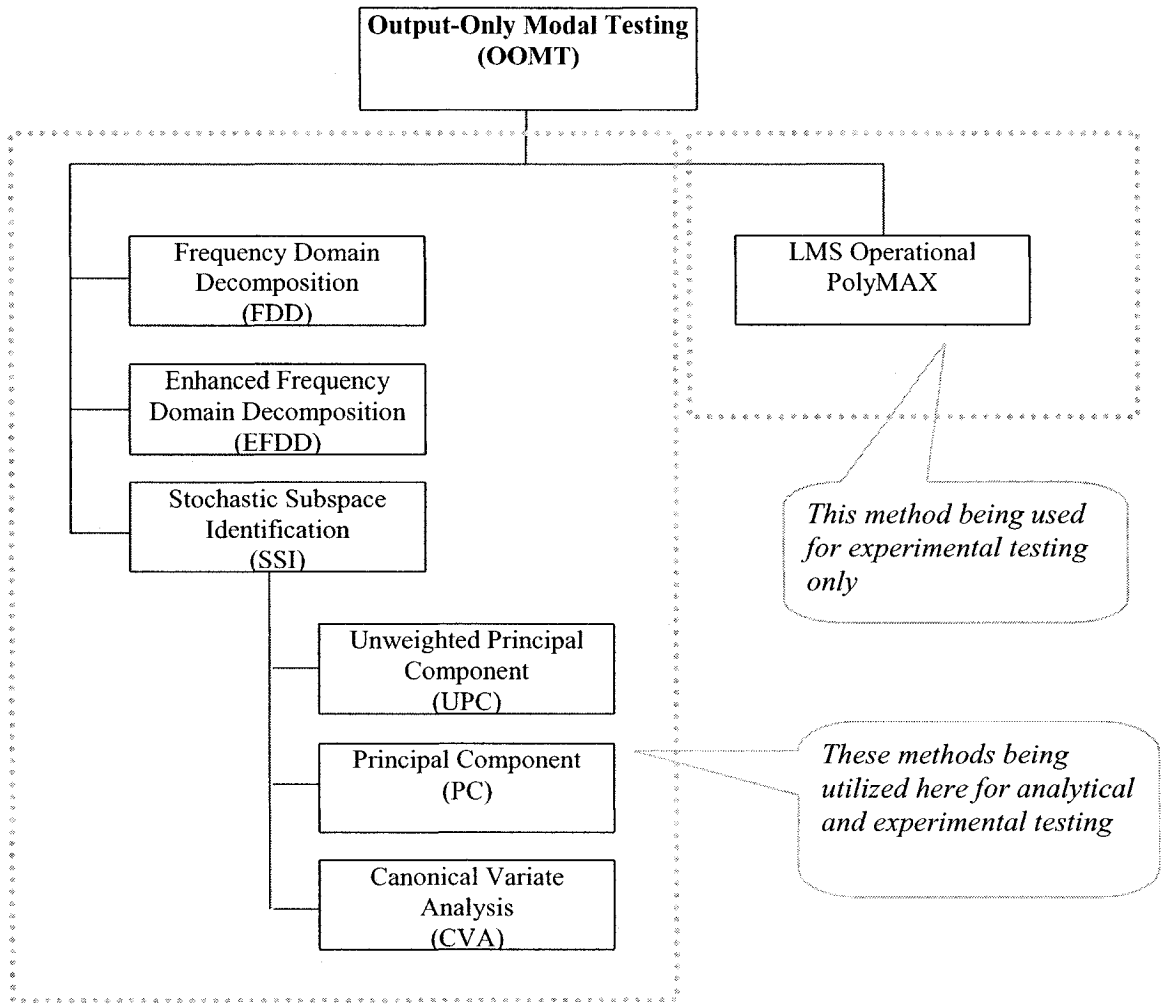

Figure 2-1: Different methods of output-only modal testing technique

2.2 OUTPUT ONLY MODAL TESTING METHODS AND THEIR ALGORITHM

2.2.1 Frequency Domain Decomposition (FDD) method

FDD is a non-parametric technique based on Singular Value Decomposition (SVD) for each frequency line of the response spectral density matrix. The singular values are interpreted as a combination of auto-power spectra for a set of Single Degree of Freedom (SDoF) systems. The physics of the structural system are obtained by looking at the plot identifying the SDoF functions and picking the peak of each function. The SDoF information (modal parameters) is then extracted from the singular values. Since information from just one single frequency line is used in this technique, natural frequencies and mode shapes are provided but no damping estimates are possible.

The relationship between the unknown inputs $x(t)$ and the measured responses $y(t)$ can be expressed as [1, 22]:

$$G_{yy}(j\omega) = \overline{H}(j\omega)G_{xx}(j\omega)H(j\omega)^T \tag{2-1}$$

where $G_{xx}(j\omega)$ is the $r \times r$ Power Spectral Density (PSD) matrix of the input, r is the number of inputs, $G_{yy}(j\omega)$ is the $m \times m$ PSD matrix of the responses. $H(j\omega)$ is the $m \times r$ Frequency Response Function (FRF) matrix, and "$\overline{(\ )}$" and superscript T denote complex conjugate and transpose, respectively.

The FRF can be written in partial fraction, i.e. pole/residue form as:

$$H(j\omega) = \sum_{k=1}^{n} \frac{R_k}{j\omega - \lambda_k} + \frac{\overline{R}_k}{j\omega - \overline{\lambda}_k} \tag{2-2}$$

where n is the number of modes, λ_k is the pole of the kth mode and R_k is the residue matrix:

$$R_k = \phi_k \gamma_k^T \tag{2-3}$$

where ϕ_k, γ_k are the mode shape vector and modal participation vector, respectively. Suppose the input is white noise i.e. PSD is constant matrix, i.e. $G_{xx}(j\omega) = C$. Then Eq. (1-1) becomes:

$$G_{yy}(j\omega) = \sum_{k=1}^{n}\sum_{s=1}^{n}\left[\frac{R_k}{j\omega - \lambda_k} + \frac{\bar{R}_k}{j\omega - \bar{\lambda}_k}\right] C \left[\frac{R_s}{j\omega - \lambda_s} + \frac{\bar{R}_s}{j\omega - \bar{\lambda}_s}\right]^H \tag{2-4}$$

where superscript H denotes complex conjugate and transpose. Multiplying the two partial fraction factors and making use of the Heaviside partial fraction theorem, after some mathematical manipulations, the output PSD can be reduced to a pole/residue form as follows:

$$G_{yy}(j\omega) = \sum_{k=1}^{n}\left[\frac{A_k}{j\omega - \lambda_k} + \frac{\bar{A}_k}{j\omega - \bar{\lambda}_k} + \frac{B_k}{-j\omega - \lambda_k} + \frac{\bar{B}_k}{-j\omega - \bar{\lambda}_k}\right] \tag{2-5}$$

where A_k is the kth residue matrix of the output PSD. As the output PSD itself, the residue matrix is an $m \times m$ complex conjugate transpose (Hermitian) matrix and is given by:

$$A_k = R_k C\left(\sum_{s=1}^{n}\frac{\bar{R}_s^T}{-\lambda_k - \bar{\lambda}_s} + \frac{R_s^T}{-\lambda_k - \lambda_s}\right) \tag{2-6}$$

The contribution to the residue from the k th mode is given by:

$$A_k = \frac{R_k C \bar{R}_k^T}{2\alpha_k} \tag{2-7}$$

where α_k is minus the real part of the pole $\lambda_k = -\alpha_k + j\omega_k$. As it appears, this term becomes dominant when the damping is light, and thus, in the case of light damping, the residue becomes proportional to the mode shape vector:

$$A_k \propto R_k C \bar{R}_k^T = \phi_k \gamma_k^T C \gamma_k \phi_k^T = d_k \phi_k \phi_k^T \tag{2-8}$$

where d_k is a scalar constant. At a certain frequency ω, only a limited number of modes will contribute significantly, typically one or two modes. Let this set of modes be denoted by $Sub(\omega)$. Thus, in case of lightly damped structure the response spectral density can always be written as:

$$G_{yy}(j\omega) = \sum_{k \in Sub(\omega)} \frac{d_k \phi_k \phi_k^T}{j\omega - \lambda_k} + \frac{\bar{d}_k \bar{\phi}_k \bar{\phi}_k^T}{j\omega - \bar{\lambda}_k} \tag{2-9}$$

Identification of Algorithm

In the Frequency Domain Decomposition (FDD) identification, the first step is to estimate the power spectral density matrix. The estimate of the output PSD, $\hat{G}_{yy}(j\omega)$, is known at discrete frequencies $\omega = \omega_i$ and then decomposed by taking the Singular Value Decomposition (SVD) of the matrix as:

$$\hat{G}_{yy}(j\omega_i) = U_i S_i U_i^H \tag{2-10}$$

where the matrix $U_i = [u_{i1}, u_{i2}, \cdots, u_{im}]$ is a unitary matrix holding singular vectors u_{ij}, and S_i is a diagonal matrix holding the scalar singular values s_{ij}. Near a peak corresponding to the k th mode in the spectrum, if only the k th mode is dominating, there

will only be one term in Eq. (2-9). Thus, in this case the first singular vector u_{i1} is an estimate of mode shape:

$$\hat{\phi} = u_{i1} \tag{2-11}$$

and the corresponding singular value is the auto power spectral density function of the corresponding SDoF system. This power spectral density function is defined around the peak by comparing the mode shape estimate $\hat{\phi}$ with the singular vectors for the frequency lines around the peak.

2.2.2 Enhanced Frequency Domain Decomposition (EFDD) method

The FDD is generally a good approach to estimate natural frequencies and mode shapes but cannot be used to identify the modal damping. The EFDD provides the modal damping and also a better estimation of other modal parameters (natural frequencies and mode shapes). Damping and improved natural frequencies are estimated from the corresponding SDoF normalized auto-correlation functions in the time domain.

It performs a detailed analysis in the neighborhood of a natural frequency identified by the FDD, by means of a suitable use of the Modal Assurance Criterion (MAC) that identifies, for each mode, a single degree of freedom spectral density of the response and puts zero on the rest of the response. In this way the spectral response of a single degree of freedom is obtained so that it can be transformed back to the time domain where damping and improved natural frequencies are estimated from the corresponding SDOF normalized auto-correlation functions.

A suitable frequency interval for the analysis of each single mode, identified by the FDD, is determined by using an appropriate MAC threshold value. In the neighborhood of a picked frequency corresponding to an FDD identified mode shape, a MAC is computed between the reference vector and the singular vectors in the selected range. If the largest MAC value of this vector is above the threshold MAC value, the corresponding singular value is considered in the response of that modal coordinate, while the others are put to zero. To improve the modes estimate, the singular vectors are weighted by the MAC values determined above. At this point damping and natural frequency of that mode are estimated by inverse transformation of the single DoF spectra into the time domain, which provides a single DoF correlation function, by a simple regression analysis. This correlation function is an almost damped harmonic response. The natural frequency can be estimated from the logarithmic decrement of this damped signal.

2.2.3 Sub-Space Identification (SSI) method

SSI technique is more modern approach than frequency domain approach. Basically these techniques are doing the same thing as the normal time domain techniques do. With this modern approach the Ibrahim Time Domain (ITD) developed by Ibrahim and Milkulcik [2], Polyreference developed by Vold et al. [5] and Eigen Realization Algorithm (ERA) developed by Juang and Pappa [7] are included a noise model that is believed to reduce the necessary number of noise modes. This might be important especially in cases with many data sets where the problem of pole pairing between data sets (a certain mode must be visible in all data sets) might become significant. Three different implementation of Stochastic Subspace Identification technique are:

- *Unweighted Principal Component (UPC)*
- *Principal Component (PC)*
- *Canonical Variate Analysis (CVA)*

In SSI, all these techniques use the same estimation-engine for estimation of state space realizations (models). In general, the input to this engine is a weighted version of the so-called Common SSI Input matrix that consists of compressed time series data. The difference between the three Stochastic Subspace Identification techniques is basically how this matrix is weighted.

The Unweighted Principal Component algorithm is the simplest one as no weighting is applied. Thus the input of the estimation engine is the Common SSI Input matrix itself. This algorithm works best with data having modes with comparable energy level. In such cases it will produce good results using reasonable small state dimensions. The algorithm is also named as Numerical algorithm for Subspace state space system IDentification (N4SID).

In Principal Component (PC) technique, the algorithm works in the same way as algorithm for Unweighted Principal Component (UPC) but the way the weighting function is used, is different from the UPC. This algorithm also gives best results with modes and comparable energy level whereas Canonical Variate analysis (CVA) technique has the ability to estimate modes with larger difference in energy level. That is why it can use a larger state space dimension. In order to see low excited modes among well-excited

modes, it is necessary to force a large state space dimension. So for low excited modes the CVA would be better choice. If the data is only with well-excited modes then the Unweighted Principal Component or Principal Component algorithm can be the best choice. The mathematical formulations are briefly discussed here. For more detailed information, one can refer to Ref. [20].

The continuous structure may be discretized into appropriate finite elements using finite element technique and subsequently the governing differential equation can be cast to the following form:

$$M\ddot{U}(t) + C\dot{U}(t) + KU(t) = e(t) \tag{2-12}$$

where M, C and K are the $n \times n$ time-invariant mass, damping and stiffness matrices respectively; $U(t), \dot{U}(t), \ddot{U}(t)$ are $n \times 1$ vectors of displacement, velocity and acceleration and $e(t)$ is an $n \times 1$ vector of external excitation for a system with n degrees of freedom. The eigenvalue problem associated with Eq. (2-12) is given by

$$(\lambda_i^2 M + \lambda_i C + K)\Phi_i = 0, \qquad i = 1, 2, \cdots, 2n \tag{2-13}$$

where λ_i and Φ_i are the eigenvalues and eigenvectors, respectively. They can be real or complex. In the later case they occur in pairs of complex conjugates and the eigenvalues can be expressed as [20]:

$$\lambda_q = -\eta_q \omega_q \pm j\omega_q \sqrt{1 - \eta_q^2} \qquad q = 1, 2, \cdots, n \tag{2-14}$$

where ω_q is the natural frequency (rad/s) of the dynamic system; η_q is its damping ratio and j represents the imaginary unit. The goal is to identify the eigenvalues and eigenvectors of the Eq. (2-13) using response measurements in time domain.

Let $y(t)$ be the observation of degrees of freedom of system; $y(t)$ is a $p \times 1$ vector of measurement and is described by:

$$y(t) = L_{ij} U(t) \tag{2-15}$$

where L_{ij} is equal to one if sensor i observes the degrees of freedom j, and zero otherwise. It is noted that L is $p \times n$ matrix. Eq. (2-12) can be rewritten as a first-order system of differential equations in a number of ways. One commonly used reformulation is a state-space representation as:

$$\dot{x}(t) = Ax(t) + B e(t) \tag{2-16}$$

$$y(t) = Hx(t) \tag{2-17}$$

where $H = [L \quad 0]$ is a $p \times 2n$ matrices and matrices A, B and state vector $x(t)$ are describes as:

$$A = \begin{bmatrix} 0 & I \\ -M^{-1}K & -M^{-1}C \end{bmatrix}, \quad B = \begin{bmatrix} K & 0 \\ 0 & -M \end{bmatrix}^{-1}, \quad x(t) = \begin{bmatrix} U(t) \\ \dot{U}(t) \end{bmatrix} \tag{2-18}$$

where A is a $2n \times 2n$ matrix called the system matrix and B is a $2n \times n$ input matrix. In the case of time-equally spaced sampling, with Δt as constant sampling interval, the discrete time form state-space model [16, 19, 53] is:

$$x_{k+1} = Fx_k + Ge_k \tag{2-19}$$

$$y_k = Hx_k \tag{2-20}$$

where $F(t) = \exp(A\Delta t)$ and is a $2n \times 2n$ matrix which is called the state transition matrix of the linear dynamic structure and $G = \int_0^{\Delta t} \exp(A\tau) B d\tau = (F - I) A^{-1} B$.

The eigenvalues μ_i and eigenvectors Ψ_i of the state transition matrix F are related to the modal characteristics of the vibrating system [16, 53] as:

$$\mu_i = \exp(\lambda_i \Delta t) \text{ and } H\Psi = L\Phi \tag{2-21}$$

where the matrix Ψ contains the eigenvectors Ψ_i and the matrix Φ contains the eigenvectors Φ_i. The eigen-structure of the state transition matrix F contains all the vibrating characteristics of the mechanical structure and identifying the set of pairs $(\mu, H\Psi)$, from output-only measurements, is equivalent to the same task for the set of $(\lambda, L\Phi)$ given by Eq. (2-13). Therefore the global modal parameters for the qth mode can be determined by:

$$\omega_q = \frac{1}{2\Delta t}\sqrt{\left[\ln(\mu_q \mu_q^*)\right]^2 + 4\left[\cos^{-1}\left(\frac{\mu_q + \mu_q^*}{2\sqrt{\mu_q \mu_q^*}}\right)\right]^2} \tag{2-22}$$

$$\eta_q = \sqrt{\frac{\left[\ln(\mu_q \mu_q^*)\right]^2}{\left[\ln(\mu_q \mu_q^*)\right]^2 + 4\left[\cos^{-1}\left(\frac{\mu_q + \mu_q^*}{2\sqrt{\mu_q \mu_q^*}}\right)\right]^2}} \tag{2-23}$$

where μ_q and μ_q^* are the pair of complex conjugate roots. Our purpose is to obtain the modal parameters of a vibrating system, from the discrete observation data $y(k)$, which is measured.

2.2.4 LMS Operational PolyMAX method:

Frequency-domain Operational Modal Analysis methods, such as PolyMAX require output spectra as primary data [54]. Under the assumption of white noise input, output

spectra can be modeled in a very similar way as FRFs. The modal decomposition of an FRF matrix is [35] as:

$$[H(\omega)] = \sum_{i=1}^{n} \frac{\{v_i\} < l_i^T >}{j\omega - \lambda_i} + \frac{\{v_i^*\} < l_i^H >}{j\omega - \lambda_i^*} \tag{2-24}$$

where n is the number of modes; $\bullet^*$ is the complex conjugate of a matrix; $\bullet^H$ is the complex conjugate transpose (Hermitian) of a matrix; $\{v_i^l\} \in C^m$ are the mode shapes and $< l_i^T >$ modal participation factors and λ_i are the poles, which occur in complex-conjugate pairs and are related to the eigenfrequencies ω_i and damping ratio ξ_i as follows:

$$\lambda_i, \lambda_i^* = -\xi_i \omega_i \pm \sqrt{1-\xi_i^2}\,\omega_i \tag{2-25}$$

The input spectra $[S_{uu}] \in C^{m \times m}$ and output spectra $[S_{yy}] \in C^{l \times l}$ of a system represented by the FRF matrix $[H(\omega)]$ are related as:

$$[S_{yy}] = [H(\omega)][S_{uu}][H(\omega)]^H \tag{2-26}$$

In case of operational data the output spectra are the only available information. The deterministic knowledge of the input is replaced by the assumption that the input is white noise. A property of white noise is that it has a constant power spectrum. Hence $[S_{uu}]$ is independent of the frequency in Eq. (2-26). The modal decomposition of the output spectrum matrix is obtained by inserting Eq. (2-24) into Eq. (2-26) and converting to the partial fraction form [42, 55, 56] as:

$$[S_{yy}(\omega)] = \sum_{i=1}^{n} \frac{\{v_i\} < g_i >}{j\omega - \lambda_i} + \frac{\{v_i^*\} < g_i^* >}{j\omega - \lambda_i^*} + \frac{\{g_i\} < v_i >}{-j\omega - \lambda_i} + \frac{\{g_i^*\} < v_i^* >}{-j\omega - \lambda_i^*} \tag{2-27}$$

where $< g_i > \in C^l$ are the so-called operational reference factors, which replace the modal participation factors in cases where only output data are available. Their physical interpretation is less obvious as they are a function of all modal parameters of the system and the constant input spectrum matrix. Note that the order of the power spectrum model is twice the order of the FRF model. The goal of Operational Modal Analysis is to identify the right hand side terms in Eq. (2-27) based on the measured output data pre-processed into output spectra, which is mentioned in the next section.

Pre-processing operational data

Power spectra are defined as the Fourier Transform of the correlation sequences. The most popular non-parametric spectrum estimate is the so-called *weighted averaged periodogram* (also known as *modified Welch's periodogram*). Weighting means that the signal is weighted by one of the classical windows, (Hanning, Hamming, ...) to reduce leakage. Welch's method start with computing Discrete Fourier Transform (DFT) of the weighted outputs as:

$$Y(\omega) = \sum_{k=0}^{N-1} w_k y_k \exp(-j\omega k\Delta t) \tag{2-28}$$

where w_k denotes the time window. An unbiased estimate of the spectrum is the weighted periodogram as:

$$S_{yy}^{(i)}(\omega) = \frac{1}{\sum_{k=0}^{N-1} |w_k|^2} Y(\omega) Y^H(\omega) \tag{2-29}$$

The variance of the estimate is reduced by splitting the signal in possibly overlapping segments, computing the weighted periodogram of all segments and taking the average

$$S_{yy}(\omega) = \frac{1}{P}\sum_{i=1}^{P} S_{yy}^{(i)}(\omega) \tag{2-30}$$

where P is the number of segments and superindex i denotes the segment index. Another non-parametric spectrum estimate is the so-called *weighted correlogram.* It will be shown that this estimate has some specific advantages in a modal analysis context. First the correlations have to be estimated as:

$$R_i = \frac{1}{N}\sum_{k=0}^{N-1} y_{k+i} y_k^T \tag{2-31}$$

High-speed (FFT-based) implementation exists to compute the correlations as in Eq. (2-31) [57]. The weighted correlogram is the DFT of the weighted estimated correlation sequence

$$S_{yy}(\omega) = \sum_{k=-Q}^{Q} w_k R_k \exp(-j\omega k\Delta t) \tag{2-32}$$

where Q is the maximum number of time lags at which the correlations are estimated. This number is typically much smaller than the number of the data samples to avoid the greater statistical variance associated with the higher lags of the correlation estimates. In the modal analysis context, the weighted correlogram has the following advantages

- It is sufficient to compute the so-called *half spectra* which are obtained by using only the correlations having a positive time lag in Eq. (2-32):

$$S_{yy}^{+}(\omega) = \frac{w_0 R_0}{2} + \sum_{k=1}^{Q} w_k R_k \exp(-j\omega k\Delta t) \tag{2-33}$$

  The relation between the half spectra in Eq. (2-33) and the full spectra in Eq. (1-32) is the following:

$$S_{yy}(\omega) = S_{yy}^{+}(\omega) + \left(S_{yy}^{+}(\omega)\right)^H \tag{2-34}$$

It can be shown [42, 58] that the modal decomposition of these half spectra only consists of the first two terms in Eq. (2-27):

$$\left[S^{+}_{yy}(j\omega)\right] = \sum_{i=1}^{n} \frac{\{v_i\} < g_i >}{j\omega - \lambda_i} + \frac{\{v_i^*\} < g_i^* >}{j\omega - \lambda_i^*} \tag{2-35}$$

The advantage in modal analysis is that models of lower order can be fitted without affecting the quality.

- Under the white noise input assumption, the output correlations are equivalent to impulse responses. Thus just like in an impact testing, it seems logical to apply an exponential window to the correlations before computing the DFT. The exponential window reduces the effect of leakage and the influence of the higher time lags, which have a larger variance. Moreover, the application of an exponential window to impulse responses or correlations is compatible with the modal model and the pole estimates can be corrected. This is not the case when a Hanning window is used: such a window always leads to biased damping estimation.

2.3 CRITERIA FOR BETTER ESTIMATION OF MODAL PARAMETERS

The operational (output-only) modal analysis is typically used in cases where the excitation is relatively broad-banded. It can also be used in cases involving rotating machinery if broadband noise from bearings or other excitation forces is present. Similarly, it can be used for measurements on rotating machinery performing run-up / down tests.

For the output-only modal testing, we just need to make sure that the loading is reasonably random in time and space. In output-only testing, there are two main rules to be followed: Multiple input load and good quality and quantity of data.

One way to identify the multiple input loads is to perform singular value decomposition of the spectral matrix of the measured data and plot the singular values as a function of frequency. If a family of singular values is observed, this is a good indication that multiple loading is exciting the structure. If the excitation is single input, then only one singular value curve will be significant, and all the other singular values will be close to zero mainly describing noise in the data. The second rule is to get good quantity of data. To make sure that there is good amount of data, we can use the following simple rule of thumb. The correlation time for a certain mode can be defined as $(\varsigma_k \omega_k)^{-1}$ [23]. This means that the data segments should at least have that length to reasonably suppress the influence of leakage. If we consider 100 averages then the minimum duration of the continuous measurement should be

$$T = \max\left\{\frac{100}{\varsigma_k \omega_k}\right\} \tag{2-36}$$

One of the reasons why output-only modal testing had very little appeal to engineers in the past is that the principles of good testing were not well understood, and erroneous testing procedures were adopted in many projects, leading to severe problems in the identification phase.

It is not only necessary to have good quality and quantity of data but also to have good equipment, experience and good planning while measuring the data for better estimation of modal parameters. Some guidelines are given here [59]:

- ***Measured Degrees-Of-Freedoms (Measurement Points):*** It is necessary to decide at how many points one wants to know the mode shapes, i.e. the spatial resolution of the mode. For simple structures it might be just 5-10 points, for complex structures it might be 100-200 points. If there are no closely spaced modes and we are not interested in the mode shapes, but only in the natural frequencies and the damping, we can do with only one measurement point.

- ***Data Sets (Setups):*** We should decide how to distribute the many measurement points in groups, the so-called data sets or setups. Typically, a smaller set of transducers or accelerometers, like 8, 12 or 16, are used to estimate mode shapes. In theory, only one accelerometer need to be kept at the same location (the reference point) where others can be moved until the time series from all the measurement points are obtained. However, in practice, one would normally use two or three reference points between data, in order to reduce adverse effects of errors or noise in a single data set.

- ***Reference Points:*** The reference points are the measurement points that are common in all data sets. The main rule is, that the reference points should be placed in such a way, that all modes contribute well to the response signal at

the reference points. If close modes are expected, it is necessary to have these modes well represented in the reference signals.

- ***Data Acquisition:*** We need to decide first how to filter and how many data points are needed in the time series. A good rule is to sample a little higher than is needed and then decimate the signal afterwards. However, a rule of thumb is to collect sample points, at least, corresponding to 500 cycles of the lowest expected natural frequency. This is when the data is totally noise-free and when there is no close mode. In most cases it is necessary to take time series corresponding to say 1000 cycles or more of the lowest natural frequency.

2.4 OUTPUT ONLY DATA PROCESSING

Operation modal analysis module of B&K PULSE software works on the response data in time domain whereas LMS Operational PolyMAX works on the cross power spectrum directly or on time domain throughput file. So data need to be recorded either in time domain or preprocessed to identify the cross power spectrum.

For PULSE, there are two types of files needed in standard format so-called universal file format to perform the modal parameters estimation from output data. One is the configuration file which contains the test article and set-up configuration information including, number of nodes, number of elements, lines, surfaces, sampling interval, reference node, and direction of response measured, whereas the other one is the data file

which contains the response data in time domain. These two types are required to be in either Universal File Format (UFF) or Structural Vibration Solutions (SVS) ASCII format and can be edited using MATLAB or any other ASCII file editor. To generate these kinds of files some Matlab codes are developed and enclosed in APPENDIX-I. Once these files are ready then they can be fed-into the PULSE software for modal parameters identification using different methods i.e. FDD, EFDD and SSI.

The cross power spectrum in frequency domain generated by the LMS spectrum analysis (data acquisition) module can be used in Operation PolyMAX to identify the modal parameters.

2.5 ADVANTAGES AND LIMITATIONS OF OUTPUT ONLY MODAL TESTING METHODS

The output-only frequency domain methods (e.g. FDD and EFDD) have been widely used for a long time and have been proved to be efficient in many cases. However, there are some limitations with these methods in dealing with the heavy damping and closely spaced modes. If a structure has very closely spaced modes or very heavy damping, these frequency domain methods would not identify accurate modal parameters. The reason for the limitation is essentially modal interference and hence some individual modes and natural frequencies cannot be observed. While, the time domain techniques (e.g. SSI-UPC, SSI-PC and SSI-CVA) use all response data available and fit them in the time domain. The assumption for these advanced time-domain methods is that the input to the

structure model is a stationary force signal that can be approximated by filtered, zero-mean, Gaussian white-noise.

2.6 SUMMARY

In this chapter a brief overview of output only modal testing has been presented. The algorithms of the output-only modal testing techniques including data processing techniques have been illustrated. This chapter also indicates the guidelines to obtain better estimation of modal parameters. At the end the advantages and limitations of output only modal testing technique have been described.

In the next chapter the analytical study of modal parameters extraction using output-only modal testing techniques are presented.

CHAPTER 3

ANALYTICAL STUDY OF MODAL PARAMETERS EXTRACTION USING OUTPUT-ONLY MODAL TESTING

3.1 INTRODUCTION

As stated in the Chapter 1 and 2, output only modal testing technique is quite convenient to identify the modal parameters of satellite appendages under space environmental conditions. These satellite appendages can be modeled as simple beam or plate type of structures. In this chapter, modal parameters of these satellite appendages modeled as beam or plate model are identified first using simple modal analysis. Then, with the random input excitation approach, modal parameters are extracted using output only modal testing technique from the finite element transient response data for both beam and plate models. The objective for this analytical study is to investigate output-only modal testing techniques and to conduct the experimental testing more effectively. It has been evaluated analytically from the performance of output only modal testing under different excitations condition that will exist in the experiment. The results have been presented and compared with the modal parameters obtained from modal analysis.

3.2. MODAL ANALYSIS OF SIMPLE STRUCTURES

3.2.1 Modal analysis of beam and plate models

Modal analysis of beam and plate models is presented here for two main reasons. First to identify the modal parameters of the beam and plate models and second is to evaluate the finite element modeling, which will be used for dynamic transient response analysis.

a) Cantilever beam

The bending natural frequencies of a cantilever beam can generally be expressed in the following form [60]:

$$f_i = \frac{\lambda_i^2}{2\pi a^2}\sqrt{\frac{EI}{m}} \qquad i = 1, 2, 3\ldots \tag{3-1}$$

where EI is the bending rigidity of the beam and m is the mass per unit length. The properties and dimensions of the beam studied are presented in Table 3-1 to identify the natural frequencies of the beam.

Table 3-1: Properties of beam and its dimensions

Material type	Aluminum 6061-T6
Modulus of Elasticity, E	$68.7\times10^{9}\ N/m^2$
Length of the beam, a	$1.22\ m$
Width of the beam, b	$0.3048\ m$
Thickness of the beam, h	$0.00635\ m$
Density, ρ	$2.71\times10^{3}\ kg/m^3$
Area moment of inertia, I	$0.65\times10^{-8}\ m^4$

Using Eq. (3-1), the natural frequencies of the beam with material and geometric characteristics given in Table 3-1 are presented in Table 3-2.

Table 3-2: Analytical bending natural frequencies of cantilever beam

Index	Dimensionless Parameter, λ_i	Natural frequencies, (Hz)
1	1.8751	3.46
2	4.6941	21.73
3	7.8548	60.83
4	10.9955	119.20
5	14.1372	197.06
6	17.27879	294.38

b) Cantilever plate

Similarly, the natural frequencies of the cantilever rectangular plate can be written as [60-63]

$$f_{ij} = \frac{\lambda_{ij}^2}{2\pi a^2}\sqrt{\frac{Eh^3}{12\gamma(1-\nu^2)}}; \qquad i = 1, 2, 3\ldots \ and \ j = 1, 2, 3\ldots \tag{3-2}$$

where i is the number of half-waves in mode shape along horizontal axis, j is the number of half-waves in mode shape in vertical axis, and γ is the mass per unit cross-sectional area . The cantilever beam studied before is now modeled as plate. The properties and dimensions of the plate studied are presented in Table 3-3 to identify the natural frequencies of the plate.

Table 3-3: Properties of plate and its dimensions

Material type	Aluminum 6061-T6
Modulus of Elasticity, E	$68.7\times10^9\ N/m^2$
Length of the beam, a	1.22 m
Width of the beam, b	0.3048 m
Thickness of the beam, h	0.00635 m
Density, ρ	$2.71\times10^3\ kg/m^3$
Poisson's ratio, ν	0.3

The identified bending natural frequencies are provided in Table 3-4. A general closed-form solution does not exist for the vibration of a rectangular plate. The approximate natural frequencies can be expected to be 5% of the exact solution. The Table 3-4 represents the upper and lower bounds of the natural frequencies for the first five modes. The natural frequencies lie in between these two bounds when the model is considered as a beam.

Table 3-4: Upper and lower bound of bending natural frequencies of plate

Aspect Ratio, $\frac{a}{b}=4$	Dimensionless Frequency Parameter, λ_{ij}^2		Natural Frequencies (Hz)	
	Lower bounds	Upper bounds	Lower bounds	Upper bounds
1	3.3306	3.4332	3.44	3.55
2	20.822	21.475	21.53	22.20
3	58.356	60.292	60.34	62.34
4	114.57	118.59	118.46	122.62
5	189.63	196.62	196.08	203.30

3.2.2 Modal analysis using finite element software

a) Natural frequencies and mode shapes of the cantilever beam

Modal parameters of cantilever beam model (using 10 beam elements) have been obtained using finite element software NASTRAN [64] with the dimensions that are used in the previous section (Table 3-4) in order to compare the results. The results are presented in Table 3-5.

Table 3-5: Natural frequencies of cantilever beam using NASTRAN

Mode	Natural frequencies, (Hz)
1	3.462
2	21.69
3	60.74
4	119.09
5	197.12
6	295.22

Corresponding mode shapes originated from NASTRAN are represented in Figure 3-1.

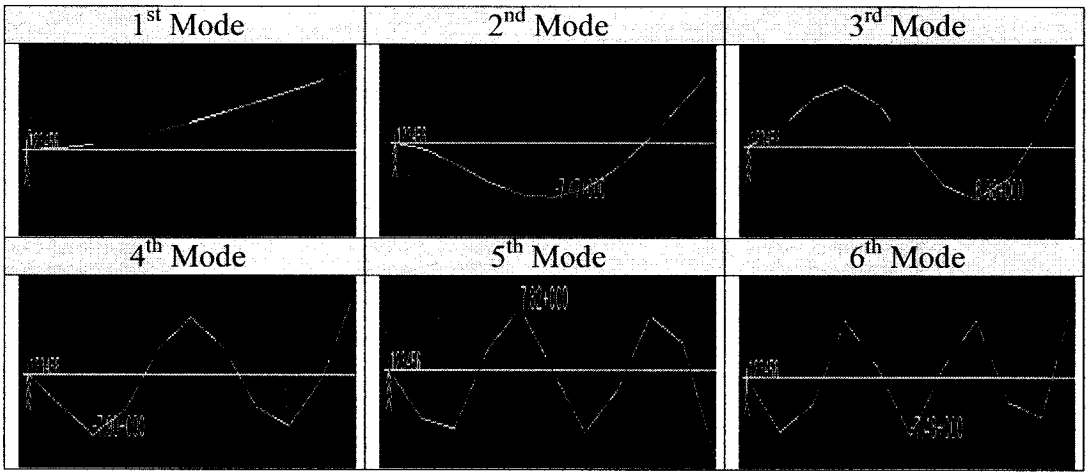

Figure 3-1: First six modes of cantilever beam from NASTRAN

Table 3-6 presents a comparison of natural frequencies for the beam model for two modal analysis approaches.

Table 3-6: Comparison of natural frequencies of the cantilever beam

Mode	Nat. Freq. (Hz) (Analytical modal analysis)	Nat. Freq. (Hz) (NASTRAN modal analysis)
1	3.46	3.462
2	21.73	21.69
3	60.83	60.74
4	119.20	119.09
5	197.06	197.12
6	294.38	295.22

Based on the presented results it can be concluded that the natural frequencies obtained from finite element model are in excellent agreement with those obtained analytically. Since the beam modeling is validated, NASTRAN results can be considered as the base modal parameters to be compared with analytical output only modal testing for cantilever beam model.

b) Natural frequencies and mode shapes of the cantilever plate

Similarly, modal parameters of cantilever plate model (with 760 bending panel elements) have been obtained using finite element software NASTRAN with the dimensions that are used in the previous section (Table 3-3) in order to compare the results. The results are given in Table 3-7. The reason for considering a plate model in this analysis is to find the effect of output only modal testing technique in some torsional mode as well.

Table 3-7: Natural frequencies of the cantilever plate

Index	Natural frequencies, (Hz)	Mode category
1	3.51	1st bending
2	22.00	2nd bending
3	28.33	1st torsion
4	61.90	3rd bending
5	87.52	2nd torsion
6	122.12	4th bending
7	203.29	5th bending

The first six modes originated from NASTRAN are shown in Figure 3-2.

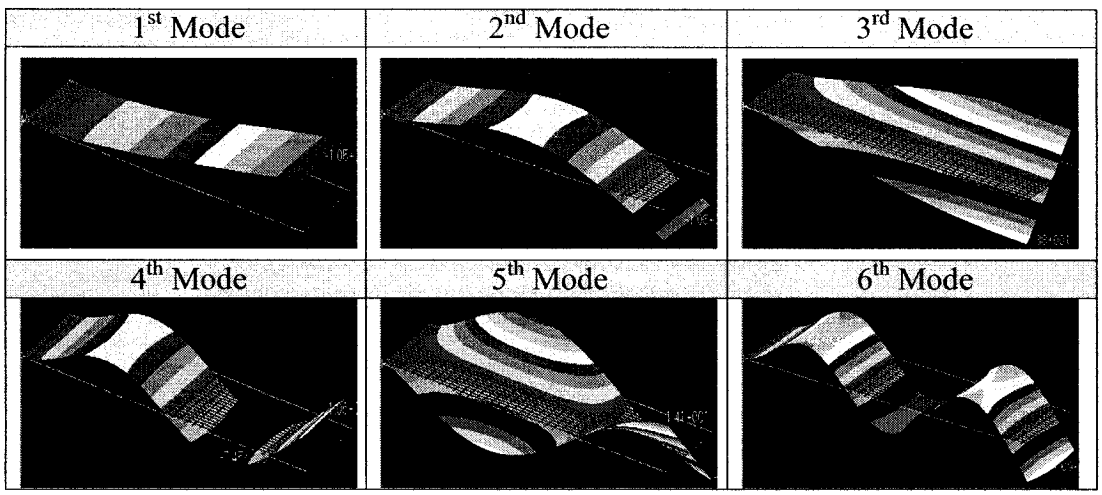

Figure 3-2: First six mode shapes of cantilever plate from NASTRAN

The effect of different number of elements on the natural frequencies is given in Table 3-8.

Table 3-8 Frequencies of cantilever plate with different number of elements

Index	Nat. Freq. (Hz) [No. of Elements=16]	Nat. Freq. (Hz) [No. of Elements=40]	Nat. Freq. (Hz) [No. of Elements=180]
1	3.51	3.51	3.51
2	23.51	22.27	22.06
3	28.47	28.27	28.28
4	73.73	64.26	62.28
5	94.58	88.18	87.52
6	151.52	131.87	124.11

Comparison of natural frequencies for the plate model for two modal analysis approaches is shown in Table 3-9.

Table 3-9: Comparison of bending natural frequencies of cantilever plate

Index	Nat. Freq. (Hz) (Analytical modal analysis)		Nat. Freq. (Hz) (NASTRAN modal analysis) [No. of Elements= 760]
	Lower bounds	Upper bounds	
1	3.44	3.55	3.51
2	21.53	22.20	22.00
3	60.34	62.34	61.90
4	118.46	122.62	122.12
5	196.08	203.30	203.29

Based on the presented results we can conclude that the natural frequencies very closely agree thus validating the finite element model. It is noted that for simple analytical study we will consider a plate model with 16 elements as it provides accurate natural frequencies for the first two modes and also makes it computationally less extensive to extract nodal response on data to be used by output-only modal testing. Thus modal parameters associated with the plate model with 16 elements will be considered as the reference natural frequencies for the plate.

3.3 TRANSIENT RESPONSE ANALYSIS AND VALIDATION OF OUTPUT ONLY MODAL TESTING TECHNIQUE

3.3.1 Process description

After validating the beam and plate finite element model created in NASTRAN, the next step is to identify analytically the modal parameters using output only modal testing technique.

For this purpose, the structures have been excited with random base acceleration as it has been shown that output only modal technique works better under random type excitation in time and space. The modal parameters have been extracted using output only modal testing technique software PULSE from the response data computed from NASTRAN for random base excitation. Along with this type of excitation, two other types of (random point and multi-point) excitations that have also been used on the beam and plate models to compare the obtained modal parameters with those obtained from finite element modal analysis.

First, in order to perform the transient response analysis using NASTRAN, it is necessary to create random input fields, which can be done by MATLAB "randtool" toolbox [65].

The parameters considered to generate the random signal are given in Table 3-10.

Table 3-10: Parameters for random signal

Signal type	Random
Mean, μ	0
Time block	32 sec
Time resolution	0.00390625

The reason for considering the time block for 32 second is because in attitude control the excitation exists for only a few seconds as discussed in Chapter 1. An example of random signal generated in MATLAB is shown in Figure 3-3.

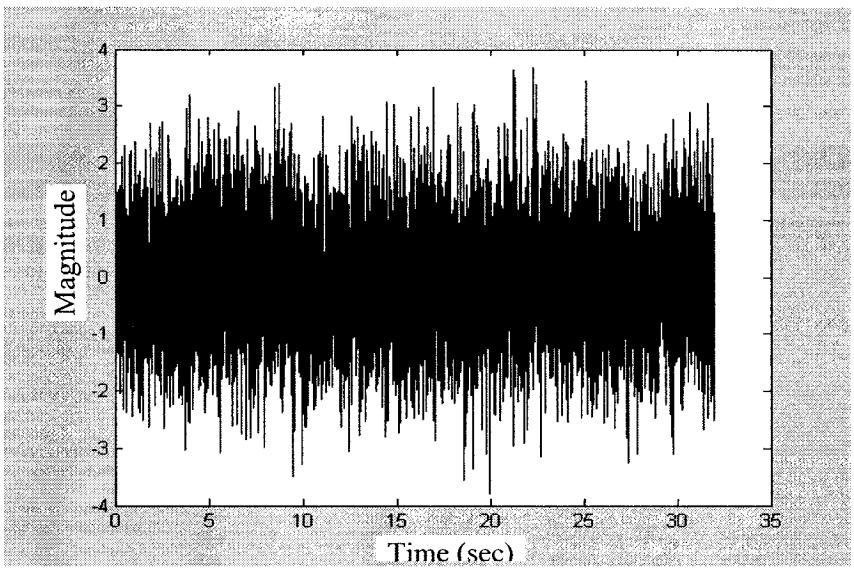

Figure 3-3: Random signal generated from MATLAB

Once the random input signal is generated, transient random response analysis is carried out using NASTRAN with different kinds of excitations, which are briefly discussed as follows:

i) Base excitation

In order to provide the base excitation, we need to restrict the motion in all the Degrees-of-Freedom (DoF) at the base except the translational DoF in the out-of-plane direction. The translational random input acceleration is applied at the base in the out-of-plane direction and is shown in Figure 3-4.

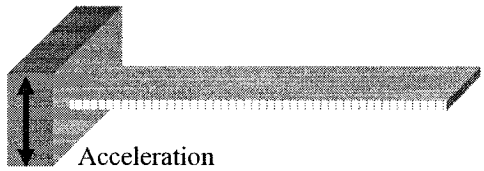

Figure 3-4: Base excitation for beam or plate

ii) Tip excitation

With the tip excitation, we need to restrict movement in all the DoF at the base. The tip excitation has to be applied at the tip as random force input as shown in Figure 3-5.

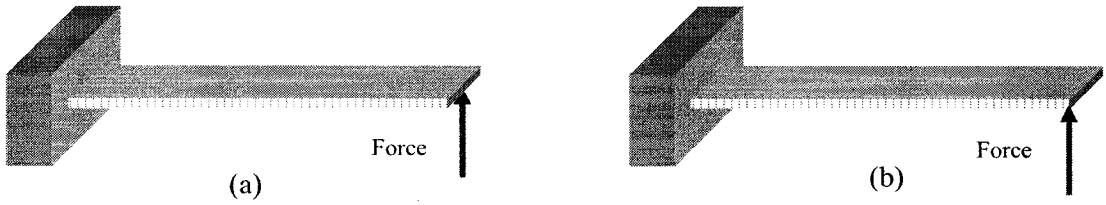

Figure 3-5: Tip excitation for (a) beam and (b) plate

iii) Multipoint excitation

With the multi-point excitation, we need to restrict movement in all the DoF at the base. The multi-point random force excitation has to be applied at several points of the structure as shown in Figure 3-6.

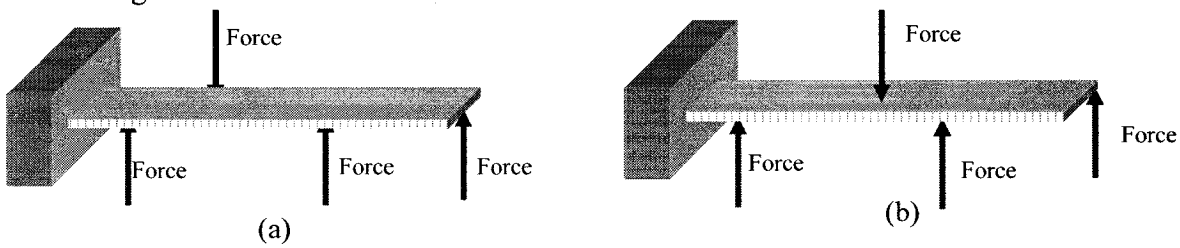

Figure 3-6: Multi-point excitation for (a) beam and (b) plate

Once the random response analysis has been done with these setups, the responses at all the nodes, in the vertical direction of beam and out-of-plane direction of plate, are recorded and converted into universal file format in order to be processed in output only modal testing PULSE software. Some sample MATLAB codes for this purpose are given in APPENDIX-I.

3.3.2 Extraction of modal parameters

Using material and geometric characteristics given in Table 3-1 and Table 3-3 for beam and plate models, respectively the transient response analysis is done using NASTRAN for base, tip and multi-point excitations. The response data from the finite element transient response analysis are divided into two parts. One is due to the free decay part and the other part is due to the forced excitation. It is found that the free decay portion of the response data set provides more stabilized modal parameters compared to the excitation portion of the response data. Thus here only free decay portion of the data set is processed. Figure 3-7 represents the sample response for plate at one of the corner tip under base excitation.

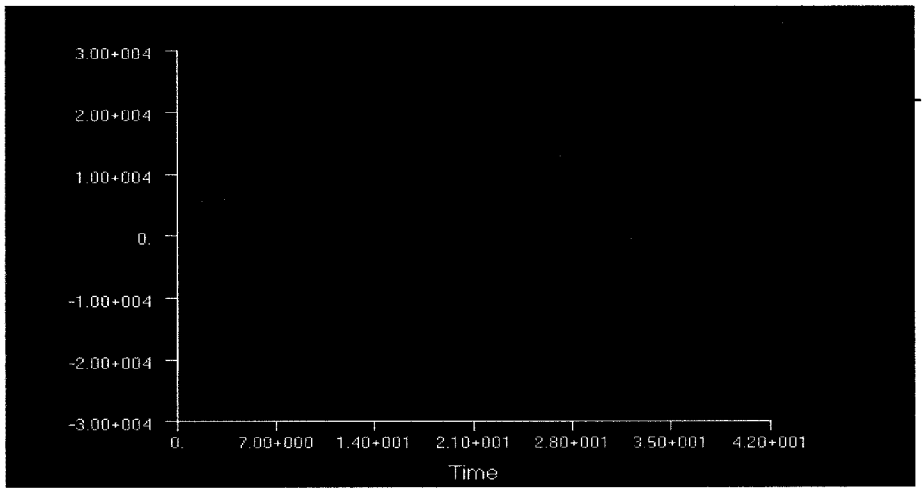

Figure 3-7: Nodal response acceleration for the plate under base excitation

Total 7 seconds of free decay data is processed for identification of modal parameters. Once the data has been processed using output only modal testing module of PULSE, the spectral density matrix of the time series data can be obtained as shown in the Figure 3-8. The figure represents the singular value curves generated from the nodal acceleration responses of 25 nodes of the plate. The solid line on the top shows the average normalized curve of all the 25 curves.

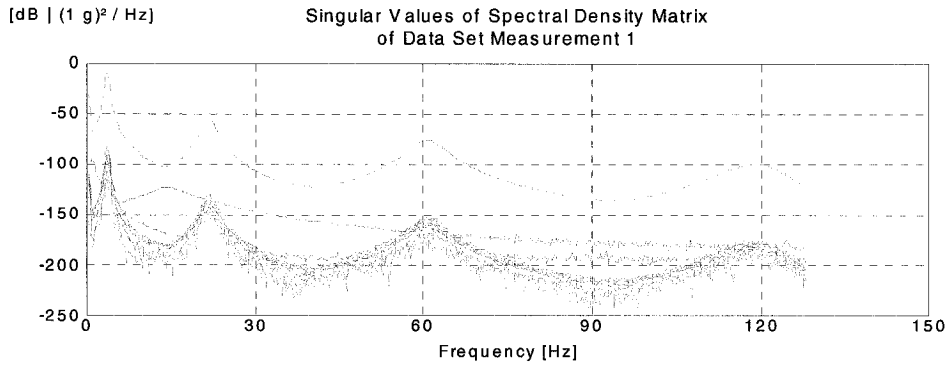

Figure 3-8: Singular values of spectral density matrix for base excitation

As we can see the curves are well defined. The average of the normalized singular values of spectral density curve could be found as a single firm line on top of the SVD lines. The peaks of the curve can be picked using FDD and EFDD window by which natural frequencies and the damping ratios can be found as shown in Figure 3-9.

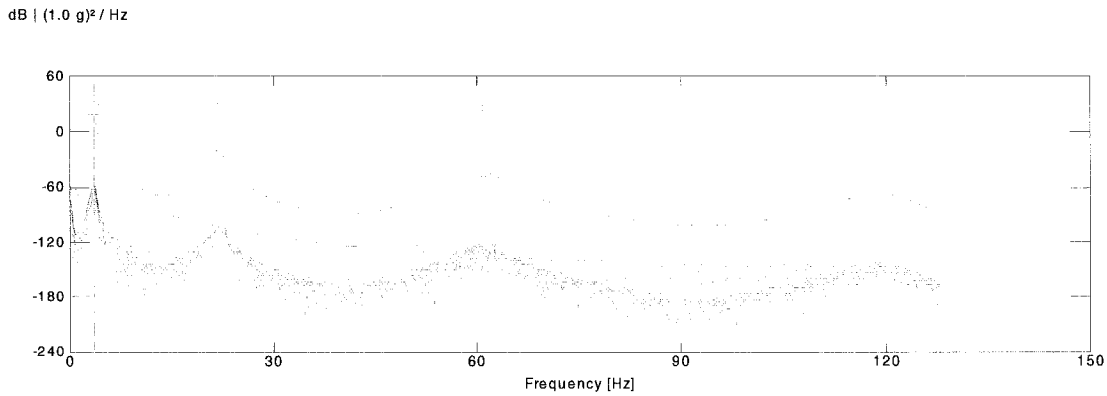

Figure 3-9: Peak picking of average normalized singular values for base excitation

Also, Figure 3-10 presents stabilized diagram of stochastic state space technique. The dark '+' represents the stabilized mode, dark '×' represent the unstabilized and the light '×' represent the noise modes. The stabilized modes can be selected and the modal parameters can be extracted. Only Principal Component window of the SSI method is presented here. The stabilization diagrams for other two SSI method i.e. Unweighted Principal Component and Canonical Variate Analysis are almost similar to Figure 3-10.

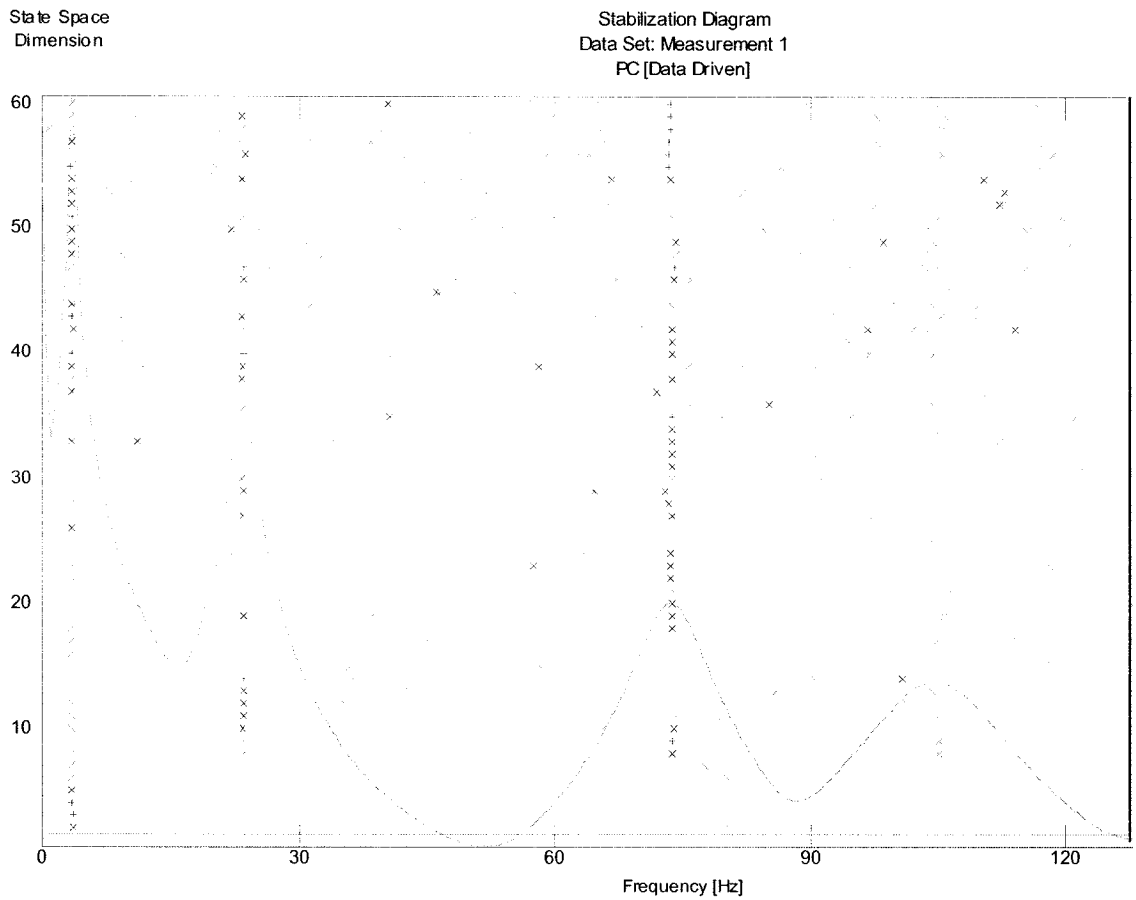

Figure 3-10: Stabilized state space diagram for base excitation

a) Modal parameters extracted for cantilever beam under base excitation using output only modal testing techniques:

The natural frequencies of the beam model for base excitaion are tabulated in Table 3-11.

Table 3-11: Natural frequencies of beam under base excitation

Mode	Output only modal testing methods					Finite element Modal analysis f (Hz)
	FDD f (Hz)	EFDD f (Hz)	SSI			
			UPC f (Hz)	PC f (Hz)	CVA f (Hz)	
1	3.5	3.47	3.46	3.46	3.46	3.46
2	21.75	21.75	21.69	21.69	21.69	21.69
3	60.75	60.72	60.74	60.74	60.74	60.74
4	119.5	118.7	119.1	119.1	119.0	119.09

As it can be realized excellent agreement exists between the extracted natural frequencies using output-only modal testing techniques and those obtained using modal analysis in NASTRAN. The extracted damping ratios are also presented in Table 3-12.

Table 3-12: Damping ratios of beam under base excitation

Mode	Output only PULSE methods					Finite element Modal analysis ξ (%)
	FDD ξ (%)	EFDD ξ (%)	SSI			
			UPC ξ (%)	PC ξ (%)	CVA ξ (%)	
1	-	5.0	5.0	5.0	4.94	5.0
2	-	4.88	5.0	5.0	5.0	5.0
3	-	4.23	5.0	4.98	4.97	5.0
4	-	3.45	5.0	4.97	5.0	5.0

As it can be seen, very good agreement exists between the damping ratios extracted from different SSI methods and those of finite element analysis. However, for EDFF method, although first mode damping ratio agrees very well with that of finite element modal

analysis, damping ratios for higher modes are not in very good with those set in finite element modal analysis. This discrepancy may be explained from the normalized curve. Figure 3-11 represents the normalized correlation based on time lag for the 1st mode for MAC value 0.8. By changing the ranges of the MAC values, the damping can be adjusted so that the straight line shown in the Figure 3-12 becomes in-line with curve.

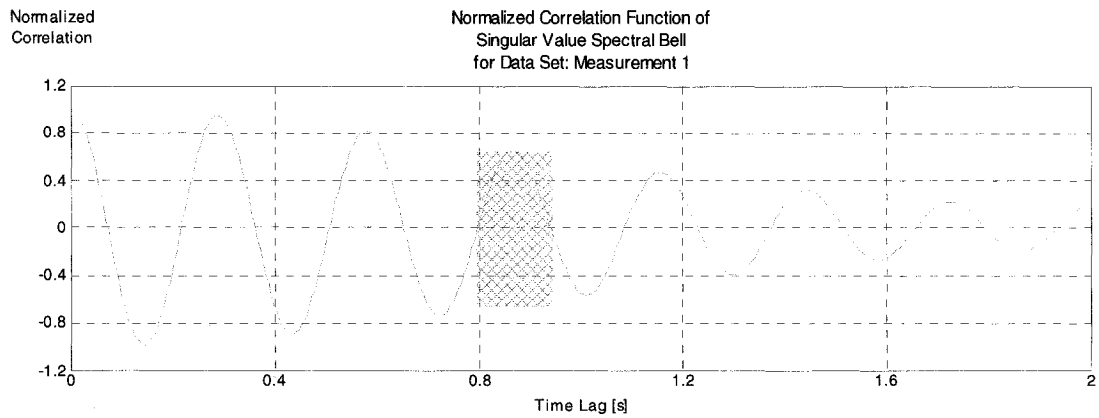

Figure 3-11: Normalized correlation curve for 1st mode

Figure 3-12 represents the well-fitted slope with normalized correlation curve in log scale. Since the slope is matched with the curve, the estimation of percentage damping matched with the value obtained for base excitation.

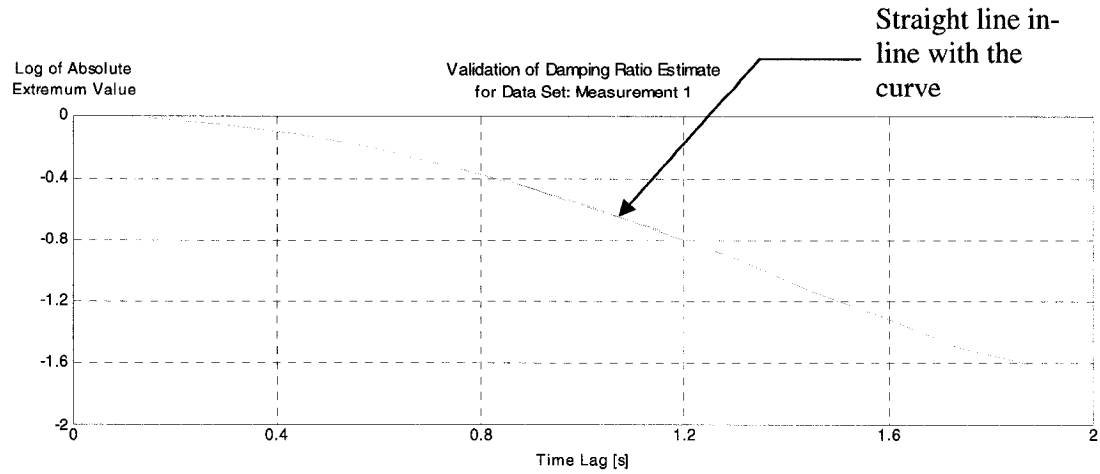

Figure 3-12: Log of absolute extreme value for 1st mode

Now, if we look at the same graphs for the 4th mode as shown in Figure 3-13, it can be seen that the normalized autocorrelation has significant rise and falls. There is no gradual slope of the curve as it had for mode 1 in Figures 3-11 and 3-12.

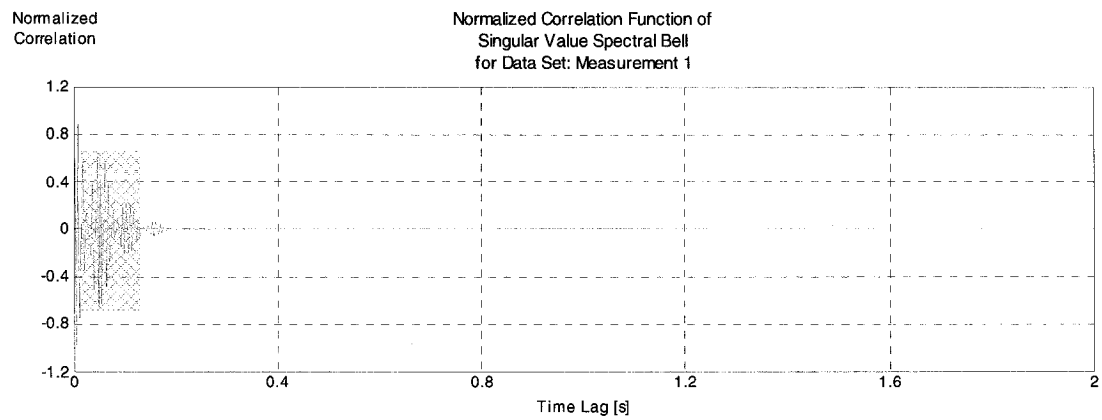

Figure 3-13: Normalized correlation curve for 4th mode

If we examine the log of absolute extreme value graph shown in Figure 3-14, it could be found that the slope does not fall into a gradual variation. The percentage damping estimation for a particular mode by EFDD method is dependent on the normalized correlation function, which can be optimized by using suitable MAC value.

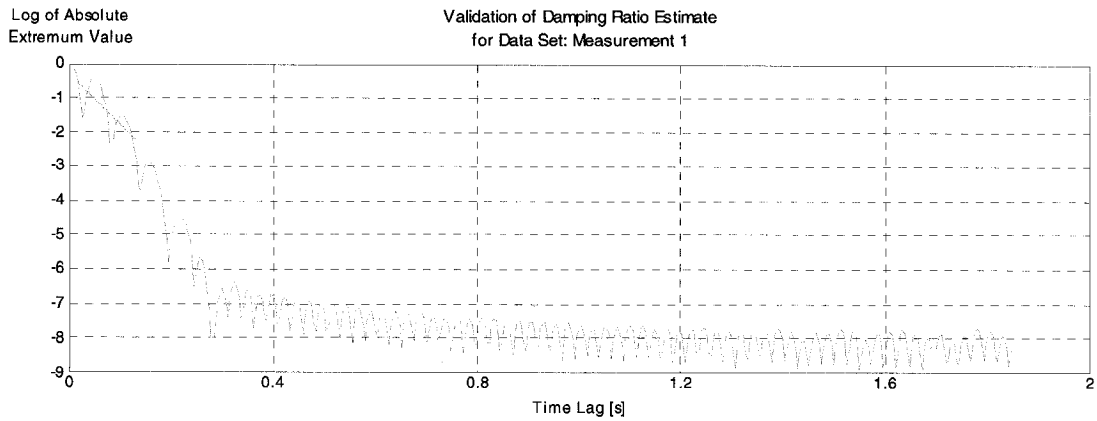

Figure 3-14: Log of absolute extreme value for 4th mode

The mode shapes for FDD, EFDD and SSI are shown in Figure 3-15. It can be seen that the mode shapes identified by output only modal testing techniques are quite similar to those obtained from finite element modal analysis.

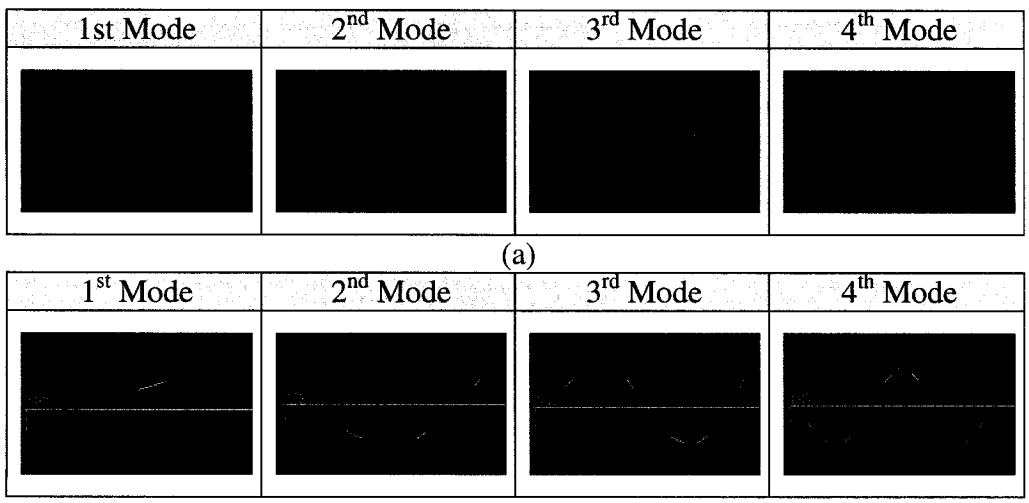

Figure 3-15: Comparison of mode shapes between (a) PULSE and (b) NASTRAN for beam under base excitation

b) Modal parameters extracted for cantilever beam under tip force random excitation using output-only modal testing techniques

The natural frequencies of beam model for random tip force excitaion extracted by different output-only modal testing techniques are tabulated in the Table 3-13:

Table 3-13: Natural frequencies of beam under tip excitation

Mode	Output only modal testing methods					Finite element Modal analysis f (Hz)
	FDD f (Hz)	EFDD f (Hz)	SSI			
			UPC f (Hz)	PC f (Hz)	CVA f (Hz)	
1	3.50	3.48	3.46	3.46	3.46	3.46
2	21.75	21.75	21.69	21.69	21.64	21.69
3	60.75	60.71	60.74	60.74	60.74	60.74
4	118.5	118.4	119.1	119.1	119.1	119.09

By comparison of results in Tables 3-11 and 3-13, it can be realized that the natural frequencies obtained for single-point random force excitation and the base random acceleration excitation agree well. The extracted damping ratios for the tip excitation are given in Table 3-14. Since it is observed that the damping ratios for the 3rd and 4th mode in EFDD method are significantly deviated from the imposed of 5.0 value. One reason could be the explanation mentioned before for random base excitation. Also, it is found in reference [21] that the output only modal testing works better with randomly distributed loading conditions.

Table 3-14: Damping ratios of beam under tip excitation

Mode	Output only PULSE methods					Finite element Modal analysis ξ (%)
	FDD ξ (%)	EFDD ξ (%)	SSI			
			UPC ξ (%)	PC ξ (%)	CVA ξ (%)	
1	-	5.01	5.0	5.0	5.0	5.0
2	-	4.88	5.0	5.0	4.86	5.0
3	-	3.90	4.97	5.0	5.0	5.0
4	-	3.58	5.0	5.0	5.0	5.0

Similar to the base excitation, the PULSE mode shapes and the NASTRAN mode shapes are identical for the beam under tip excitation as shown in Figure 3-16.

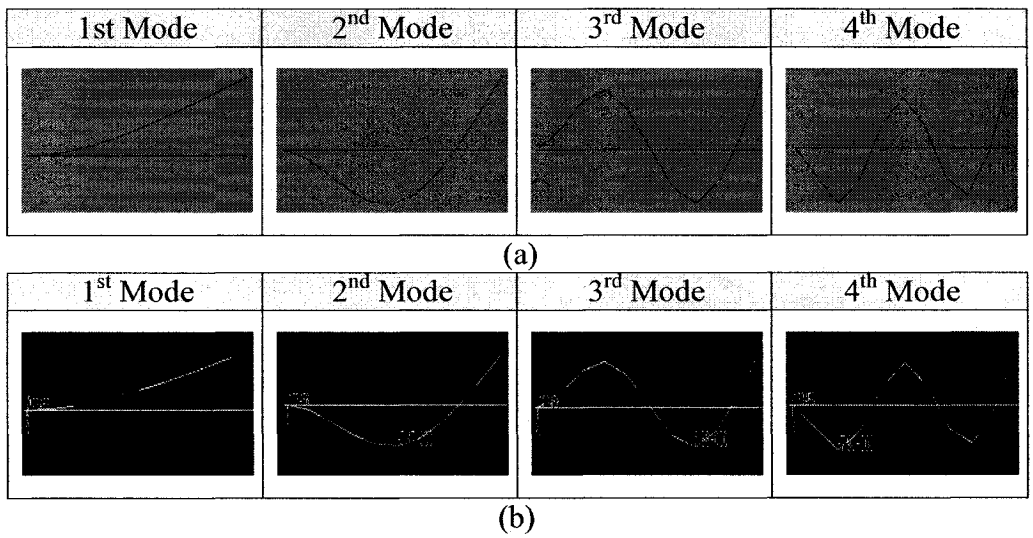

Figure 3-16: Comparison of mode shapes between (a) PULSE and (b) NASTRAN for beam under tip excitation

c) Modal parameters extracted for cantilever beam under multi-point random force excitation using output-only modal testing techniques

In this case, four uncorrelated multiple point random loads have been applied and the modal parameters have been extracted from the responses data using output-only modal testing techniques. The natural frequencies and the damping ratios are tabulated in the Table 3-15 and Table 3-16, respectively. Examination of the results reveals that multi-point excitation provides better results compared with the single point excitation and in some cases with base excitation. Even for this case, the problem associated with the damping in 4th mode has not been eliminated. One reason could be attributed to the bandwidth i.e. 128 Hz that has been used for all these excitations.

Table 3-15: Natural frequencies of beam under multiple-point excitation

Mode	Output only modal testing methods					Finite element Modal analysis f (Hz)
	FDD f (Hz)	EFDD f (Hz)	SSI			
			UPC f (Hz)	PC f (Hz)	CVA f (Hz)	
1	3.5	3.47	3.46	3.46	3.46	3.46
2	21.75	21.69	21.69	21.69	21.69	21.76
3	60.50	60.69	60.74	60.74	60.74	60.74
4	119.0	118.82	119.1	119.1	119.1	119.09

Table 3-16: Damping ratios of beam under multiple-point excitation

Mode	Output only PULSE methods					Finite element Modal analysis ξ (%)
	FDD ξ (%)	EFDD ξ (%)	SSI			
			UPC ξ (%)	PC ξ (%)	CVA ξ (%)	
1	-	5.01	5.0	5.0	5.0	5.0
2	-	4.57	5.0	5.0	5.0	5.0
3	-	4.27	5.0	5.0	5.0	5.0
4	-	3.39	5.0	5.0	5.0	5.0

The mode shapes obtained by the PULSE for multipoint excitation and NASTRAN software are shown in Figure 3-17.

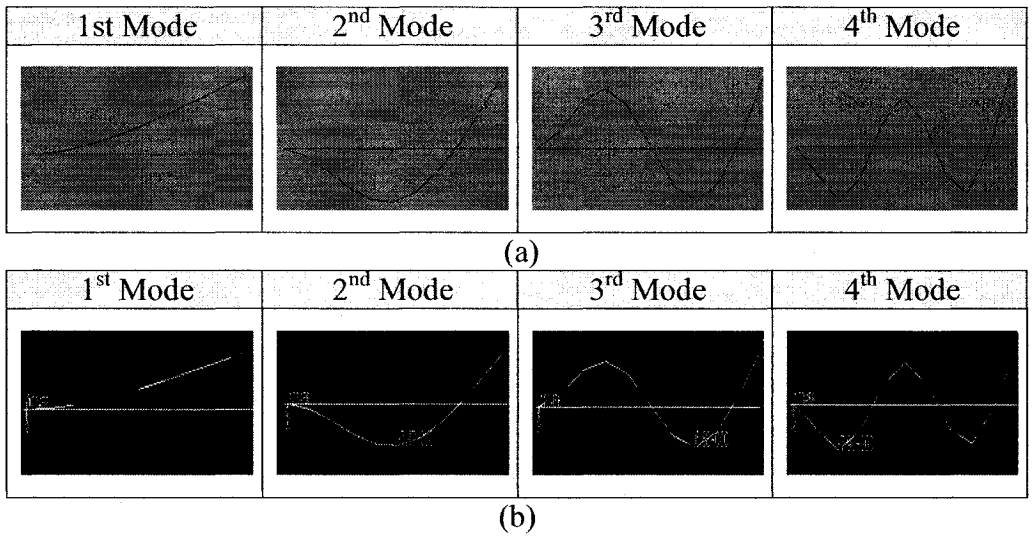

Figure 3-17: Comparison of mode shapes between (a) PULSE and (b) NASTRAN for beam under multi-point excitation

It can be concluded that, the output only modal testing technique provides good estimation of the modal parameters for the beam model.

Similarly, the transient response analysis is done using base, tip and multi-point excitations analytically in the NASTRAN and then processed response data are fed into output only modal testing technique to extract modal parameters. Some plate torsional modes are also present in this case. Here also, the free decay part of the response has been processed for modal parameter extractions.

d) Modal parameters extracted for cantilever plate under random base excitation using output only modal testing techniques

Natural frequencies for cantilever plate using PULSE are identified and compared with modal natural frequencies in Table 3-17. Since the base excitation can only excite the bending modes (out of plane) of the plate model, thus the modal parameters corresponding to only the bending modes can be extracted and no results for 3rd and 5th modes, which are torsional modes are reported. As it can be seen the results are in close agreement with the actual values.

Table 3-17: Natural frequencies of plate under base excitation

Mode	Output only modal testing methods					Finite element Modal analysis f (Hz)
	FDD f (Hz)	EFDD f (Hz)	SSI			
			UPC f (Hz)	PC f (Hz)	CVA f (Hz)	
1	3.50	3.51	3.51	3.51	3.51	3.51
2	23.54	23.54	23.51	23.55	23.38	23.51
3	-	-	-	-	-	28.47
4	73.75	73.70	73.73	73.84	73.77	73.73
5	-	-	-	-	-	94.58

The damping ratios extracted by different methods of output-only modal testing techniques are given in Table 3-18 and compared with actual values.

Table 3-18: Damping ratios of plate under base excitation

Mode	Output only PULSE methods					Finite element Modal analysis ξ (%)
	FDD ξ(%)	EFDD ξ (%)	SSI			
			UPC ξ (%)	PC ξ (%)	CVA ξ (%)	
1	-	5.06	4.52	4.78	4.78	5.0
2	-	4.56	5.00	4.80	4.04	5.0
3	-	-	-	-	-	5.0
4	-	4.15	4.96	4.70	4.89	5.0
5	-	-	-	-	-	5.0

The bending modes from PULSE for the base excitation and NASTRAN are shown in Figure 3-18, they agree very well.

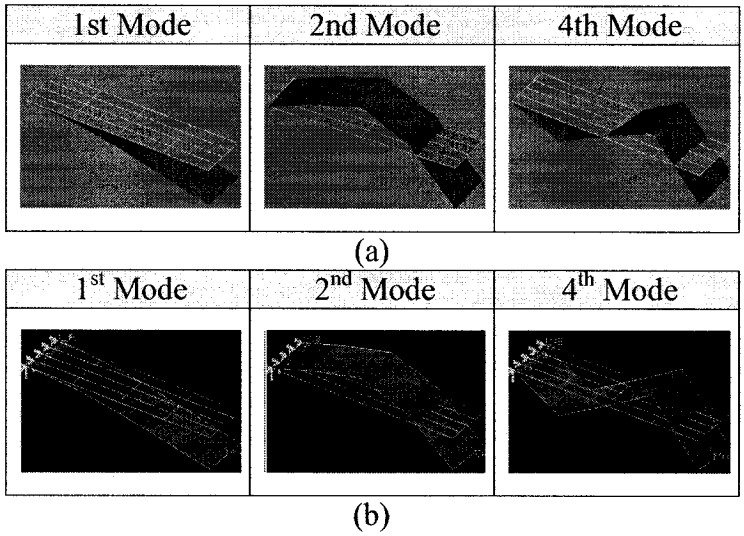

Figure 3-18: Comparison of mode shapes between (a) PULSE and (b) NASTRAN for plate under base excitation

e) Modal parameters extracted for cantilever plate under tip random load excitation using output only modal testing techniques

The extracted natural frequencies of the cantilever plate for tip (point) excitation are given in Table 3-19. For this case, torsional modes are also excited with the corner-tip excitation. There is a good agreement between the extracted results by the output only modal testing and by finite element method with tip (single point) excitation.

Table 3-19: Natural frequencies of plate under tip excitation

Mode	Output only modal testing methods					Finite element Modal analysis f (Hz)
	FDD f (Hz)	EFDD f (Hz)	SSI			
			UPC f (Hz)	PC f (Hz)	CVA f (Hz)	
1	3.50	3.51	3.52	3.51	3.56	3.51
2	23.50	23.50	23.28	23.51	23.60	23.51
3	28.50	28.37	28.49	28.54	28.38	28.46
4	74.25	73.70	73.70	73.72	73.73	73.73
5	94.58	94.81	94.47	94.52	94.50	94.58

From the damping information given in Table 3-20, it can be seen that the damping ratios are very close with actual damping applied in finite analysis, unlike in the case of beam.

Table 3-20: Damping Ratios of plate under tip excitation

Mode	Output only PULSE methods					Finite element Modal analysis ξ (%)
	FDD ξ (%)	EFDD ξ (%)	SSI			
			UPC ξ (%)	PC ξ (%)	CVA ξ (%)	
1	-	5.20	4.70	5.0	4.69	5.0
2	-	5.13	4.10	4.99	4.87	5.0
3	-	5.03	4.98	4.99	4.81	5.0
4	-	5.19	4.96	4.99	5.00	5.0
5	-	4.62	4.99	4.99	4.95	5.0

The mode shapes obtained from PULSE and NASTRAN are also quite similar as shown in Figure 3-19.

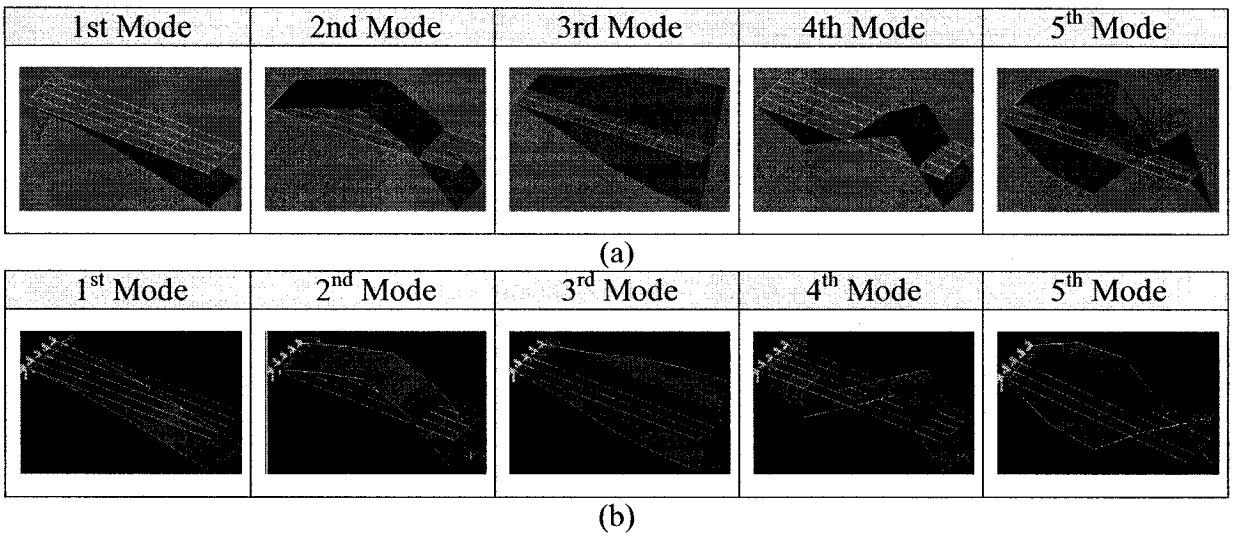

Figure 3-19: Comparison of mode shapes between (a) PULSE and (b) NASTRAN for plate under tip excitation

f) Modal parameters extracted for cantilever plate model under multiple-point force random excitation using output only modal testing techniques

The extracted natural frequencies of the cantilever plate and damping ratios for multiple point excitations are given in Table 3-21 and Table 3-22, respectively.

Table 3-21: Natural frequencies of plate model under multiple-point excitation

Mode	Output only modal testing methods					Finite element Modal analysis f (Hz)
	FDD f (Hz)	EFDD f (Hz)	SSI			
			UPC f (Hz)	PC f (Hz)	CVA f (Hz)	
1	3.50	3.51	3.51	3.49	3.50	3.51
2	23.50	23.63	23.51	23.54	23.51	23.51
3	28.25	28.35	28.47	28.49	28.47	28.46
4	74.25	73.61	73.73	73.74	73.73	73.73
5	94.75	94.73	94.58	94.57	94.58	94.58

Table 3-22: Damping ratios of plate under multiple-point excitation

Mode	Output only PULSE methods					Finite element Modal analysis ξ (%)
	FDD ξ(%)	EFDD ξ (%)	SSI			
			UPC ξ (%)	PC ξ (%)	CVA ξ (%)	
1	-	5.14	5.0	4.91	4.97	5.0
2	-	4.45	5.0	4.96	5.0	5.0
3	-	4.95	5.0	4.96	5.0	5.0
4	-	4.89	5.0	4.94	5.0	5.0
5	-	4.75	5.0	5.0	5.0	5.0

It is seen that there is better agreement in natural frequencies and damping ratios for multiple point excitation compared to the other two-excitation methods.

The mode shapes are also similar to those identified for single point excitation, and agree closely with actual mode shapes obtained from modal analysis in NASTRAN as shown in Figure 3-20.

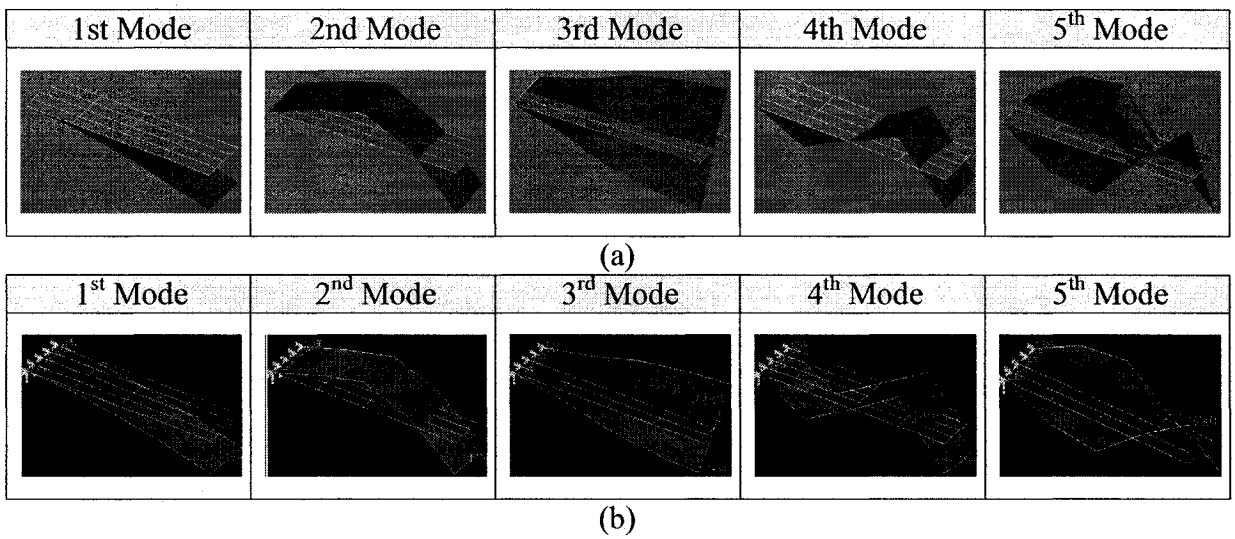

Figure 3-20: Comparison of mode shapes between (a) PULSE and (b) NASTRAN for plate under multipoint excitation

3.4 SUMMARY

In this chapter it has been shown that the transient response data obtained from the finite element modeling for simple beam or plate structures under different types of random excitation can be effectively used to extract modal parameters using different output-only modal testing techniques in PULSE software.

In all cases for both beam and plate model, the natural frequencies are in very good agreement with those obtained from the modal analysis. It has been observed that the damping ratios extracted for the case of multiple-point excitation are in better agreement with actual values compared to the base or single point excitations for both beam and plate

model. It is apparent that randomly distributed loading condition is an optimum excitation method for output-only modal testing. However, it could not be concluded analytically between base and single point excitation which excitation is better to extract modal parameters. This might be identified when the experimental testing is carried out with the driven base and single point excitation in the next chapter.

CHAPTER 4

EXPERIMENTAL TESTING

4.1 INTRODUCTION

In the previous chapter we have observed that multiple-point excitation is potentially better excitation method compared with base and single point excitations. However, analytically it could not be concluded between base and single point excitation, which excitation provides accurate modal parameters. To further elaborate on this issue, this chapter describes some experimental tests with base and single point excitation. The experimental data are acquired using LMS software and processed for modal information using LMS PolyMAX (for reference modal parameters), LMS Operational PolyMAX and also PULSE software. The results are presented and discussed. In addition, this experimental phase of the project fulfils another objective of this research, namely investigation of the application of output-only modal testing on-orbit satellite appendages experimentally.

Vibration measurements are done on the test fixture at first to find out its natural frequencies, and to see whether the fixture remains rigid in the frequency range of interest in the tests.

4.2 INSTRUMENTATION AND DATA ACQUISITION

The instrumentation that are used to perform the experimental testing include:

1) Shaker (for driven base excitation)

2) Portable exciter (for point excitation)

3) Shaker amplifier

4) Multi-channel data acquisition and processing LMS system

5) Force sensors (for point excitation)

6) Accelerometers and cables

The schematic of the test set-up is presented in Figure 4-1.

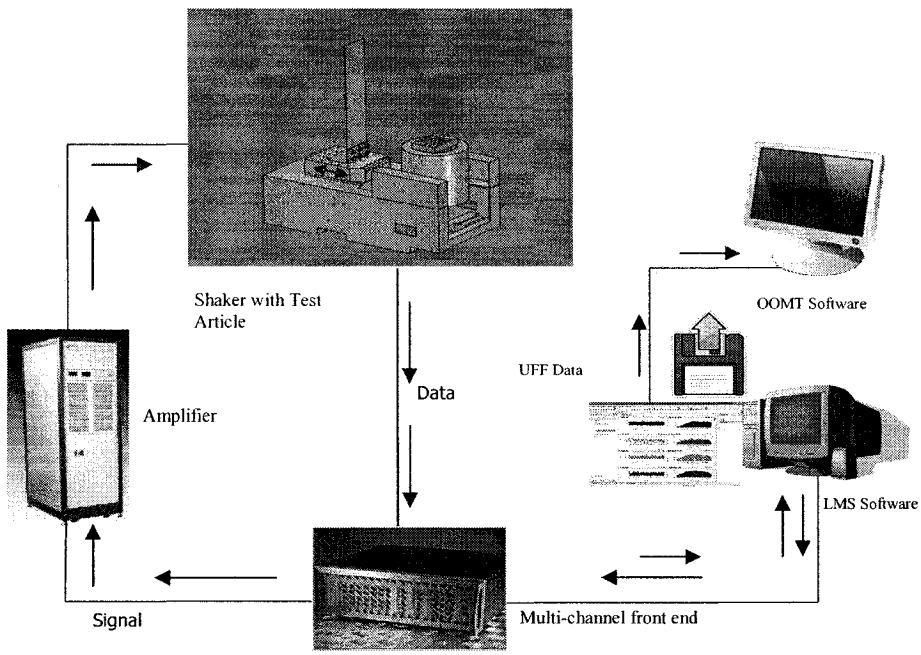

Figure 4-1: Schematic diagram for the test set-up

The test article is placed vertically on the slip table of shaker trough a fixture for both base and point excitation. The shaker is used to perform the driven base excitation whereas a single point portable exciter is hung on a frame and attached to the test article using a force sensor and a stinger. The accelerometers are glued on the test article and connected to the front end through cables. With the help of LMS PolyMAX, the data is processed to identify the modal parameters from the frequency response function. The FRF's consists of response acceleration over input acceleration for base excitation method whereas for point excitation it is response acceleration over input force. Also, using cross-power densities of the processed data the modal parameters are extracted with the help of LMS operational PolyMAX. Finally, time series data are exported in universal file format to be processed in PULSE operational modal analysis software to extract the modal parameters.

The experimental set-up for driven base excitation is shown in Figures 4-2.

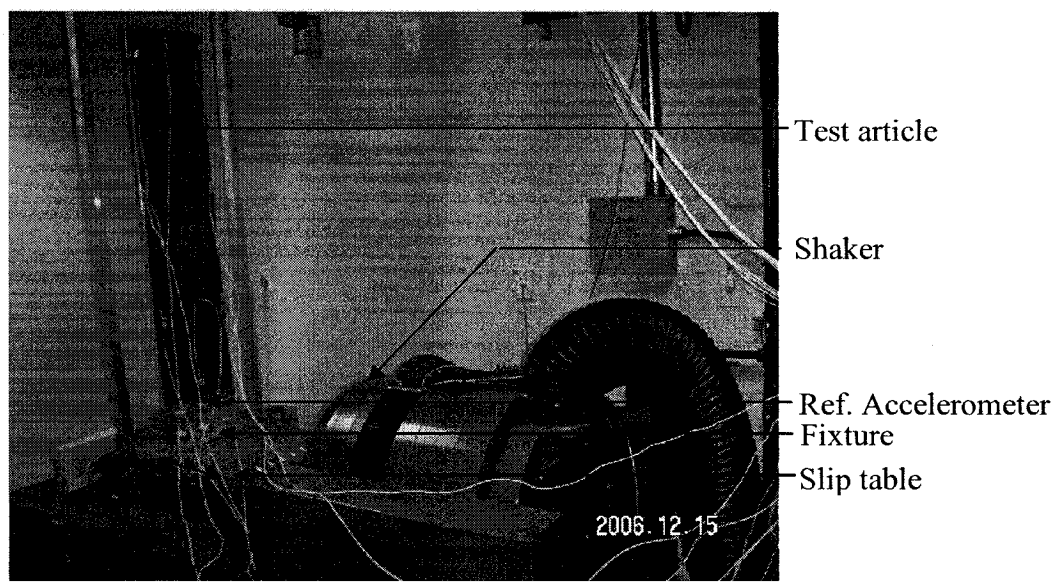

Figure 4-2: Test-setup for base excitation

For the case of base excitations, 9 accelerometers are attached on the test article and a reference accelerometer is placed on the upper part of the fixture as shown in the Figure 4-3.

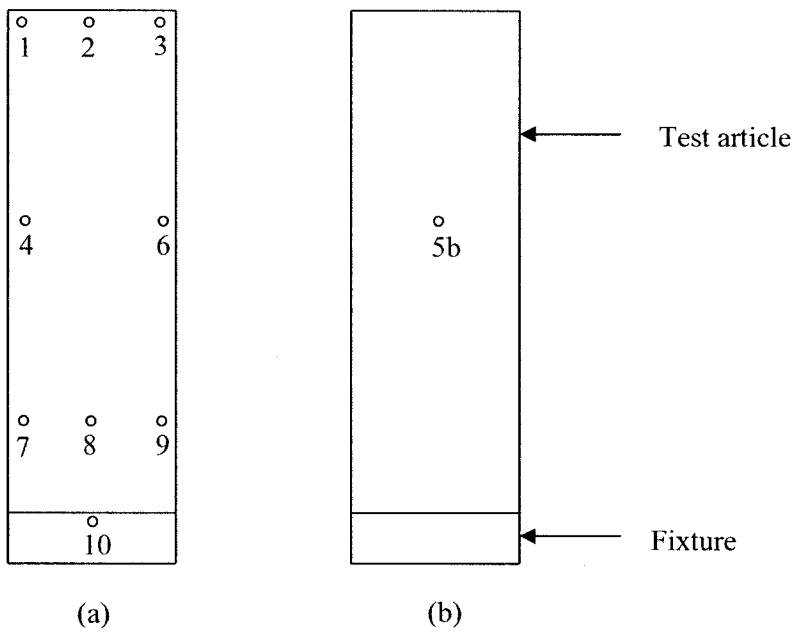

Figure 4-3: Accelerometers locations at (a) front (b) back face of test article and fixture for base excitation

There are 8 accelerometers are placed at location points 1, 2, 3, 4, 6, 7, 8, and 9 on front face as shown in Figure 4-3. Also, the 9th accelerometer is attached at location point 5b on the back face of the test article as the location point 5 at the front face is allocated for force sensor for point excitation. The reference accelerometer is attached at the location point 10 on the fixture.

In the point excitation a portable exciter is placed on a support frame and connected to the test article via a force sensor and stinger as shown in Figure 4-4. In this case, the slip table remains fixed. The response accelerations and input force are recorded and processed.

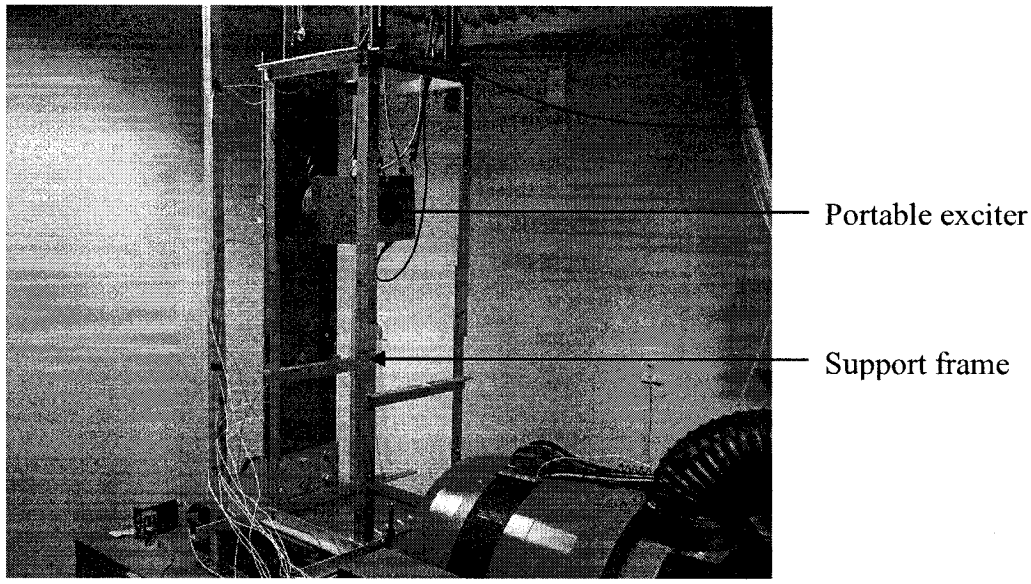

Figure 4-4: Test-setup for point excitation

For the point excitation, 9 accelerometers and a force sensor are attached on the test article as shown in the Figure 4-5.

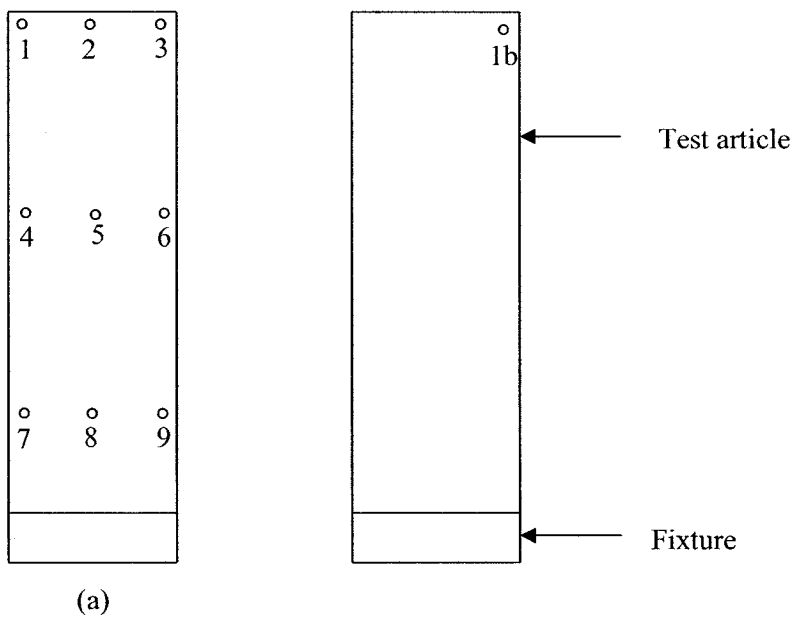

Figure 4-5: Accelerometers and force sensor locations at (a) front (b) back face of test article for portable excitation

There are 8 accelerometers attached at location points 1, 2, 3, 4, 6, 7, 8, and 9 as shown in above Figure 4-5. Also, the 9th accelerometer is attached at location point 1b on the back face of the test article, which is used as reference accelerometer. Location point 1b is the point at the back of location point 1. The location point 5 at front face is used for force sensor and the portable exciter is attached with it.

The parameters that are considered for both the driven base excitation and point excitation methods are represented in Table 4-1.

Table 4-1: Parameters for both driven base excitation and point excitation

Method	FRF PolyMAX	Operational PolyMAX	PULSE
Bandwidth	128 Hz	128 Hz	128 Hz
No. of frequency lines	4096	4096	8192
Frequency resolution	0.03125	0.03125	0.25
No. of averages	30	15	22
Signal type	75% burst random	100% random	100% random

4.3 Fixture survey

At the beginning of the experiment a FRF based modal survey has been carried out on fixture using LMS PolyMAX to ensure that the fixture is rigid enough in the frequency range of interest. There are ten accelerometers mounted on the fixture as shown in Figure 4-6 and a reference accelerometer is placed at the end side of the slip table.

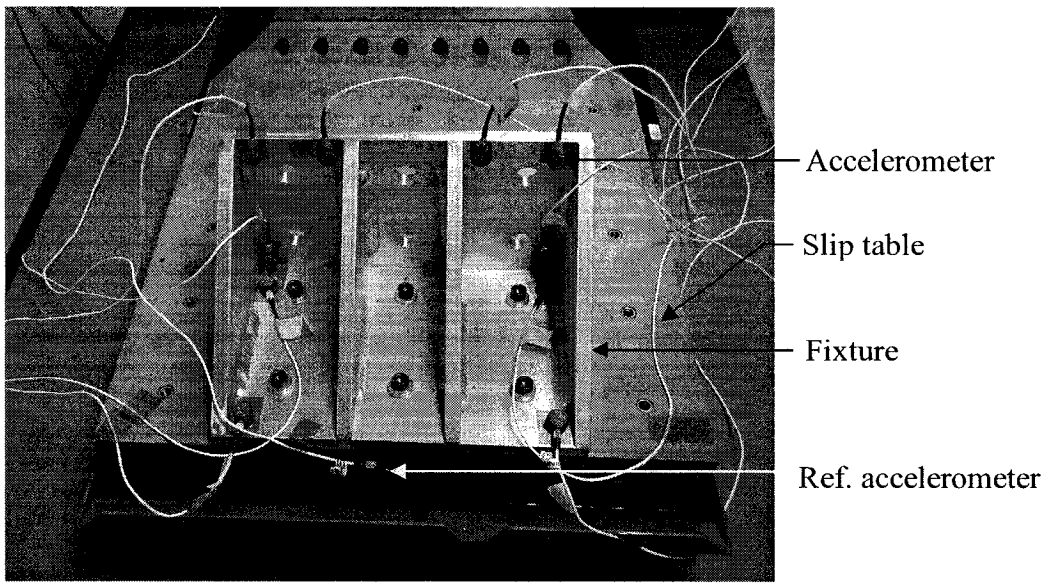

Figure 4-6: Fixture testing

The parameters used for the driven base testing of the fixture are presented in Table 4-2.

Table 4-2: Parameters for fixture testing

Excitation	Driven base
Location of Ref. accelerometer	At the side of the slip table
Bandwidth	512 Hz
No. of frequency lines	11000
Frequency resolution	0.04655
No. of averages	30
Signal type	75% burst random

Using these parameters the experiments have been carried out and the FRF's are obtained for processing using LMS.

Two FRF samples, one for point location fixture-1 (at top left corner of the vertical surface) and another for point location fixture-3 (at the bottom left corner on the vertical surface) shown in Figure 4-6, are demonstrated in Figure 4-7.

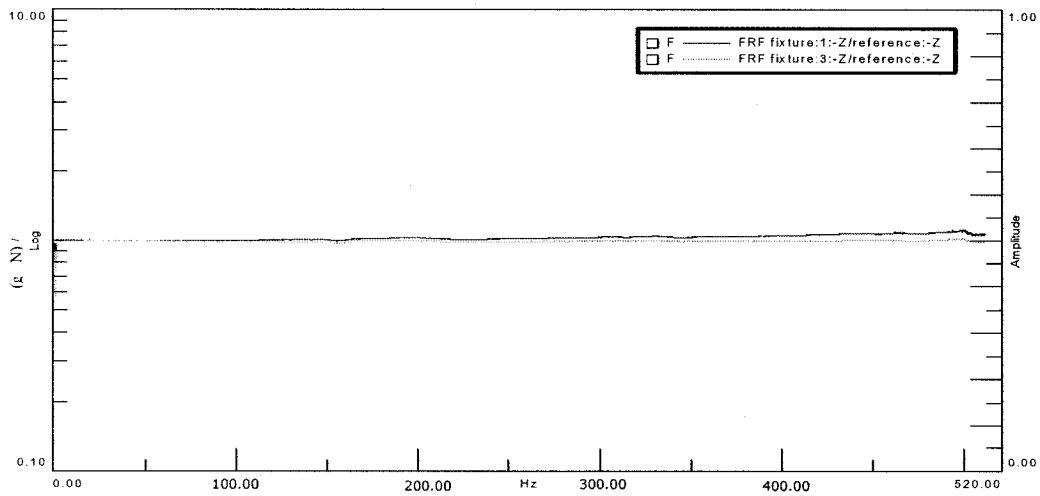

Figure 4-7: FRF for base excitation of the fixture

There is no sharp peak observed in the FRF window. Now if we look at the stabilization diagram we can find that the first and second modes are at about 55 Hz and 157 Hz.

Corresponding modes for the first and second frequencies are shown in Figure 4-8.

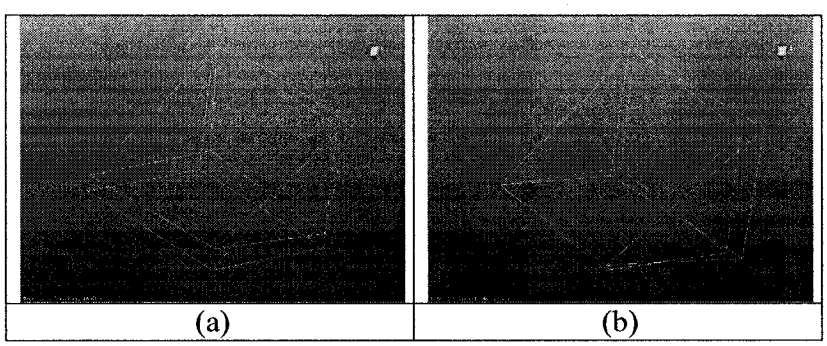

Figure 4-8: Fixture (a) 1st mode at 55 Hz (b) 2nd Mode at 157 Hz

4.4 EXPERIMENTAL RESULTS AND COMPARISON

4.4.1. Base Excitation

Once the data acquisition is done the next thing to do is to process the FRFs with PolyMAX to identify the natural frequencies and damping ratios of the modes. These modal parameters are to be used as reference for comparison with the values extracted with operational modal technique.

Figure 4-9 shows two examples of FRF's measured from the driven base excitation.

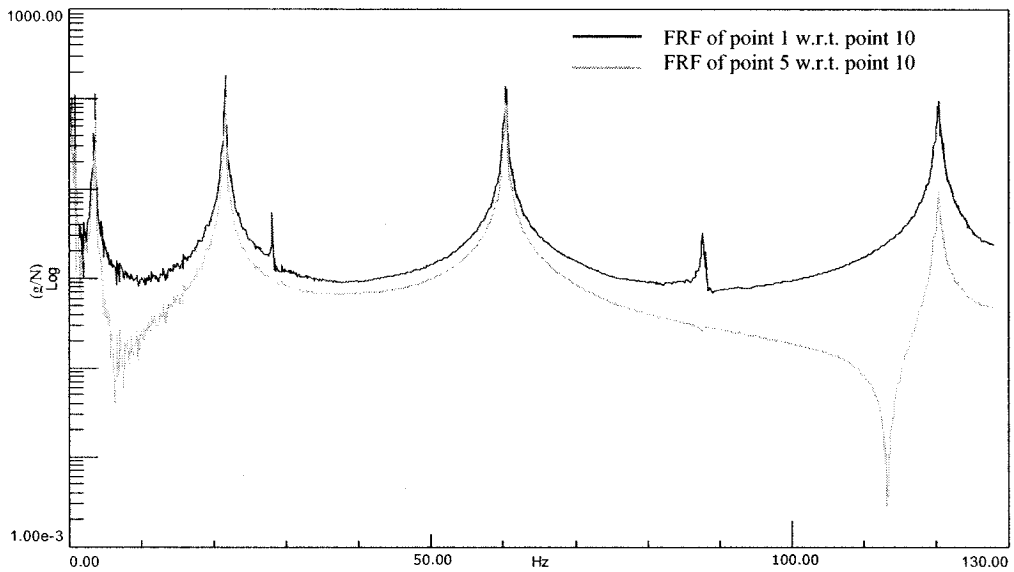

Figure 4-9: Sample FRFs from driven base run

The upper curve represents the FRF at the point 1 location whereas the lower curve represents the FRF at the point 5 at the back face of the test article as shown in Figure 4-3. upper curve shows some torsion peaks at about 28 Hz and 87 Hz but the lower curve does not show the torsion modes as it is located at the centerline along the length of the test article.

The modal parameters obtained by the stabilized poles of the stabilization diagram of PolyMAX are considered as the reference modal parameters of the test article for comparison purposes.

In order to use the Operational PolyMAX, we need cross power spectra to identify the modal parameters. In this method the cross powers spectra are used instead FRF's in PolyMAX. The stabilized poles are selected from the stabilization diagram of Operational PolyMAX to identify the modal parameters. An example of the cross power spectra for base excitation run is demonstrated in Figure 4-10.

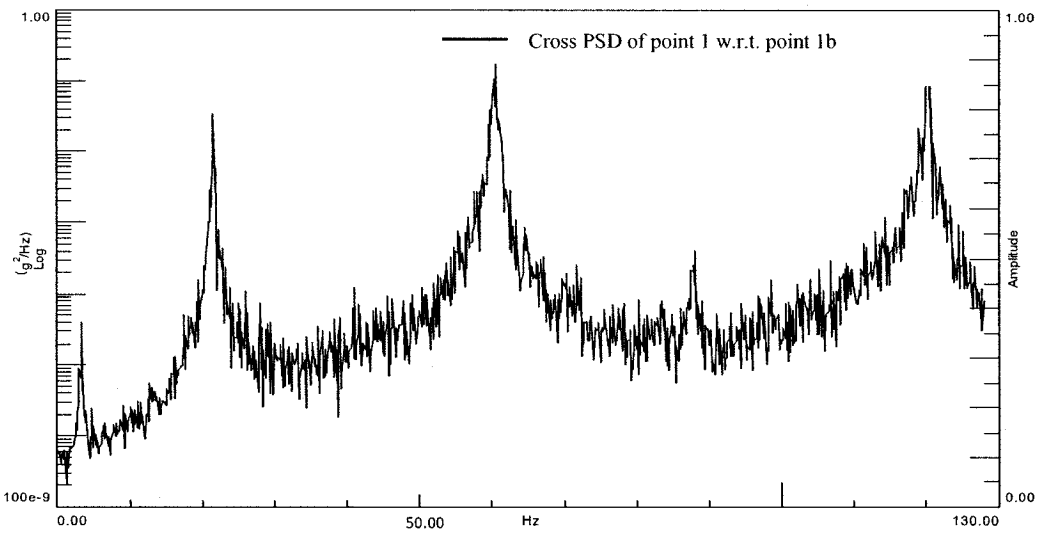

Figure 4-10: Sample cross PSD for the driven base excitation

In order to use the PULSE operational modal analysis, we need time series output data. A time dependent output file in universal file format is generated. Using these data and with standard processing in PULSE the modal parameters are identified.

FRF PolyMAX, Operation PolyMAX and B&K PULSE are used to obtain modal parameters from base excitation. The identified natural frequencies are presented in Table 4-3.

Table 4-3: Natural frequencies of test article model under base excitation

Mode	LMS PolyMAX (Reference) f (Hz)	Operational PolyMAX f (Hz)	PULSE methods				
			FDD f (Hz)	EFDD f (Hz)	SSI		
					UPC f (Hz)	PC (Hz)	CVA f (Hz)
1	3.48	3.35	3.45	3.45	3.46	3.46	3.46
2	21.54	21.49	21.38	21.50	21.53	21.52	21.53
3	28.15	-	-	-	-	-	-
4	60.43	60.39	60.5	60.49	60.52	60.45	60.45
5	87.84	-	87.75	87.77	87.77	87.77	87.69
6	120.5	120.29	120.6	120.4	120.5	120.4	120.5

It can be seen that the frequencies are very close except for the missing information about the 3rd and 5th torsional modes by output-only modal testing techniques. Two things should be remembered. First thing is that the output-only modal testing works on output responses only and there is every chance of losing data and the second thing is that base excitation can excite only the bending modes.

The damping ratios for the three different approaches are given in Table 4-4.

Table 4-4: Damping ratios of test article under base excitation

Mode	FRF PolyMax (Reference) ξ (%)	Operational PolyMax ξ (%)	PULSE methods				
			FDD ξ (%)	EFDD ξ (%)	SSI		
					UPC ξ (%)	PC ξ (%)	CVA ξ (%)
1	0.40	1.43	-	0.59	0.78	0.59	0.84
2	0.14	0.28	-	0.39	0.23	0.21	0.23
3	0.02	-	-	-	-	-	-
4	0.13	0.2	-	0.19	0.27	0.33	0.34
5	0.20	-	-	0.24	0.24	0.33	0.34
6	0.14	0.11	-	0.35	0.23	0.54	0.36

The damping ratios identified by different output-only modal testing approaches agree well with reference FRF PolyMAX results. Actually the damping in the system is negligible. So, the identified damping ratios using output-only approaches do not exist physically. The differences in the values are not significant.

The mode shapes for driven base run using FRF curve fit are shown in Figure 4-11. Mode shapes for FRF, Operational PolyMAX and PULSE output only modal testing are close to each other except for the 3rd and 5th mode in Operational PolyMAX and 3rd mode in PULSE which are missing. It can be noticed that this excitation could excite the torsional modes which have been identified from FRFs. In some cases output only could generate the information about these modes and some cases not, due to the fact that it can miss the data regarding the unexcited modes.

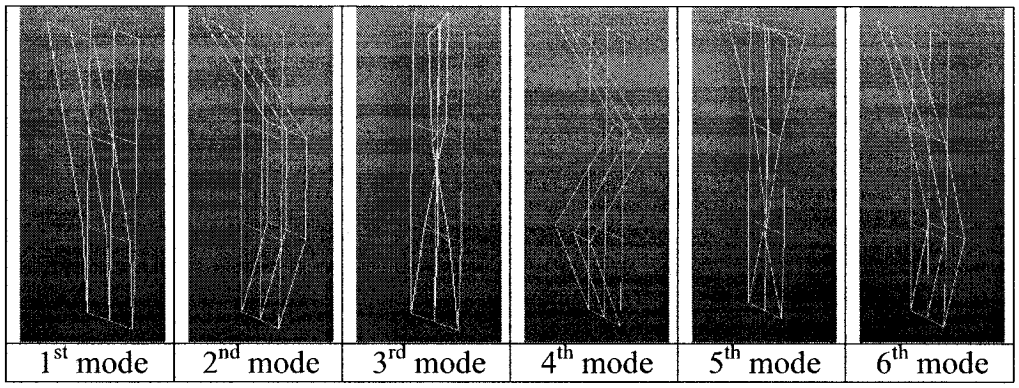

Figure 4-11: Mode shape from FRF and output only approaches for driven base run

4.4.2. Point Excitation

The sample FRFs for two nodes is represented in Figure 4-12. The upper curve represents the FRF at point 1 location whereas the bottom (darker line) curve represents the FRF at point 5 at the back face of the test article. The peaks for the torsional modes as presented in upper curve can be found from the FRF at location point 1.

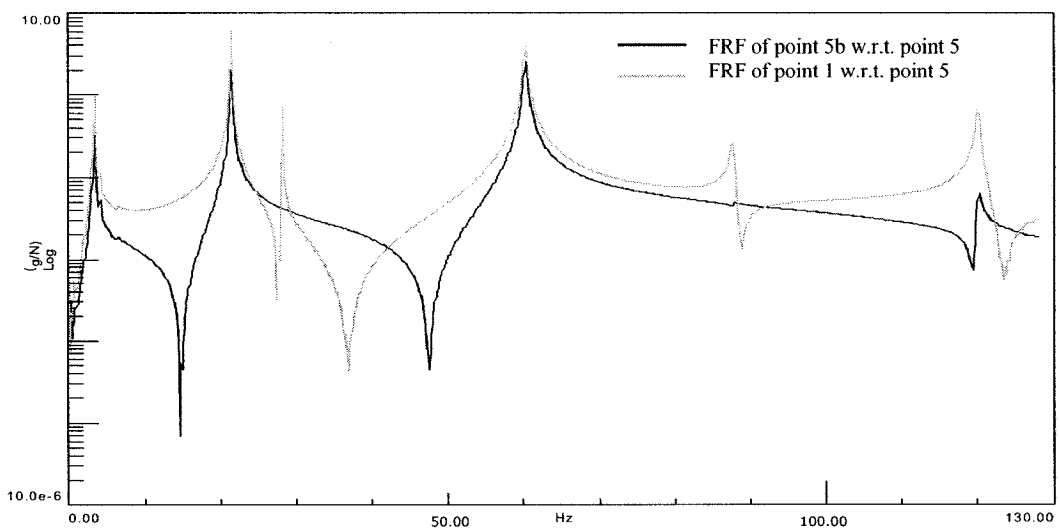

Figure 4-12: Sample FRFs for point excitation run

As we can see from the figure, the point at the top left corner possesses the torsion mode peaks. The modal parameters obtained by the stabilized poles of the stabilization diagram of PolyMAX are considered as the reference modal parameters of the test article as processed in the base excitation method. For Operational PolyMAX, the cross power spectra are used to identify the modal parameters. A sample cross-power spectra for point excitation run is shown in Figure 4-13.

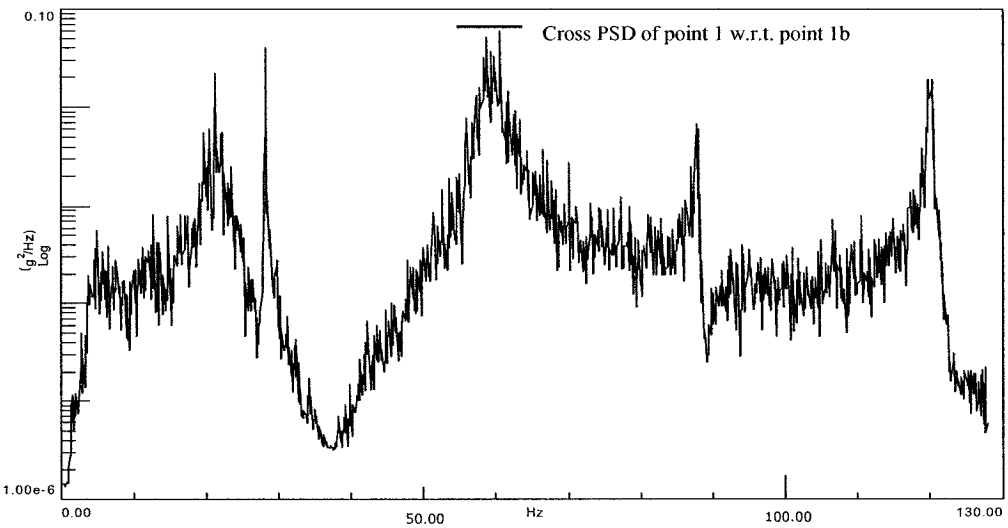

Figure 4-13: Sample cross PSD for portable excitation run

Since PULSE requires time series data, so another run is taken to generate the response data in universal file format. Using these data and with standard processing in PULSE, the modal parameters are identified.

The identified natural frequencies using these different approaches are provided in Table 4-5.

Table 4-5: Natural frequencies of test article under point excitation

Mode	FRF PolyMax (Ref.) f (Hz)	Operational PolyMax f (Hz)	PULSE methods				
			FDD	EFDD	SSI		
			f (Hz)	f (Hz)	UPC f (Hz)	PC (Hz)	CVA f (Hz)
1	3.47	4.98	4.85	4.60	4.60	4.75	4.84
2	21.50	21.39	21.0	21.11	21.21	21.33	21.41
3	28.26	28.25	28.25	28.31	28.28	28.28	28.28
4	60.39	59.28	59.50	59.38	59.49	59.43	59.45
5	87.84	87.91	87.75	87.78	87.81	87.81	87.81
6	120.1	120.1	120.5	120.0	120.1	119.8	120.1

As it can be realized that there is close agreement in the values of natural frequencies identified using the different approaches with those of reference except for the first mode. The reason for this discrepancy for the identified fundamental mode can be attributed to the fact that the test article is a flexible structure but when it is connected with the portable exciter it becomes a bit stiffened at the point of exciter by the set-up and thus the first natural frequency becomes a little bit higher as it expected. The damping ratios for three different approaches are given in Table 4-6.

Table 4-6: Damping ratios of test article under point excitation

Mode	FRF PolyMax (Ref.) ξ (%)	Operational PolyMax ξ (%)	PULSE methods				
			FDD	EFDD	SSI		
			ξ (%)	ξ (%)	UPC ξ (%)	PC ξ (%)	CVA ξ (%)
1	0.95	1.86	-	0.76	1.85	1.36	2.0
2	0.21	0.44	-	0.26	1.87	2.51	2.23
3	0.08	0.02	-	0.59	0.20	0.19	0.19
4	0.34	0.74	-	1.96	1.60	1.96	1.95
5	0.27	0.02	-	0.29	0.23	0.21	0.22
6	0.22	0.11	-	0.37	0.26	0.36	0.29

There are significant differences in the damping information due to the fact that the point excitation technique depends highly on the point where the excitation is given and to what extent it is able to evoke response in the linear range.

The generalized mode shapes identified for driven base run using FRF curve fit is shown in Figure 4-14. Mode shapes identified by Operational PolyMAX and PULSE output only modal testing are identical with the FRF modes and are not presented here.

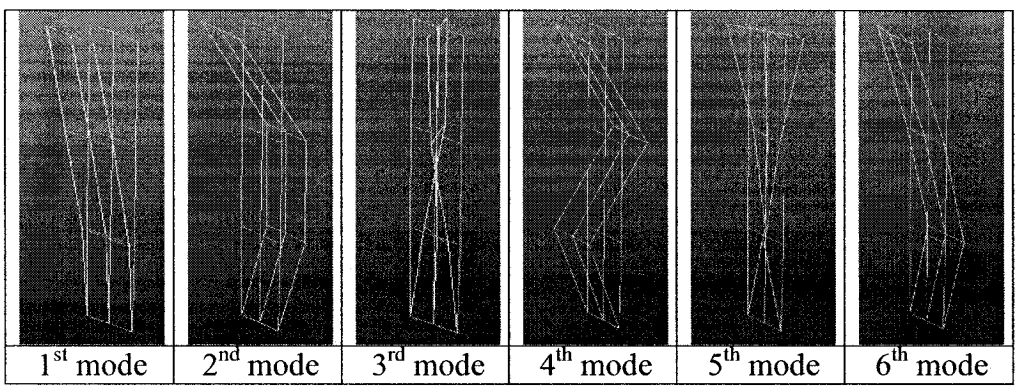

Figure 4-14: Mode shape from FRF and output only approaches for point excitation

4.5 SUMMARY

At beginning of this chapter an experimental survey on the fixture has been presented. It has also been confirmed that the fixture remains basically rigid. The fundamental frequency of the fixture is identified to be around 55 Hz confirming that there is no movement of the fixture at the frequency range of interest.

Also, in this chapter two types of testing are carried out and results have been presented and discussed. Although our main focus is on the performance of output only modal

testing technique in satellite appendages under driven base excitation, we have performed a single point test to investigate how this technique performs under single point loading condition.

Although in analytical approach it could not be concluded between the base and single point excitation loading condition which one provide better results in output only modal testing technique, from the experimental testing it can be confirmed that, the base excitation is better, even though we have some significant discrepancy in the damping ratios. The identified percentage damping is about 0.4% by FRF PolyMAX which is very small amount of damping. When the damping becomes so small it becomes very difficult to identify the true value. So any errors associated with the damping information could be ignored.

In conclusion, it has been established both analytically and experimentally that output only modal testing works very well. In next chapter the actual simulation of the solar panel will be performed to represent the real case scenario of a spacecraft appendage using analytical simulation.

CHAPTER 5

SIMULATION OF SOLAR PANEL

5.1 INTRODCUTION

In the previous two chapters we have confirmed that the output only modal testing technique works very well with translational random driven base excitation on simple structure.

In this chapter, the model of a solar panel appendage will be excited analytically at the base with rotational step input excitation as provided by the spacecraft thrusters to change its orientation or course (discussed in the dynamics of spacecraft appendages in Chapter 1). Only, few nodal responses will be processed to identify the modal parameters of the structure as would be the case for a real life scenario.

5.2 DESIGN CONSIDERATIONS OF SOLAR PANEL

The solar panel appendage is selected as a 'template' for our analysis due to the simplicity of its boundary conditions and availability of some of its properties and characteristics. The dimensions of the panel are taken as 6 m long and 1.2 m wide based on the dimension of solar panel of Communication Technology Satellite (CTS) [48]. The materials used to manufacture these panels are glass-fibre with a Kapton layer on it. With the nominal thickness of such a panel, the fundamental frequency comes out to be very low.

We know that the fundamental frequency increases with the increase of the stiffness (including modulus of elasticity) and decreases with the increase of material density. Normally, in the real solar panel structure, supports and stiffeners are used to increase the fundamental frequency of the panel to about 3~4 Hz. Here in this study, the effects of stiffeners are smeared over the panel considering the panel is designed with an isotropic material that has properties to reach the fundamental frequency between 3~4 Hz.

Figure 5-1 represents the solar panel, which is excited at the base. The translational displacement DoF in the out of plane direction is allowed free to undergo motion.

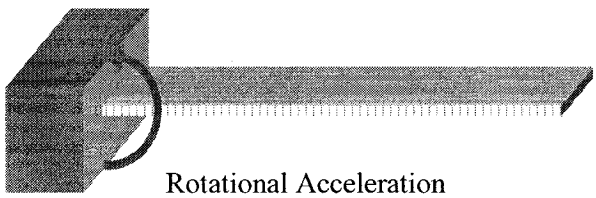

Figure 5-1: Solar panel simulation

The finite element model of the panel is shown in Figure 5-2.

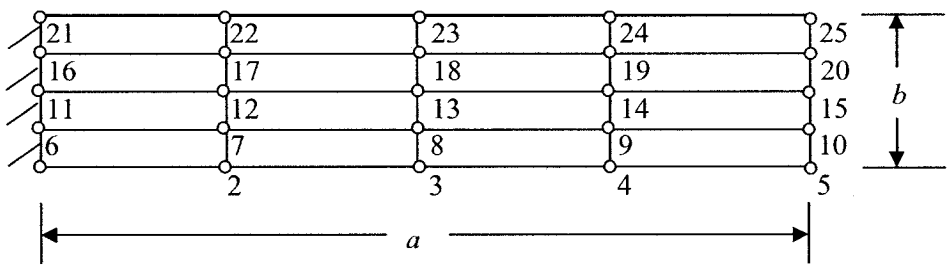

Figure 5-2: Finite element model of the solar panel

Material properties and dimension of the solar panel are given in Table 5-1.

Table 5-1: Properties of solar panel and its dimensions

Material type	Isotropic material
Modulus of Elasticity, E	$207\times10^{9}\ N/m^{2}$
Length of the panel, a	$6.48\ m$
With of the panel, b	$1.32\ m$
Thickness of the panel, h	$0.0228\ m$
Density, ρ	$0.1548\times10^{3}\ kg/m^{3}$
Poisson's ratio, ν	0.3

Table 5-2 provides information regarding finite element model.

Table 5-2: Finite element design consideration

Number of element	16
Number of nodes	25
Time resolution	0.0025 sec
Excitation time	6 sec

An input field representing rotational base excitation caused by thruster has been created using NASTRAN field as shown in Figure 5-3.

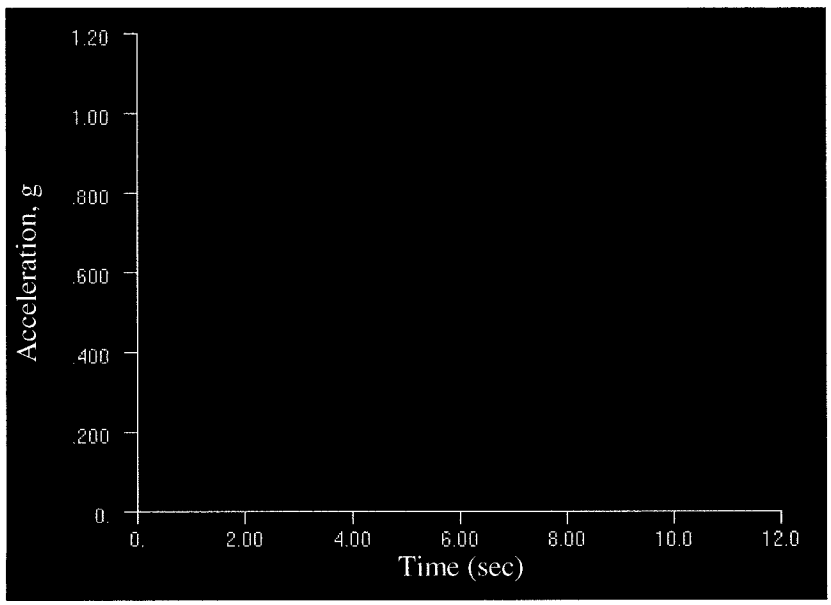

Figure 5-3: Step input field for rotational base excitation

Rotational transient excitation at the base is applied and the acceleration responses at all the nodes are recorded. The damping ratio considered in this analysis is 2%. The response at node 5 is shown in Figure 5-4.

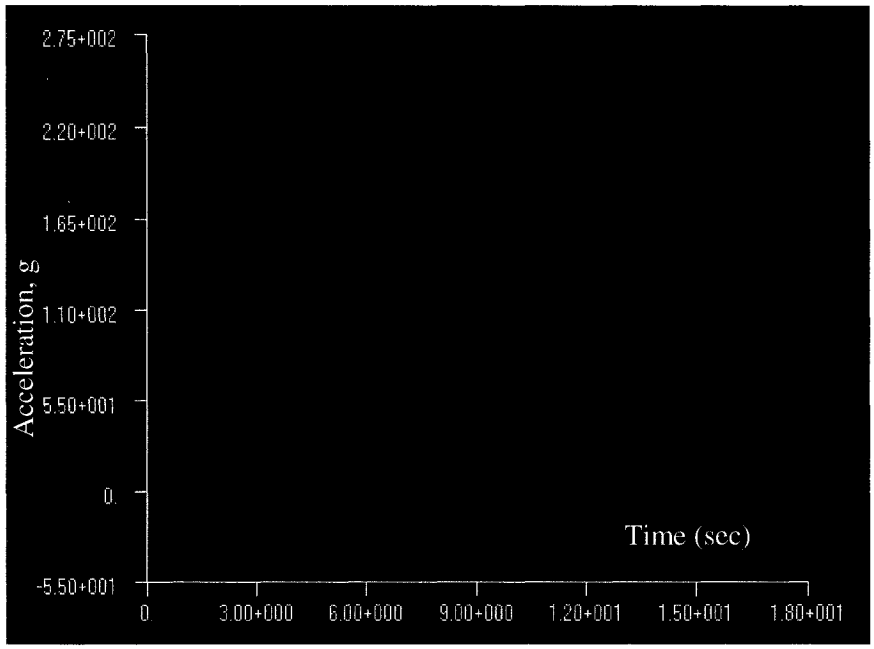

Figure 5-4: Responses at node number 5

The nodal responses for all nodes are then transformed into a universal file format. This universal file is then processed in output only modal testing software to extract the modal parameters of the solar panel. While processing this universal file four kinds of nodal responses are considered. These are including (i) responses for all the nodes, (ii) responses for 4 nodes (e.g. node 3, node 5, node 23, and node 25), (iii) response for node 3 and (iv) response for node 5.

5.3 SIMULATED RESULTS

After processing these nodal responses, modal parameters are extracted using output only modal testing methods. The methodology is the same as described earlier in analytical approach presented in Chapter 3.

5.3.1 Modal parameters based on all nodal responses

The extracted natural frequencies of the solar panel for all the nodal responses are given in Table 5-3

Table 5-3: Identified natural frequencies based on all nodal responses

Mode	Output only modal testing methods					Finite element Modal analysis f (Hz)
	FDD f (Hz)	EFDD f (Hz)	SSI			
			UPC f (Hz)	PC f (Hz)	CVA f (Hz)	
1	3.125	-	3.30	3.0	3.25	3.24
2	21.48	21.65	21.76	-	21.75	21.75
3	68.75	68.25	68.72	-	68.78	68.22
4	140.6	140.2	141.6	-	142.4	140.25

The errors in natural frequencies are tabulated in Table 5-4.

Table 5-4: Percentage errors in identified natural frequencies based on all nodal responses

Mode	Output only modal testing methods				
	FDD Nat. Freq. Error (%)	EFDD Nat. Freq. Error (%)	SSI		
			UPC Nat. Freq. Error (%)	PC Nat. Freq. Error (%)	CVA Nat. Freq. Error (%)
1	-3.5	-	1.85	-7.40	0.03
2	-1.30	-0.46	0.05	-	0.0
3	0.77	0.04	0.07	-	0.82
4	0.25	-0.04	0.09	-	1.53

The small errors represent that there is close agreement between the identified natural frequencies and those obtained from modal analysis. The identified damping ratios based on all nodal responses is given in Table 5-5.

Table 5-5: Damping ratio based on all nodal responses

Mode	Output only PULSE methods					Finite element Modal analysis ξ (%)
	FDD ξ (%)	EFDD ξ (%)	SSI			
			UPC ξ (%)	PC ξ (%)	CVA ξ (%)	
1	-	-	2.1	2.4	3.3	2.0
2	-	1.98	2.0	-	2.3	2.0
3	-	1.99	2.0	-	1.96	2.0
4	-	1.88	2.0	-	2.4	2.0

The errors in extracted percentage damping for all the nodal responses are given in Table 5-6.

Table 5-6: Percentage errors in damping ratios for all nodal responses

Mode	Output only modal testing methods				
	FDD Damp. ratio Error (%)	EFDD Damp. ratio Error (%)	SSI		
			UPC Damp. ratio Error (%)	PC Damp. ratio Error (%)	CVA Damp. ratio Error (%)
1	-	-	5.0	20.0	65.0
2	-	-1.0	0.0	-	15.0
3	-	-0.5	0.0	-	-2.0
4	-	-6.0	0.0	-	20.0

The errors in the damping ratio are quite acceptable in most cases although there are some significant errors in some modes. The real damping ratios values can easily be identified by comparing the damping ratios identified by different methods.

Corresponding mode shapes are presented in Figure 5-5. The mode shapes from output only approach is identical to the mode shape identified by NASTRAN.

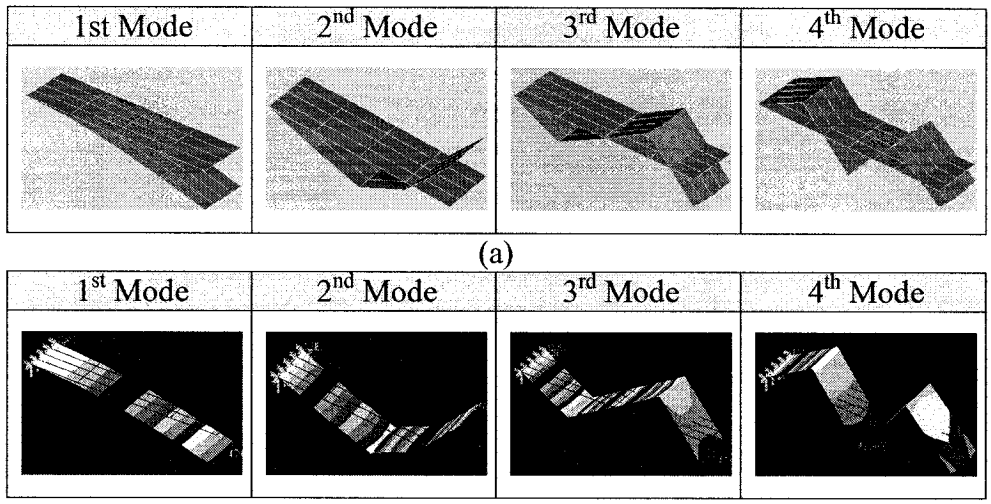

Figure 5-5: Comparison of mode shapes between (a) PULSE and (b) NASTRAN

5.3.2 Modal parameters based on the four nodal responses

The extracted natural frequencies of the solar panel for nodal responses of arbitrary nodes 3, 5, 23 and 25 are given in Table 5-7.

Table 5-7: Identified natural frequencies based on nodal responses of four nodes

Mode	Output only modal testing methods					Finite element Modal analysis f (Hz)
	FDD f (Hz)	EFDD f (Hz)	SSI			
			UPC f (Hz)	PC f (Hz)	CVA f (Hz)	
1	3.125	-	3.30	3.30	3.30	3.24
2	21.68	21.69	21.71	21.14	21.70	21.75
3	68.36	68.26	68.22	-	68.20	68.22
4	140.8	140.5	140.1	-	140.2	140.25

The errors in natural frequencies are tabulated in Table 5-8.

Table 5-8: Percentage errors in identified natural frequencies based on nodal responses of four nodes

Mode	Output only modal testing methods				
	FDD Nat. Freq. Error (%)	EFDD Nat. Freq. Error (%)	SSI		
			UPC Nat. Freq. Error (%)	PC Nat. Freq. Error (%)	CVA Nat. Freq. Error (%)
1	-3.5	-	1.85	1.85	1.85
2	-0.32	-0.28	-0.18	-	-0.23
3	0.21	0.06	0.0	-	-0.03
4	0.39	-0.04	-0.10	-	-0.03

The results show that there is close agreement between the identified natural frequencies using just nodal responses of four nodes and the finite element results. The identified damping ratios for four nodal responses are given in Table 5-9.

Table 5-9: Damping ratio based on nodal responses of four nodes

Mode	Output only PULSE methods					Finite element Modal analysis ξ (%)
	FDD ξ (%)	EFDD ξ (%)	SSI			
			UPC ξ (%)	PC ξ (%)	CVA ξ (%)	
1	-	-	2.0	2.0	2.7	2.0
2	-	1.85	2.0	1.9	2.0	2.0
3	-	1.80	2.0	-	2.0	2.0
4	-	1.60	2.0	-	2.0	2.0

The errors in extracted damping ratios are given in Table 5-10. From the previous analysis in Chapters 3 and 4, it was shown that there is some uncertainty in identifying modal parameters using EFDD. At the same time we can rely on the results from more

advanced method i.e. SSI since the percentage damping results have close agreement with real values.

Table 5-10: Percentage errors in damping ratios

based on nodal responses of four nodes

Mode	Output only modal testing methods				
	FDD	EFDD	SSI		
	Damp. ratio Error (%)	Damp. ratio Error (%)	UPC Damp. ratio Error (%)	PC Damp. ratio Error (%)	CVA Damp. ratio Error (%)
1	-	-	0.0	0.0	35.0
2	-	-7.5	0.0	5.0	0.0
3	-	-10.0	0.0	-	0.0
4	-	-20.0	0.0	-	0.0

Since we have processed only four nodal responses it is impossible to extract the correct mode shapes of the solar panel. So, the modes shapes are not presented here.

5.3.3 Modal parameters based on nodal response at node 3

The extracted natural frequencies of the solar panel based on nodal responses at node 3 are given in Table 5-11.

Table 5-11: Identified natural frequencies based on nodal response at node 3

Mode	Output only modal testing methods					Finite element Modal analysis f (Hz)
	FDD f (Hz)	EFDD f (Hz)	SSI			
			UPC f (Hz)	PC f (Hz)	CVA f (Hz)	
1	3.32	-	3.30	3.30	3.29	3.24
2	21.68	-	21.75	21.43	21.75	21.75
3	68.75	-	68.23	68.19	68.03	68.22
4	140.2	-	140.22	140.5	140.2	140.25

The errors in natural frequencies are tabulated in Table 5-12.

Table 5-12: Percentage errors in identified natural frequencies based on nodal response at node 3

Mode	Output only modal testing methods				
	FDD Nat. Freq. Error (%)	EFDD Nat. Freq. Error (%)	SSI		
			UPC Nat. Freq. Error (%)	PC Nat. Freq. Error (%)	CVA Nat. Freq. Error (%)
1	2.47	-	1.85	1.85	1.54
2	-0.32	-	0.0	-1.47	0.0
3	0.0	-	0.01	-0.04	-0.28
4	-0.04	-	-0.02	0.17	-0.04

Since nodal responses of only one node are considered, the modal parameters cannot be identified using EFDD since zero crossing found to estimate natural frequencies and damping ratios. Percentage errors show that there is close agreement between the identified natural frequencies using response of only node 3 and the finite element results.

The damping ratios based on nodal response at node 3 are given in Table 5-13.

Table 5-13: Damping ratio based on nodal response at node 3

Mode	Output only PULSE methods					Finite element Modal analysis ξ (%)
	FDD ξ (%)	EFDD ξ (%)	SSI			
			UPC ξ (%)	PC ξ (%)	CVA ξ (%)	
1	-	-	1.88	2.2	2.17	2.0
2	-	-	2.0	1.47	2.0	2.0
3	-	-	2.01	2.85	1.9	2.0
4	-	-	2.0	2.12	1.9	2.0

The errors in extracted percentage damping are given in Table 5-14.

Table 5-14: Percentage errors in damping ratios based on nodal response at node 3

Mode	Output only modal testing methods				
	FDD	EFDD	SSI		
	Damp. ratio Error (%)	Damp. ratio Error (%)	UPC Damp. ratio Error (%)	PC Damp. ratio Error (%)	CVA Damp. ratio Error (%)
1	-	-	-6.0	10.0	8.5
2	-	-	0.0	-26.5	0.0
3	-	-	0.5	42.5	-5.0
4	-	-	0.0	6.0	-5.0

The errors in extracted percentage damping ratio are reasonable except for 2nd and 3rd mode of the PC method. The mode shapes are not presented here as mode shape of one node does not carry any information and can not be distinguished.

5.3.4 Modal parameters based on the nodal response at node 5

The extracted natural frequencies of the solar panel based on the nodal response at node 5 are given in Table 5-15.

Table 5-15: Identified natural frequencies based on nodal response at node 5

Mode	Output only modal testing methods					Finite element Modal analysis
	FDD	EFDD	SSI			
	f (Hz)	f (Hz)	UPC f (Hz)	PC f (Hz)	CVA f (Hz)	f (Hz)
1	3.3	-	3.30	3.30	3.30	3.24
2	21.68	-	21.75	21.64	21.74	21.75
3	68.55	-	68.22	68.90	68.22	68.22
4	140.6	-	140.3	139.4	140.3	140.25

The errors in natural frequencies are tabulated in Table 5-16.

Table 5-16: Percentage errors in identified natural frequencies based on nodal response at node 5

Mode	Output only modal testing methods				
	FDD Nat. Freq. Error (%)	EFDD Nat. Freq. Error (%)	SSI		
			UPC Nat. Freq. Error (%)	PC Nat. Freq. Error (%)	CVA Nat. Freq. Error (%)
1	1.85	-	1.85	1.85	1.85
2	-0.32	-	0.0	-0.69	-0.05
3	0.48	-	0.0	0.99	0.0
4	0.24	-	0.03	-0.61	0.04

The errors represents that there is close agreement between the identified natural frequencies using just response of node 5 and the NASTRAN.

The damping ratios based on nodal response at node 5 are given in Table 5-17.

Table 5-17: Damping ratios based on nodal response at node 5

Mode	Output only PULSE methods					Finite element Modal analysis ξ (%)
	FDD ξ(%)	EFDD ξ (%)	SSI			
			UPC ξ (%)	PC ξ (%)	CVA ξ (%)	
1	-	-	2.0	2.0	2.0	2.0
2	-	-	2.0	1.8	2.0	2.0
3	-	-	2.0	1.6	2.0	2.0
4	-	-	2.0	1.8	1.9	2.0

The errors in extracted percentage damping are given in Table 5-18.

Table 5-18: Percentage errors in damping ratios based on nodal response at node 5

Mode	Output only modal testing methods				
	FDD	EFDD	SSI		
	Damp. ratio Error (%)	Damp. ratio Error (%)	UPC Damp. ratio Error (%)	PC Damp. ratio Error (%)	CVA Damp. ratio Error (%)
1	-	-	0.0	0.0	0.0
2	-	-	0.0	-10.0	0.0
3	-	-	0.0	-20.0	0.0
4	-	-	0.0	-10.0	5.0

It is found that the modal parameters identified for all the four cases have good agreement with the finite element results. Upon careful observations of the damping ratios any unrealistic value can easily be identified and avoided. The mode shapes are also not presented here as mode shape of one node does not carry any information and cannot be distinguished.

5.4. SUMMARY

In this chapter the simulation of a solar panel appendage under real operation condition on-orbit (thruster excitation) is presented.

The natural frequencies and damping ratios identified by output only modal testing technique are in close agreement with the results from NASTRAN. Usually, in real cases, only few nodal responses are recorded and processed which is applied in this chapter. It is shown that the acceptable natural frequencies and damping ratios can be identified even by using nodal response at single node. Although some optimization in the number and location of nodal responses is required to minimize the errors in identification.

CHAPTER 6

CONCLUSIONS AND RECOMMENDATIONS

6.1 CONCLUSIONS

The investigation is devoted to the implementation of the different techniques for on-orbit output only modal testing on satellite appendages in space. The present work put emphasizes on the analytical and experimental data to investigate the applicability of output only modal testing technique on-orbit application. The conclusions drawn on this study will help in real applications of such on-orbit testing of satellites.

The most important conclusions and contributions from the current work are listed as follows:

- An effective analytical approach has been investigated considering dynamics of satellite appendages and associated excitation methods to identify the modal parameters. In this method, the solar panel, antenna or other appendages are modeled as simple plate structure under real operation condition in space.

- Based on the results from analytical approach a plate type test article has been designed for experimental testing. Output only modal testing technique has been successfully implemented in the experimental testing. Modal parameters are extracted for the test article for driven base and single point excitation. Although the satellite appendages experience driven base excitation, single point loading

was also used in output only modal testing to compare the extracted modal parameters.

- Analytically it has been confirmed that the multiple-point excitation is better compared to other two-excitation methods i.e. driven base and single point excitation. Also, experimentally is has been found that between the driven base and single point excitation, driven base is better choice for the extraction of modal parameters using output-only modal testing techniques.

- With the help of simulation technique the modal parameters have been identified using just few nodal responses, which is typically a real case scenario. Hence, output only modal testing technique can be effectively implemented in the satellite appendages when they experience driven base excitation. This finding will help working with more complex satellite appendages under driven base load condition.

6.2 RECOMMENDATIONS FOR FUTURE WORK

The methodologies developed and presented in this study have been successfully applied to the satellite appendages modeled as simple plate type of structure considering the real relevant case satellite environment.

The recommendations for future work are:

- This research has been carried out on analytical and test data, however it is important to check the applicability of output only modal testing technique on real

operation data from space. Some optimization is required on the number and location of nodal responses based on the mass and instrumentation, cost, and operational limitations required for output only modal testing.

- This thesis is focused on a simple linear structure. In actual case, the structures of the solar panel are composed of flexible non-linear and complicated structure. Thus these tests should be carried-out on such structures. Also, study has been carried-out on the structure with widely spaced modes. Similar kind of analysis can be done on structure with closely spaced modes.

- Finally, the experimental testing has been executed using base-excitation in the out-of-plane direction and the data are acquired in the out-of-plane direction. But in practical cases in the space, satellite solar panels are excited with rotational base excitation. So, experiments should be carried out using rotational type base excitation.

REFERENCES

[1]. Bendat, J. S. and Piersol, A. G., *"Engineering applications of correlation and spectral analysis"*, John Wiley, New York, 1993

[2]. Ibrahim, S. R. and Milkulcik, E. C.,*"A time domain modal vibration test technique"*, Shock and vibration bulletin vol. 43 pp. 21-37, 1973

[3]. Ibrahim, S. R. and Milkulcik, E. C., *"The experimental determination of vibration parameters from time response"*, Shock and vibration bulletin vol.46 pp.187-196, 1976

[4]. Ibrahim, S. R. and Milkulcik, E. C.,*"A method for the direct identification of vibration parameters from the response"*, Shock and vibration bulletin vol. 47(4) pp. 183-198, 1977

[5]. Vold, H., Kundrat, J. and Rocklin, G. T., *"A multi-input modal estimation algorithm for mini-computers"*, SAE technical paper No.820194, 1982

[6]. Vold, H. and Rocklin, G. T., *"A numerical implementation of multi-input modal estimation method for mini-computers"*, Proceedings of the 1st international modal analysis conference, pp. 542-548, 1982

[7]. Juang, J.-N. and Pappa, R. S., *"An eigensystem realization algorithm for modal parameter identification and modal reduction"*, AIAA Journal of guidance, control, and dynamics, vol. 8(5) pp. 620-627, 1985

[8]. Juang, J.-N. and Pappa, R. S., *"Galileo Spacecraft Modal identification using an eigensystem realization algorithm"*, AIAA paper number 84-1070, 1984, pp. 18.

[9]. Cooper, J. E. and Wright J. R., *"Spacecraft in-orbit identification using eigensystem realization methods"*, AIAA Journal of guidance, control, and dynamics, vol. 15(2) pp. 352-359, 1992

[10]. Fukuzono, K., *"Investigation of multiple reference Ibrahim time domain parameter estimation technique,* M.S. thesis, dept. of mechanical and industry engineering, University of Cincinnati, 1986

[11]. Zhang, L., Brincker, R. and Andersen, P., *"A unified approach for two-stage time domain modal identification"*, Proceedings of the international conference on structural dynamics modeling-test, analysis, correlation, and validation, Madeira Island, 2002

[12]. Van Overschee, P. and De Moor, B., *"Subspace identification for linear systems: theory, implementation and applications"*, Kluwer Academic Publishers, Dordrecht (Netherlands), 1996

[13]. Van Overschee, P. and De Moor, B., *"Subspace algorithm for the stochastic identification problem"*, Automatica vol. 29 (3), pp. 649-660, 1993

[14]. Van Overschee, P. and De Moor, B., *"N4SID: Subspace algorithms for the identification of combined deterministic stochastic systems"*, Automatica vol. 30(1), pp. 75-93, 1994

[15]. Van Overschee, P. and De Moor, B., *"A unifying theorem for three subspace system identification algorithms"*, Automatica vol. 31(12), pp. 1853-1864, 1995

[16]. Pandit, S. M., *"Modal and spectrum analysis: data dependent systems in state space"*, John Wiley & Sons, Inc., New York, 1991

[17]. Peeters, B. and De Roeck, G., *"Reference-based stochastic subspace identification for output-only modal analysis"*, Mechanical systems and signal processing, vol. 13(6), pp. 855-878, 1999

[18]. Peeters, B. and De Roeck, G., *"Stochastic system identification for operational modal analysis"*, Journal of dynamics, measurement, and control, ASME, vol. 123, pp. 659-667, 2001

[19]. Lardies, J., *"Detection of mechanical changes in vibration systems"*, Proceedings of the 13th international modal analysis conference, pp. 1057-1062, 1995

[20]. Lardies, J., *"Modal Parameter Identification from output-only measurements"*, Mechanics Research Communications, vol. 24(5) pp. 521-528, 1997

[21]. Ren, W.-X. and Zong, Z.-H., *"Output only modal parameter identification of civil engineering structure"*, Journal of structural engineering and mechanics, vol. 17(3-4) pp. 1-16, 2004

[22]. Brincker, R., Zhang, L. and Andersen, P., *"Modal identification of output-only systems using frequency domain decomposition"*, Proceedings of European COST F3 conference on System Identification and Structural Health Monitoring, Madrid (Spain), 2000

[23]. Brincker, R., Ventura, C. E., Andersen, P., *"Why output-only modal testing is a desirable tool for a wide range of practical applications"*, Proceedings of 21st international modal analysis conference on Structural Dynamics, Kissimmee, Orlando, Florida, 2003

[24]. Bricker, R. and Andersen, P., *"A way of getting scaled mode shapes in output-only modal testing"*, Proceedings of 21st international modal analysis conference on structural dynamics , Kissimmee, Orlando, Florida, 2003

[25]. Doebling, S. W. and Farrar, C. R., *"Computation of structural flexibility for bridge health monitoring using ambient modal data"*, Proceedings of the 11th ASCE engineering mechanics conference, pp.1114-1117, 1996

[26]. Deweer, J. and Dierckk, B., *"Obtaining a scaled modal model of panel type structures using acoustic excitation"*, Proceedings of the 17th international modal analysis conference, pp. 2042-2048, 1999

[27]. Randall, R. B., Gao, Y. and Swevers, J., *"Updating modal models from response measurements"*, Proceedings of the 23rd international conference on noise and vibration engineering (ISMA23), pp. 1153-1160, 1998

[28]. Parloo, E., Verboven, P., Guillaume, P., and Van Overmeire, M., *"Sensitivity-based operational mode shape normalization in mechanical systems and signal"*, Mechanical systems and processing vol. 16(5) pp. 757-767, 2002

[29]. Sestieri, A., and D'Ambrogio, W., *"Frequency response function versus output-only modal testing identification"*, Proceedings of 21st international modal analysis conference on structural dynamics, Kissimmee, Orlando, Florida, Feb 3-6, 2003

[30]. Schwarz, B. and Richardson, M., *"Scaling mode shapes obtained from operating data"*, Proceedings of international modal analysis conference on structural dynamics, Kissimmee, Orlando, Florida, Feb 3-6, 2003

[31]. Abdelghani, M., Goursat, M., Biolchini, T., Hermans, L. and Van Der Auweraer, H., *"Performance of output-only identification algorithms for modal analysis of aircraft structures"*, Proceedings of the 17th International Modal Analysis Conference, Kissimmee, Orlando, Florida, 1999

[32]. Richardson, M. and Schwarz, B., *"Modal parameter estimation from operating data"*, Journal of Sound and Vibration, 2003

[33]. Guillaume, P., Verboven, P., and Vanlanduit, S., *"Frequency-domain maximum likelihood identification of modal parameters with confidence intervals"*, International proceedings of ISMA 23, Leuven, Belgium, pp. 16-18, 1998

[34]. Guillaume, P., Pintelon, R. and Schoukens, J., *"Frequency domain- a survey"*, In proceedings of ISMA 21, Leuven, Belgium, pp. 651-658, 1966

[35]. Heylen, W., Lammens, S., and Sas, P., *"Modal analysis theory and testing"*, Department of Mechanical Engineering, Leuven, Belgium, 1995

[36]. Verboven, P., *"Frequency domain system identification for modal analysis"*. PhD Thesis, Belgium, 2002

[37]. Pintelon, R. and Schoukens, J., *"System identification: a frequency domain approach"* IEEE Press, New York, 2001

[38]. Van der Auweraer, H., Guillaume, P., Verboven, P. and Vanlanduit, S., *"Application of a fast-stabilizing frequency domain parameter estimation method,* ASME Journal of Systems, Measurement, and Control vol. 4, pp. 451-658, 2001

[39]. Guillaume, P., Verboven, P., Vanlanduit, S., and Van der Auweraer, H., *"A poly-reference implementation of the least-squares complex frequency-domain estimator",* In proceedings of IMAC 21, the International Modal Analysis Conference, Kissimmee, Orlando, Florida, 2003

[40]. Peeters, B., Guillaume, P., Van der Auweraer, H., Cauberghe, P., Verboven, P., and Leuridan, L., *"Automotive and aerospace applications of PolyMAX modal parameter estimation method",* In proceedings of IMAC 22, the International Modal Analysis Conference, Dearborn (MI), 2004

[41]. Peeters, B., Pauwels, S., and Debille, J., *"Enhanced exploration of vibration test data by the PolyMAX modal parameters estimation method",* In proceedings of the 5th international symposium on Environmental Testing for Space programs, Noordwik, The Netherlands, 2004

[42]. Hermans, L., Guillaume, P. and Van der Auweraer, H., *"A frequency domain maximum likelihood approach for the extraction of modal parameters from output-only data"*, In proceedings of ISMA 23, the international conference on Noise and Vibration Engineering, Leuven, Belgium, 1998

[43]. Canadian RADARSAT-2 Satellite, Satellite image from Canadian Space Agency website, 2007

[44]. Fortescue, P. and Stark, J., *"Spacecraft Systems Engineering",* John Wiley and Sons, New York, 1991

[45]. Wertz, J. R. and Larson, W. J., *"Space mission analysis and design",* 3rd edition, Dordrecht, Netherlands; Boston, 1999

[46]. Fraser, D., Kleespies, H. and Vasicek, C., *"Spacecraft structure",* Texas Space grant consortium, Texas, 1991

[47]. Freeman, M. T., *"Spacecraft on-orbit deployment anomalies: what can be done?",* IEEE AES Systems Magazine, pp. 3-15, 2003.

[48]. Zhang, L. and Chen, Y., *"The on-orbit thermal-structure analysis of the spacecraft component using MSC/NASTRAN"*, Beijing Inst. of spacecraft system engineer, CAST, MSC Aerospace Users' Conference Proceedings, China, 1999

[49]. Vigneron, F. R., Parthasarathy, A., and Harrison, T. D., *"Analysis of the structural dynamics of a flexible solar array and correlation with ground-testing"*, AIAA/CASI 6th Communications Satellite System Conference, AIAA Paper no. 76-242, pp.1-9, 1976

[50]. Modi, V. J. and Ng, A. C., *"Dynamics of interconnected flexible members in the presence of environmental Forces: a formulation with applications"*, Acta Astronautica Vol. 19(6/7), pp. 561-571, 1989

[51]. Modi, V. J. and Ibrahim, A. M., *"Dynamics of the orbiter based construction of structural components for Space platforms"*, Acta Astronautica Vol. 12(10), pp. 879-888, 1985

[52]. Brüel and Kjaer, *"Output- only modal testing techniques"*, User Guide, Magazine No. 1, 2003

[53]. Mickleborough, N. C. and Pi, Y. L., *"Modal parameter identification using z-transformations"*, International journal for numerical methods in engineering, vol. 28(10), pp 2307-2321, 1989

[54]. Peeters, B. and Van der Auweraer, H., *"PolyMAX: A revolution in operational modal analysis"*, Proceedings of the 1st international Operational Modal Analysis Conference, Denmark, 2005

[55]. Peeters, B., *"System identification and damage detection in civil engineering"*, PhD thesis, Department of Civil Engineering, K U Leuven, Belgium, 2000

[56]. Hermans, L. and Van der Auweraer, H., *"Modal testing and analysis of structures under operational conditions: industrial applications"*, Mechanical systems and signal processing, vol. 13(2) pp. 193-216, 1999

[57]. Oppenheim, A. V. and Schafer, R. W., *"Digital signal processing"*, Prentice-Hall, New Jersey, 1975

[58]. Cauberghe, B., *"Applied frequency-domain system identification in the field of operational modal analysis,"* PhD thesis, Department of Mechanical Engineering, Brussels, Belgium, 2004

[59]. B&K's PULSE software User guide, 2003

[60]. Blevins, R. D., *" Formulas for natural frequency and mode shape"*, Published by Van Nostrand Reinhold company, New York, 1979

[61]. Warburton, G. B., *"The vibration of rectangular plates"*, Proceedings of the institute of mechanical engineers, part A, power and process engineering, vol. 168, pp. 371-384, 1954

[62]. Martin, A. I., *"On the vibration of a cantilever plate"*, The quarterly journal of mechanics and applied mathematics, vol. 9(1), pp. 94-102, 1956

[63]. Leissa, A. W., *"The free vibration of rectangular plates"*, Journal of sound and vibration, vol. 31, pp. 257-293, 1973

[64]. MSC.Nastran™ and MSC.Patran® User Guide v2005 r3, 2005

[65]. MATLAB User Guide, Version 7.0, 2004

APPENDIX-I

% MATLAB Codes to generate a configuration file in universal file format

```
%************************************************************************
clc
clear all

uf = fopen('configuration.uff','w');

fprintf(uf,'%6d\n',-1);
fprintf(uf,'%6d\n',15);

m=input('Numbers of Nodes = ');
A=[m,7];
for i=1:m
    A(i,1)=input('Node Number = ');
    A(i,2)=0;
    A(i,3)=0;
    A(i,4)=0;
    A(i,5)=input('x-coordinate = ');
    A(i,6)=input('y-coordinate = ');
    A(i,7)=input('z-coordinate = ');
end

for j=1:m;
    fprintf(uf,'%10d%10d%10d%10d%13.5e%13.5e%13.5e\n',A(j,1),A(j,2),...
        A(j,3),A(j,4),A(j,5),A(j,6),A(j,7));
    j=j+1;
end

fprintf(uf,'%6d\n',-1);

%************************************************************************
fprintf(uf,'%6d\n',-1);
fprintf(uf,'%6d\n',82);

p=input('Number of Global Trace Lines = ');
B=[p,3];
for k=1:p
    B(k,1)=0;
    B(k,2)=input('Global Trace Line from Node1=');
    B(k,3)=input('Global Trace Line to Node2=');
end

fprintf(uf,'%10d%10d%10d\n',1,3*p,0);
fprintf(uf,'%s\n','Global Trace Lines');

%************************************************************************
```

```
iter = floor(p/8);
left = rem(p,8);
i = 1;
for line=1:iter
    fprintf(uf,'%10d%10d%10d%10d%10d%10d%10d%10d\n',B(i,1),B(i,2),...
        B(i,3),B(i+1,1),B(i+1,2),B(i+1,3),B(i+2,1),B(i+2,2));

fprintf(uf,'%10d%10d%10d%10d%10d%10d%10d%10d\n',B(i+2,3),B(i+3,1),...
        B(i+3,2),B(i+3,3),B(i+4,1),B(i+4,2),B(i+4,3),B(i+5,1));

fprintf(uf,'%10d%10d%10d%10d%10d%10d%10d%10d\n',B(i+5,2),B(i+5,3),...
        B(i+6,1),B(i+6,2),B(i+6,3),B(i+7,1),B(i+7,2),B(i+7,3));
    i = i + 8;
end
if left == 1
    fprintf(uf,'%10d%10d%10d\n',B(i,1),B(i,2),B(i,3));

elseif left == 2
    fprintf(uf,'%10d%10d%10d%10d%10d%10d\n',B(i,1),B(i,2),B(i,3),...
        B(i+1,1),B(i+1,2),B(i+1,3));

elseif left == 3
    fprintf(uf,'%10d%10d%10d%10d%10d%10d%10d%10d\n',B(i,1),B(i,2),...
        B(i,3),B(i+1,1),B(i+1,2),B(i+1,3),B(i+2,1),B(i+2,2));
    fprintf(uf,'%10d\n',B(i+2,3));

elseif left == 4
    fprintf(uf,'%10d%10d%10d%10d%10d%10d%10d%10d\n',B(i,1),B(i,2),...
        B(i,3),B(i+1,1),B(i+1,2),B(i+1,3),B(i+2,1),B(i+2,2));

fprintf(uf,'%10d%10d%10d%10d\n',B(i+2,3),B(i+3,1),B(i+3,2),B(i+3,3));

elseif left == 5
    fprintf(uf,'%10d%10d%10d%10d%10d%10d%10d%10d\n',B(i,1),B(i,2),...
        B(i,3),B(i+1,1),B(i+1,2),B(i+1,3),B(i+2,1),B(i+2,2));
    fprintf(uf,'%10d%10d%10d%10d%10d%10d%10d\n',B(i+2,3),B(i+3,1),...
        B(i+3,2),B(i+3,3),B(i+4,1),B(i+4,2),B(i+4,3));

elseif left == 6
    fprintf(uf,'%10d%10d%10d%10d%10d%10d%10d%10d\n',B(i,1),B(i,2),...
        B(i,3),B(i+1,1),B(i+1,2),B(i+1,3),B(i+2,1),B(i+2,2));

fprintf(uf,'%10d%10d%10d%10d%10d%10d%10d%10d\n',B(i+2,3),B(i+3,1),...
        B(i+3,2),B(i+3,3),B(i+4,1),B(i+4,2),B(i+4,3),B(i+5,1));
    fprintf(uf,'%10d%10d\n',B(i+5,2),B(i+4,3));

elseif left == 7
    fprintf(uf,'%10d%10d%10d%10d%10d%10d%10d%10d\n',B(i,1),B(i,2),...
        B(i,3),B(i+1,1),B(i+1,2),B(i+1,3),B(i+2,1),B(i+2,2));

fprintf(uf,'%10d%10d%10d%10d%10d%10d%10d%10d\n',B(i+2,3),B(i+3,1),...
        B(i+3,2),B(i+3,3),B(i+4,1),B(i+4,2),B(i+4,3),B(i+5,1));
    fprintf(uf,'%10d%10d%10d%10d%10d\n',B(i+5,2),B(i+5,3),B(i+6,1),...
        B(i+6,2),B(i+6,3));
```

```
end

fprintf(uf,'%6d\n',-1);

%**********************************************************************
fprintf(uf,'%6d\n',-1);
fprintf(uf,'%6d\n',82);

q=input('Number of Additional Surface Trace Lines = ');
C=[q,3];
for l=1:q
    C(l,1)=0;
    C(l,2)=input('Additional Surface Line from Node1=');
    C(l,3)=input('Additional Surface Line to Node2=');
end

fprintf(uf,'%10d%10d%10d\n',2,3*q,0);
fprintf(uf,'%s\n','Additional Trace Lines');

%**********************************************************************
iter1 = floor(q/8);
left1 = rem(q,8);
i = 1;
for line=1:iter1
    fprintf(uf,'%10d%10d%10d%10d%10d%10d%10d%10d\n',C(i,1),C(i,2),...
        C(i,3),C(i+1,1),C(i+1,2),C(i+1,3),C(i+2,1),C(i+2,2));

fprintf(uf,'%10d%10d%10d%10d%10d%10d%10d%10d\n',C(i+2,3),C(i+3,1),...
        C(i+3,2),C(i+3,3),C(i+4,1),C(i+4,2),C(i+4,3),C(i+5,1));

fprintf(uf,'%10d%10d%10d%10d%10d%10d%10d%10d\n',C(i+5,2),C(i+5,3),...
        C(i+6,1),C(i+6,2),C(i+6,3),C(i+7,1),C(i+7,2),C(i+7,3));
    i = i + 8;
end
if left1 == 1
    fprintf(uf,'%10d%10d%10d\n',C(i,1),C(i,2),C(i,3));

elseif left1 == 2
    fprintf(uf,'%10d%10d%10d%10d%10d%10d\n',C(i,1),C(i,2),C(i,3),...
        C(i+1,1),C(i+1,2),C(i+1,3));

elseif left1 == 3
    fprintf(uf,'%10d%10d%10d%10d%10d%10d%10d%10d\n',C(i,1),C(i,2),...
        C(i,3),C(i+1,1),C(i+1,2),C(i+1,3),C(i+2,1),C(i+2,2));
    fprintf(uf,'%6d\n',C(i+2,3));

elseif left1 == 4
    fprintf(uf,'%10d%10d%10d%10d%10d%10d%10d%10d\n',C(i,1),C(i,2),...
        C(i,3),C(i+1,1),C(i+1,2),C(i+1,3),C(i+2,1),C(i+2,2));

fprintf(uf,'%10d%10d%10d%10d\n',C(i+2,3),C(i+3,1),C(i+3,2),C(i+3,3));

elseif left1 == 5
    fprintf(uf,'%10d%10d%10d%10d%10d%10d%10d%10d\n',C(i,1),C(i,2),...
        C(i,3),C(i+1,1),C(i+1,2),C(i+1,3),C(i+2,1),C(i+2,2));
```

```
    fprintf(uf,'%10d%10d%10d%10d%10d%10d%10d\n',C(i+2,3),C(i+3,1),...
        C(i+3,2),C(i+3,3),C(i+4,1),C(i+4,2),C(i+4,3));

elseif left1 == 6
    fprintf(uf,'%10d%10d%10d%10d%10d%10d%10d%10d\n',C(i,1),C(i,2),...
        C(i,3),C(i+1,1),C(i+1,2),C(i+1,3),C(i+2,1),C(i+2,2));

fprintf(uf,'%10d%10d%10d%10d%10d%10d%10d%10d\n',C(i+2,3),C(i+3,1),...
        C(i+3,2),C(i+3,3),C(i+4,1),C(i+4,2),C(i+4,3),C(i+5,1));
    fprintf(uf,'%10d%10d\n',C(i+5,2),C(i+4,3));

elseif left1 == 7
    fprintf(uf,'%10d%10d%10d%10d%10d%10d%10d%10d\n',C(i,1),C(i,2),...
        C(i,3),C(i+1,1),C(i+1,2),C(i+1,3),C(i+2,1),C(i+2,2));

fprintf(uf,'%10d%10d%10d%10d%10d%10d%10d%10d\n',C(i+2,3),C(i+3,1),...
        C(i+3,2),C(i+3,3),C(i+4,1),C(i+4,2),C(i+4,3),C(i+5,1));
    fprintf(uf,'%10d%10d%10d%10d%10d\n',C(i+5,2),C(i+5,3),C(i+6,1),...
        C(i+6,2),C(i+6,3));

end

fprintf(uf,'%6d\n',-1);

%************************************************************************
fprintf(uf,'%6d\n',-1);
fprintf(uf,'%6d\n',2412);

r=input('Number of Surface = ');
D=[r,3];
for i=1:r
    D(i,1)=input('1st Node of the Surface= ');
    D(i,2)=input('2nd Node of the Surface= ');
    D(i,3)=input('3rd Node of the Surface= ');
end

for j=1:r;
    fprintf(uf,'%10d%10d%10d%10d%10d%10d\n',j,91,1,1,0,3);
    fprintf(uf,'%10d%10d%10d\n',D(j,1),D(j,2),D(j,3));
    j=j+1;
end

fprintf(uf,'%6d\n',-1);
```

-End of codes-

```
% Matlab code to record the data from NASTRAN output file and write an
% universal data file with help of a function written in
% unv_write_time.m (mentioned in the next section)

%*************************************************************************
% Variables used:
% time_inc = Increment of time
% time_start = Strarting time
% time_line = Number of line per points
% refpoint_id = Number of the reference point
% refpoint_dir = Direction of the reference point
% no_points = Number of points
% point_id = Point identifier
% data = Matrix where all the data are stored

%*************************************************************************
function nast_trans

file_name = uigetfile('.f06','Nastran files');

if file_name == 0
    return
end

% Open the file
fid = fopen(file_name);

% Thease values need to be inserted
time_line =4000;
time_inc = 0.0078125;
time_start = 0;
refpoint_id=1;
refpoint_dir=2;

% Delete all data up to the number of points
for line=1:199
    temp = fgetl(fid);
end

% Get the number of points
temp = fscanf(fid,'%13s',[1,1]);
temp = fscanf(fid,'%13s',[1,1]);
temp = fscanf(fid,'%13s',[1,1]);
temp = fscanf(fid,'%13s',[1,1]);
temp = fscanf(fid,'%13s',[1,1]);
no_points = fscanf(fid,'%13e',[1,1]);

% Delete values up to the point id
for line=line:359
    temp = fgetl(fid);
end

% Get the first point id
temp = fscanf(fid,'%13s',[1,1]);
temp = fscanf(fid,'%13s',[1,1]);
```

```
point_id = fscanf(fid,'%13e',[1,1]);

% Remove lines up to the begenning of data
for line=line:362
    temp = fgetl(fid);
end


% First loop to gather all the points
indice = 1;
uf = fopen('Data.uff','w');

%writinf the uff 151 heading information

fprintf(uf,'%6d\n',-1);
fprintf(uf,'%6d\n',151);

fprintf(uf,'%s\n', 'Cantilever Beam');
fprintf(uf,'%s\n', 'NONE');
fprintf(uf,'%s\n', 'NASTRAN OUTPUT');
fprintf(uf,'%s\n', date);
fprintf(uf,'%s\n', 'NONE');
fprintf(uf,'%s\n', 'NONE');
fprintf(uf,'%s\n', 'NONE');

fprintf(uf,'%6d\n',-1);

%wait handle

wait_handle = waitbar(0,'Please wait exporting in progress...');
for k=1:no_points

    % Loop to get all the data blocks
    for j=1:floor(time_line/50)

        % Loop to collect the data within a complete set of data
        for i=1:50
            temp = fscanf(fid,'%13e',[1,1]);
            temp = fscanf(fid,'%13s',[1,1]);
            temp = fscanf(fid,'%13e',[1,1]);
            data(indice,1) = fscanf(fid,'%13e',[1,1]);
            temp = fgetl(fid);
            indice = indice + 1;
        end

        % Delete uncessary data in between the data sets
        for i=1:7
            temp = fgetl(fid);
        end
    end

    % Loop to collect the remaining data from an incomplete block
    for i=1:rem(time_line+1,50)
            temp = fscanf(fid,'%13e',[1,1]);
```

```
            temp = fscanf(fid,'%13s',[1,1]);
            temp = fscanf(fid,'%13e',[1,1]);
            data(indice,1) = fscanf(fid,'%13e',[1,1]);
            temp = fgetl(fid);
            indice = indice + 1;
    end

    % Obtain the second point ID

    real=data(1:4001,1);

    unv_write_time(real,time_start,time_line,time_inc,point_id,...
    refpoint_id,refpoint_dir,uf)

    temp = fgetl(fid);
    temp = fgetl(fid);
    temp = fgetl(fid);
    temp = fscanf(fid,'%13s',[1,1]);
    temp = fscanf(fid,'%13s',[1,1]);
    point_id = fscanf(fid,'%13e',[1,1]);
    temp = fgetl(fid);
    temp = fgetl(fid);
    temp = fgetl(fid);
    temp = fgetl(fid);

    waitbar(k/no_points)

end
% Close the file
fclose(fid);
fclose(uf);
delete(wait_handle);

return
```

-End of codes-

```
% MATLAB codes to transform the recorded data by nastr_trans_unv.m
% into universal file format

%*************************************************************************
% Parameters are:
% freq_inc = Increment of frequencies
% freq_start = Strarting frequency
% freq_line = Number of line per points
% refpoint_id = Number of the reference point
% refpoint_dir = Direction of the reference point
% no_points = Number of points
% point_id =  Point identifier
% real = Matrix where all the real value are stored

%*************************************************************************
function unv_write(real,time_start,time_line,time_inc,point_id,...
    refpoint_id,refpoint_dir,uf)

%  Writing of start line and dataset type line
fprintf(uf,'%6d\n',-1);
fprintf(uf,'%6d\n',58);

%  Writing of 5 id records
fprintf(uf,'%s%2d\n','Time Response of point',point_id);
fprintf(uf,'%s\n', '[UID=Response]');
fprintf(uf,'%s\n', date);
fprintf(uf,'%s\n','NONE');
fprintf(uf,'%s\n', 'NONE');

%  Writing of record 6
fprintf(uf,'%5d%10d%5d%10d %s%16d%4d %s%10d%4d\n',1,0,0,0,'NONE',...
    point_id,2,'NONE',refpoint_id,refpoint_dir);
%  Writing of record 7
fprintf(uf,'%10d%10d%10d%13.5e%13.5e%13.5e\n',2,time_line+1,1,...
    time_start,time_inc,0);

%  Writing of records 8, 9 and 10
fprintf(uf,'%10d%5d%5d%5d %s %s\n',17,0,0,0,...
    'X-axix                ','sec                  ');
fprintf(uf,'%10d%5d%5d%5d %s %s\n',12,0,0,0,...
    'NONE                  ','g                    ');
fprintf(uf,'%10d%5d%5d%5d %s %s\n', 0,0,0,0,...
    'NONE                  ','NONE                 ');
fprintf(uf,'%10d%5d%5d%5d %s %s\n', 0,0,0,0,...
    'NONE                  ','NONE                 ');

iter = floor((time_line+1)/6);
left = rem((time_line+1),6);
i = 1;
for line=1:iter
    fprintf(uf,'%13.5e%13.5e%13.5e%13.5e%13.5e%13.5e\n',...
        real(i),real(i+1),real(i+2),real(i+3),real(i+4),real(i+5));
    i = i + 6;
end
if left == 1
```

```
    fprintf(uf,'%13.5e\n',real(i));
elseif left == 2
    fprintf(uf,'%13.5e%13.5e\n',real(i),real(i+1));
elseif left == 3
    fprintf(uf,'%13.5e%13.5e%13.5e\n',real(i),real(i+1),real(i+2));
elseif left == 4

fprintf(uf,'%13.5e%13.5e%13.5e%13.5e\n',real(i),real(i+1),real(i+2),...
        real(i+3));
elseif left == 5
    fprintf(uf,'%13.5e%13.5e%13.5e%13.5e%13.5e\n',real(i),real(i+1),...
        real(i+2),real(i+3),real(i+4));
end

%  Writing of last record
fprintf(uf,'%6d\n',-1);
```

-End of codes-

```
% Configuration file written can be saved as configuation.cfg. This
% file can be used as a optional filing system necessary to read data
% in ASCII format.
```

This is the header group with the title of the project.
The title can be a string of any length.
Header
PULSE Configuration file for a Cantilever Beam

This is the sampling interval specified in seconds.
T
0.001953125

This is the node definition group.
Node Number, X-coordinate, Y-coordinate, Z-coordinate.
Nodes

1	0	0	0
2	4.8	0	0
3	9.6	0	0
4	4.4	0	0
5	9.2	0	0
6	24.0	0	0
7	28.8	0	0
8	33.6	0	0
9	38.4	0	0
10	43.2	0	0
11	48.0	0	0

This is the line definition group.
From Node Number, To Node Number.

Lines

1	2
2	3
3	4
4	5
5	6
6	7
7	8
8	9
9	10
10	11

This is the surface definition group.
From Node Number, To Node Number.
Surfaces

This is the definition group for the DOF information.
Description of the setups block
Record 1:
Field 1: (string) Data set label

Record 2:
Field 1: (string) File name where data is stored column wise in ASCII

Record 3 through end
Field 1: (non-zero positive integer) Global transducer number
Field 2: (floating point) X-directional coordinate of the transducer
Field 3: (floating point) Y-directional coordinate of the transducer
Field 4: (floating point) Z-directional coordinate of the transducer
Field 5: (floating point) Reference value to apply on dB plots of PSD
Field 6: (string) Unit of the data - No blank spaces allowed
Field 7: (string) Measurement quantity.
Field 8: (string) ID string of the transducer.

Note: Records 1 to 3 are repeated for each data set.Fields 5 through 8 are optionally. However, leaving out a field means leaving out the rest of the fields as well. The default value of field 5 is 1.0.

Setups
Measurement 1
nastran_exprcantileverbeam10elementsbase5dampexcite.asc

1	0	1	0	1	g	Acceleration	Transducer 1
2	0	1	0	1	g	Acceleration	Transducer 2
3	0	1	0	1	g	Acceleration	Transducer 3
4	0	1	0	1	g	Acceleration	Transducer 4
5	0	1	0	1	g	Acceleration	Transducer 5
6	0	1	0	1	g	Acceleration	Transducer 6
7	0	1	0	1	g	Acceleration	Transducer 7
8	0	1	0	1	g	Acceleration	Transducer 8
9	0	1	0	1	g	Acceleration	Transducer 9
10	0	1	0	1	g	Acceleration	Transducer 10
11	0	1	0	1	g	Acceleration	Transducer 11

This is the definition group for slave node equations.
Left side node should move according to the right side equation.
Equations

-End of file-

APPENDIX-II

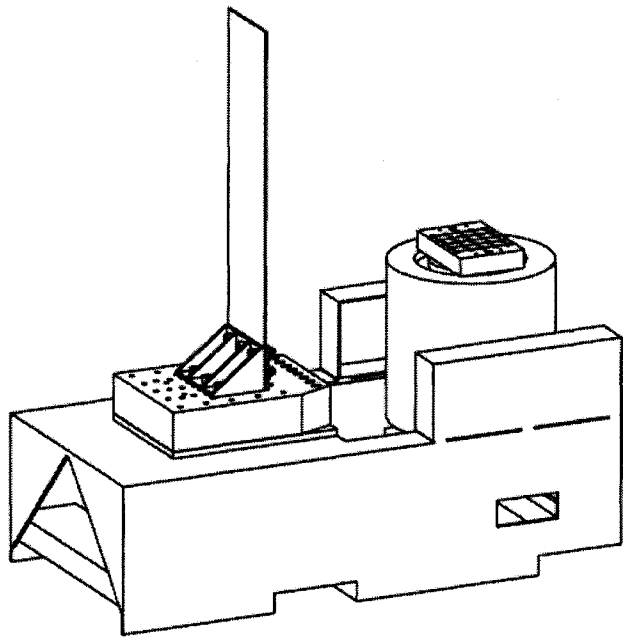

ASSEMBLY ISOMETRIC VIEW1

	Name	DATE
Drawn	malam	12/04/06
Checked		
ENG APPR		
MGR APPR		

DIMENSIONS ARE IN INCHES
ANGLE ±XX°

SOLID EDGE v19
ESA & CU JOINT PROJECT

Title OUTPUT-ONLY MODAL TESTING

SIZE A4 | DRW No. 1 | REV 1

File Name Top.dft

Scale 1:13.33 | Weight | Sheet 1 OF 1

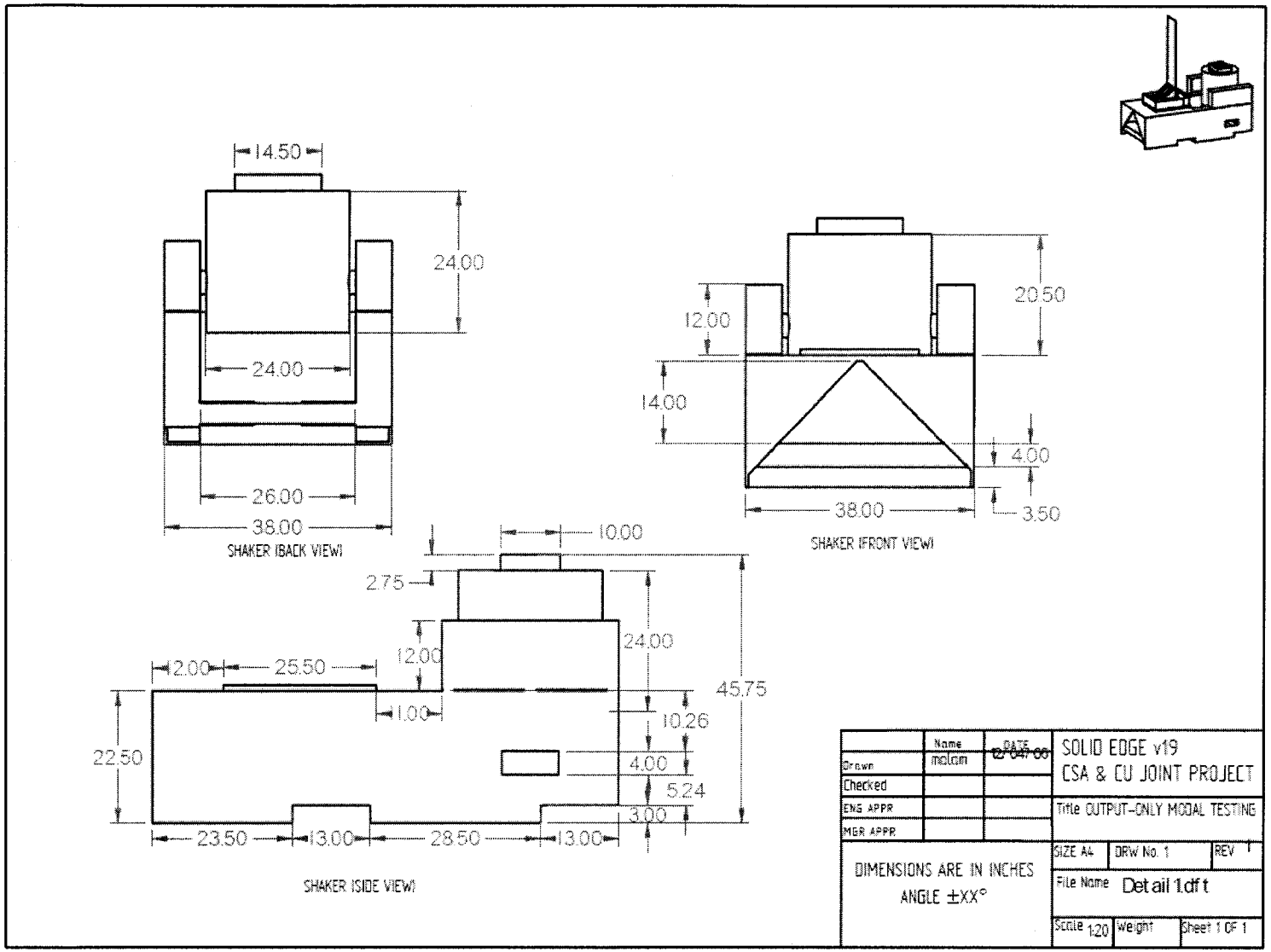
14.50
24.00
24.00
26.00
38.00
SHAKER (BACK VIEW)
20.50
12.00
14.00
4.00
38.00
3.50
SHAKER (FRONT VIEW)
10.00
2.75
24.00
12.00
2.00
25.50
45.75
1.00
10.26
22.50
4.00
5.24
3.00
23.50
13.00
28.50
13.00
SHAKER (SIDE VIEW)
Name
DATE
Drawn
malcan
12-04-00
Checked
ENG APPR
MGR APPR
SOLID EDGE v19
CSA & CU JOINT PROJECT
Title OUTPUT-ONLY MODAL TESTING
DIMENSIONS ARE IN INCHES
ANGLE ±XX°
SIZE A4
DRW No. 1
REV 1
File Name Detail1.dft
Scale 1:20
Weight
Sheet 1 OF 1

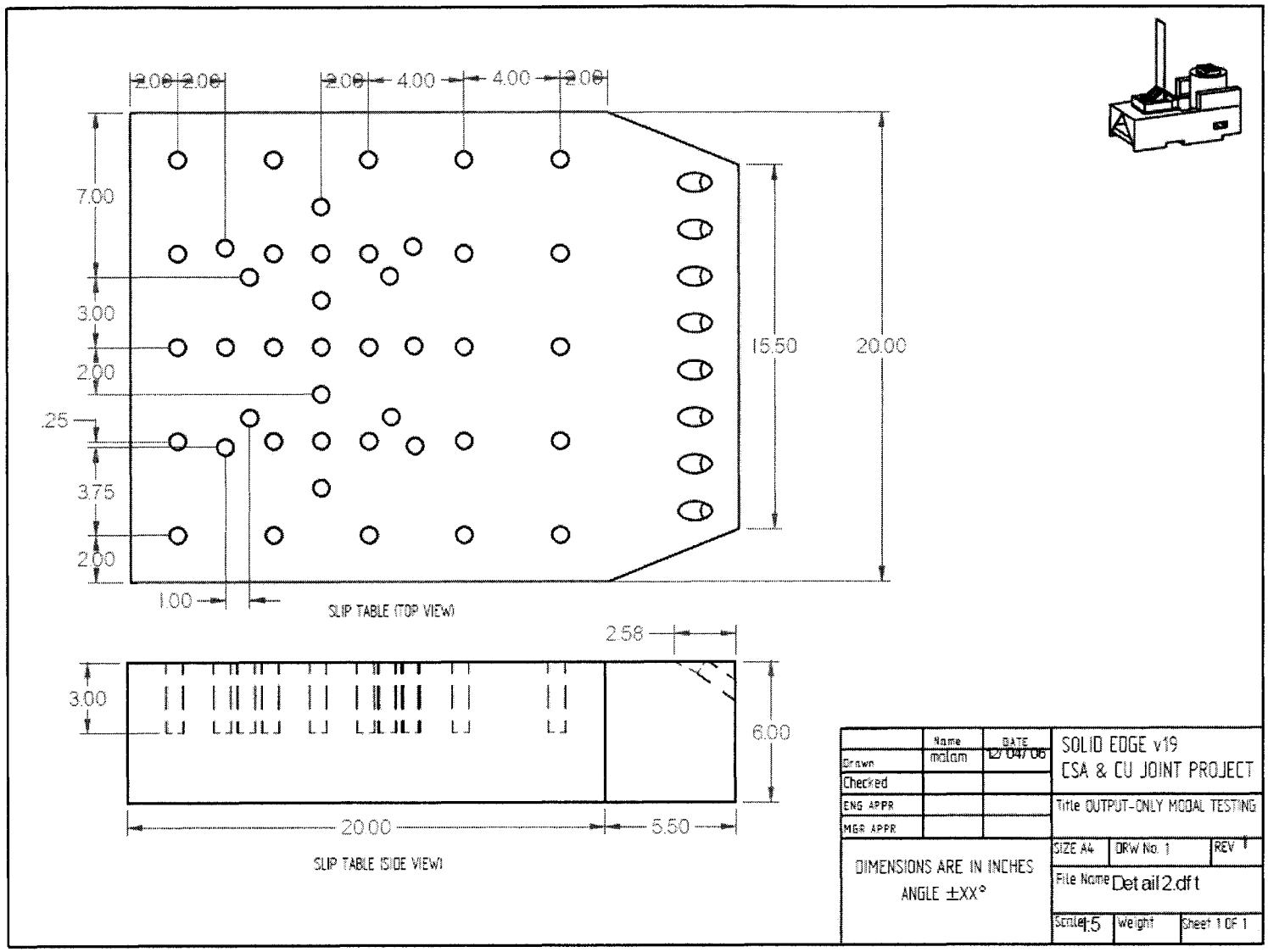
2.00
2.00
2.00
4.00
4.00
2.00
7.00
3.00
2.00
.25
3.75
2.00
1.00
15.50
20.00
SLIP TABLE (TOP VIEW)
2.58
3.00
6.00
20.00
5.50
SLIP TABLE (SIDE VIEW)
Name
DATE
Drawn
malam
12/04/06
Checked
ENG APPR
MGR APPR
SOLID EDGE v19
CSA & CU JOINT PROJECT
Title OUTPUT-ONLY MODAL TESTING
DIMENSIONS ARE IN INCHES
ANGLE ±XX°
SIZE A4
DRW No. 1
REV
File Name Detail2.dft
Scale 1:5
Weight
Sheet 1 OF 1

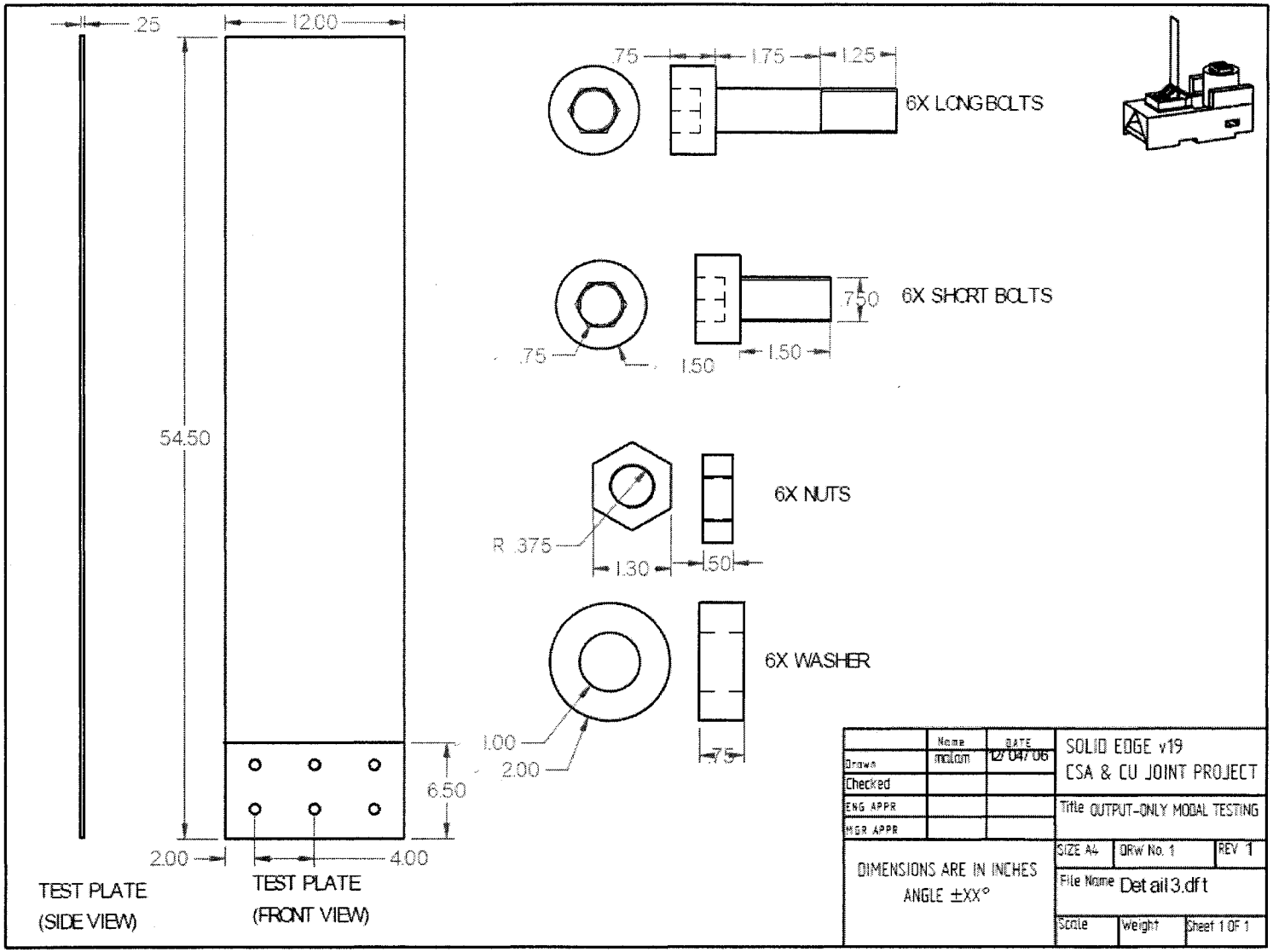
.25
12.00
54.50
6.50
2.00
4.00
TEST PLATE
(SIDE VIEW)
TEST PLATE
(FRONT VIEW)
.75
1.75
1.25
6X LONG BOLTS
.75
1.50
.75
1.50
6X SHORT BOLTS
R .375
1.30
.50
6X NUTS
1.00
2.00
.75
6X WASHER
Name
DATE
Drawn
mcl.com
12/04/06
Checked
ENG APPR
MGR APPR
SOLID EDGE v19
CSA & CU JOINT PROJECT
Title OUTPUT-ONLY MODAL TESTING
DIMENSIONS ARE IN INCHES
ANGLE ±XX°
SIZE A4
DRW No. 1
REV 1
File Name Detail3.dft
Scale
Weight
Sheet 1 OF 1